

RELIABILITY ANALYSIS AND IMPLEMENTATION OF GRID CONNECTED INVERTER FOR PV APPLICATIONS

Thesis Submitted For the Award of the Degree of

DOCTOR OF PHILOSOPHY

in

Electrical Engineering

By

Sainadh Singh Kshatri

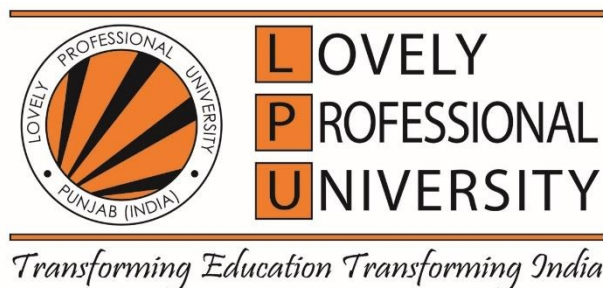
41800355

Supervised By

Dr Javed Dhillon

Co-Supervised by

Dr Sachin Mishra



LOVELY PROFESSIONAL UNIVERSITY

PUNJAB

2021

DECLARATION

I declare that the thesis entitled “**RELIABILITY ANALYSIS AND IMPLEMENTATION OF GRID CONNECTED INVERTER FOR PV APPLICATIONS**” has been prepared by me under the supervision of **Dr. Javed Dhillon**, Assistant Professor, School of Electronics and Electrical Engineering, Lovely Professional University, Punjab, India and co-supervision of **Dr. Sachin Mishra**, Associate Professor, School of Electronics and Electrical Engineering, Lovely Professional University, Punjab, India. No part of this thesis has formed the basis for the award of any degree or fellowship previously.



Sainadh Singh Kshatri

Reg. No 41800355

School of Electronics and Electrical Engineering

Lovely Professional University, Punjab

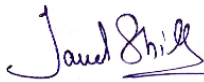
Phagwara – 144002.

Place: Phagwara

Date: 23-10-2021

CERTIFICATE

This is to certify that the thesis entitled “**RELIABILITY ANALYSIS AND IMPLEMENTATION OF GRID CONNECTED INVERTER FOR PV APPLICATIONS**” submitted by **Sainadh Singh Kshatri** to the Lovely Professional University, Punjab for the award of the degree of Doctor of Philosophy is a bonafide record of research work carried out by him under our guidance. The contents of this thesis, in full or in parts, have not been submitted to any other Institute or University for the award of any degree or diploma.



Dr. Javed Dhillon

Assistant Professor,
School of Electronics and Electrical Engineering,
Lovely Professional University, Punjab,
Phagwara – 144002.



Dr. Sachin Mishra

Associate Professor,
School of Electronics and Electrical Engineering,
Lovely Professional University, Punjab,
Phagwara – 144002.

Place: Phagwara

Date: 23-10-2021

ABSTRACT

Today inverter system is one of the enabling technologies for efficiently harnessing energy from renewable energy sources (Solar, Wind, etc.,) and for high reliable grid interfacing systems. With the advancements in power electronics, the inverter conversion efficiency is improved. The application of inverters leads to an increase in the utilization of solar energy sources and shares a notable amount of the world's total electricity generation. China leads the market with one-third of total PV installed capacity by the end of 2020. India is in the top 10 Countries of PV cumulative capacity. Total CO₂ emissions are reduced by a notable amount. Nevertheless, researchers reported PV inverter as the most unreliable device in the PV system. Generally, manufacturers specify 20 to 25 years of a lifetime for PV panels and less than 15 years for PV inverters. However, inverter costs about 59% of the total cost. Hence the reliability of the inverter plays a significant role in the performance assessment. Factors such as quality control, adequate design, electrical component failure, and other manufacturing factors influence the reliability of PV inverters. Power electronic switches in the inverter are the critical components due to thermomechanical failures. The most occurring failures are wear-out, bond-wire liftoff, etc.

Environmental factors like solar irradiance, ambient temperature (also called Mission Profile) lead to Power cycling and thermal cycling of the switch, which are the major causes for failure. Mission profile varies from location to location, regions near the equator receive relatively high solar irradiance and ambient temperature all over the year. Similarly, regions far from the equator receive relatively low solar irradiance and ambient temperature all over the year. Hence mission profile oriented reliability analysis of power electronic switch is needed.

Therefore, reliability analysis of grid-connected PV inverter and improvement solutions are proposed in this work. Real-time yearly solar irradiance and ambient temperature are considered. Solar irradiance is measured using CMP11 Pyranometer and Ambient temperature is measured using an RTD device. The measured parameters are logged with the help of a data logger. In addition to this, mission profile data at the Denmark location is considered for comparison. Denmark has cold weather conditions and India has Hot weather conditions.

A test case of a single-phase 3-kW grid-connected PV inverter is considered and simulated in the PLECS platform. Full bridge configuration is adopted, it consists of four 600V, 30A IGBT's. The thermal profile of the IGBT's is taken from the manufacturer datasheet for a realistic approach. Foster Electro-Thermal Model is implemented to estimate junction temperature. Since junction temperature calculation is indirect method validation is needed. The heat dissipated at the junction layers of IGBT flows to the case. Hence, validation is made by correlating the junction temperature of the PV inverter with the case temperature. Along with the Mission Profile, the case temperature of the PV inverter is logged. Correlation analysis is also performed between estimated junction temperature and solar irradiance, ambient temperature. Positive correlation gives the validation of Junction Temperature.

The variations of the estimated junction temperature follow irregular profiles as per the mission profile. Hence a cycle counting algorithm is needed to anticipate the variations. Rainflow counting algorithm is used to analyse the variations. From the rainflow algorithm, No. of Cycles n_i , Mean Junction Temperature T_{jm} , Cycle Amplitude ΔT , are calculated. Lifetime is evaluated using the miner's rule. In the obtained lifetime, all the parameters are constant i.e., all the devices should fail at the same rate but practically, this is not feasible, so to overcome that, the variation of 5% is considered and 10000 samples are generated using Monte Carlo simulation. All the generated samples are fitted in two parameters-based Weibull distribution and reliability function at both component level and system level is obtained and B10 lifetime is calculated.

In this work, various factors such as Installation site, the Degradation rate of PV panel, PV Panel Over Sizing, Bifacial PV Panels are considered to analyse its impact. With the change in the installation site, the reliability of the PV panel also changes, hence mission profile data of India and Denmark locations are considered. With time, the performance of the PV panel also will degrade yearly basis, this impacts the long-term operation and leads to a decrease in power output. Hence Degradation rate of 1.93% per year for five years of operation is considered at an India Location and 0.15 % per year for five years of operation is considered at Denmark Location. Panel oversizing is the common approach to yield more energy and to reduce the cost in low

irradiance locations. This increases the inverter loading and negative impact on reliability performance. To account this panel sizing ratios, $R_s = 1.0, 1.2, 1.4$ are considered. Bifacial technology is the recent advancement in the PV industry, it can harness energy from both the front side and backside. This technology inevitably affects the loading performance of the inverter, as it operates nearly the rated power for a longer duration and leads to an increase in thermal stress on power electronic components. Hence to account for this Bifacial PV panel with 0%, 30%, 50% more energy yield is considered.

Finally, Analysed the various improvement solutions to ensure the Reliability performance of the Grid Connected PV Inverter. Recent advancements in power electronic switches are SiC-based devices. SiC is provided with a wide bandgap that performs superior compared to conventional Si-based devices. The notable advantages of SiC-based devices are low switching losses, high switching speed and blocking voltage, etc., hence with the use of SiC, the performance of the system would be improved. However, the cost of SiC devices is a major concern. Hence, it is not economical to replace all the devices in the PV inverter with SiC devices. To overcome this issue a hybrid Si/SiC switch is proposed for reliability improvement of PV inverter. The hybrid Switch consists of Si-IGBT and SiC- diode and its effectiveness are analysed by comparing it with conventional Si-IGBT. Reliability improved significantly with the proposed hybrid switch.

PREFACE / ACKNOWLEDGEMENT

This thesis would not have been possible without the support of glorious people who motivated me during my doctoral study. I am thankful from my bottom of my heart toward the numerous persons who assisted me while conducting this study. First of all, I would like to thank my supervisor, Dr. Javed Dhillon, for his worthy guidance, support, and suggestions, in every step of this research project during my Ph.D. journey. Dr. Javed Dhillon has an optimistic personality with helpful nature, he has always made himself ready to clarify my doubts and it was a great opportunity to work under his supervision. He always shed light whenever I was feeling stuck in my path of research ambitions.

I would like to express my sincere gratitude to my Co- supervisor Dr. Sachin Mishra, for the continuous support of my Ph.D. study and research, for his patience, motivation, enthusiasm, and immense knowledge. His guidance helped me in all the time of research.

It is my privilege to thank my family members for their continuous encouragement throughout my research time. I am extremely thankful to the Management, Principal, HOD and all Faculty members of B V Raju Institute of Technology, Narsapur, India for supporting and providing the necessary inputs.

I would like to express my gratitude toward the entire Lovely Professional University family for providing suitable infrastructure and environment for completing my research work in a time-bound manner. Also, I like to thank the Division of Research & Development and School of Electronics and Electrical Engineering for their help and encouragement in my entire Ph.D. journey. Finally, I like to thank almighty God who helped me to achieve such a big milestone.



Sainadh Singh Kshatri

Date: 23-10-2021

TABLE OF CONTENTS

S.No	Name	Page No.
	Declaration	i
	Thesis Certificate	ii
	Abstract	iii
	Acknowledgement	vi
CHAPTER 1: INTRODUCTION & LITERATURE REVIEW		
1.1	Introduction	1
	1.1.1 Scope of Solar Energy in India	2
1.2	Reliability in Power Electronic Systems	4
1.3	Power Electronics system Failures and Field Experiences	5
	1.3.1 Critical Components in PV Inverter	8
	1.3.2 Need for Reliability Assessment	10
1.4	Review of Literature	11
	1.4.1 Grid-Connected PV Inverters	11
	1.4.2 Reliability Analysis of Grid Connected PV Inverter	12
	1.4.3 Factors affects the Reliability of PV Inverter	17
	1.4.4 Reliability Improvement of PV Inverters	20
1.5	Research Gaps and Objectives	21
1.6	Proposed Methodology	22
1.7	Organization of the Thesis	23

CHAPTER 2: MISSION PROFILE DATA LOGGING

2.1	Mission Profile	25
2.2	Mission Profile at India Location	25
2.3	Mission Profile at Denmark Location	27
2.4	Mission Profile Comparison	29
2.5	Chapter Summary	31

CHAPTER 3: ELECTRO THERMAL MODELING OF IGBT

3.1	Electro Thermal Modeling of IGBT	32
3.2	Test Case	32
3.3	IGBT Thermal Flow	34
3.4	Instantaneous Junction Temperature	35
3.5	Foster Electro Thermal Modelling of IGBT	37
3.6	Junction Temperature Calculated from Yearly Mission Profile	38
3.7	Chapter Summary	41

CHAPTER 4: VALIDATION OF ESTIMATED JUNCTION TEMPERATURE

4.1	Validation of Estimated Junction Temperature	40
4.2	Correlation Analysis	40
4.3	Correlation Analysis between Junction Temperature and Case Temperature	41
	4.3.1 Hypothesis Statement	41
	4.3.2 Correlation Analysis Parameters	42
	4.3.3 Hypothesis Conclusion	42
4.4	Correlation analysis between Junction Temperature and Solar Irradiance	42

4.4.1	Hypothesis Statement	43
4.4.2	Correlation Analysis Parameters	43
4.4.3	Hypothesis Conclusion	43
4.5	Correlation analysis between Junction Temperature and Ambient Temperature	44
4.5.1	Hypothesis Statement	44
4.5.2	Correlation Analysis Parameters	44
4.5.3	Hypothesis Conclusion	45
4.6	Chapter Summary	45
CHAPTER 5: RELIABILITY ANALYSIS OF PV INVERTER		
5.1	Reliability analysis of PV Inverter Methodology	46
5.2	Reliability Analysis of PV inverter	49
5.2.1	Rain flow Counting Analysis	49
5.2.2	Life Time Evaluation	51
5.2.3	Monte Carlo Simulation based Reliability (B_{10}) Evaluation	51
5.2.4	B_{10} Lifetime Comparison	55
5.3	Factors Effecting the Reliability of PV Inverter	56
5.3.1	Impact of Degradation Rate on PV Inverter Reliability	56
5.3.2	Impact of PV Panel Oversizing on PV Inverter Reliability	65
5.3.3	Impact of Bifacial PV Panel on PV Inverter Reliability	75
5.4	Chapter Summary	84
CHAPTER 6: RELIABILITY IMPROVEMENT SOLUTIONS		
6.1	Reliability Improvement Methodology	85
6.2	Reliability Analysis of PV inverter Considering Hybrid Si/SiC Switch	85

6.2.1	Junction Temperature Considering Hybrid Si/SiC Switch	86
6.2.2	Rain flow Analysis	87
6.2.3	Life Time Evaluation	88
6.2.4	Monte Carlo Simulation based Reliability (B_{10}) Evaluation	89
6.2.5	B_{10} Lifetime Comparison	93
6.3	Chapter Summary	94
CHAPTER 7: CONCLUSION & FUTURE SCOPE		
7.1	Conclusion	95
7.2	Future Scope	97
References		99
Appendices		115
List of Publications		117
List of Patents		119

LIST OF FIGURES

Fig. No	Description	Page No
1.1	Global PV Cumulative Capacity	1
1.2	Global Annual PV Installed Capacity	2
1.3	Annual India's growth in Conventional Power Generation	3
1.4	Annual India's growth in Renewable Power Generation	3
1.5	Scope of Power Electronics	4
1.6	Scope of Power Electronics Reliability	5
1.7	Plant Unscheduled Maintenance Events	5
1.8	PV Plant Unscheduled Maintenance Costs	6
1.9	Wind System Failure rate events	7
1.10	Wind System Down time events	7
1.11	Failure distribution in power converters	8
1.12	IGBT Cross Section layout	10
1.13	Different configurations of Grid Connected PV Inverters	11
1.14	Stages of Reliability Analysis	12
1.15	Factors affects the Reliability of PV Inverter	17
1.16	Bifacial PV Panel	18
1.17	Global annual installed bifacial solar capacity	19
1.18	Top five countries with the highest bifacial solar installed capacity	19
1.19	Proposed Methodology Block Diagram	23
2.1	CMP11 Pyranometer	25
2.2	RTD Device	26

2.3	CR3000 Data Logger	26
2.4	Schematic of experimentation	27
2.5	One Year Mission Profile Data at India Location	27
2.6	One Year Mission Profile Data at Denmark Location	28
3.1	Single phase 3-kW grid connected PV inverter	32
3.2	Thermal Flow of IGBT	34
3.3	IGBT Turn on Losses	36
3.4	IGBT Turn off Losses	36
3.5	IGBT Conduction Losses	36
3.6	Foster Electro Thermal Model of PV Inverter	37
3.7	Parameter of Foster Electro Thermal Model	37
3.8	One year Junction Temperature at India Location	38
3.9	One year Junction Temperature at Denmark Location	38
4.1	Correlation Variables	40
5.1	Reliability Analysis Flowchart	46
5.2 (a)	Rain flow Matrix India Location	50
5.2 (b)	Rain flow Matrix Denmark Location	50
5.3 (a)	Monte Carlo Simulation Lifetime Distribution at India Location	52
5.3 (b)	Monte Carlo Simulation Lifetime Distribution at Denmark Location	52
5.4 (a)	Reliability (B_{10}) Evaluation of PV Inverter at India Location Component Level	53
5.4 (b)	Reliability (B_{10}) Evaluation of PV Inverter at India Location System Level	53

5.5 (a)	Reliability (B ₁₀) Evaluation of PV Inverter at Denmark Location Component Level	54
5.5 (b)	Reliability (B ₁₀) Evaluation of PV Inverter at Denmark Location System Level	54
5.6	B ₁₀ Lifetime Comparison Chart	55
5.7 (a)	Junction Temperature with and without Degradation Rate at India Location	57
5.7 (b)	Junction Temperature with and without Degradation Rate at Denmark Location	57
5.8 (a)	Average Junction Temperature India	58
5.8 (b)	Average Junction Temperature Denmark	58
5.9 (a)	Rainflow Histogram without Degradation Rate at India	58
5.9 (b)	Rainflow Histogram with Degradation Rate at India	58
5.9 (c)	Rainflow Histogram without Degradation Rate at Denmark	58
5.9 (d)	Rainflow Histogram with Degradation Rate at Denmark	58
5.10 (a)	Monte Carlo Simulation Lifetime distribution without Degradation Rate at India	60
5.10 (b)	Monte Carlo Simulation Lifetime distribution with Degradation Rate at India	60
5.11 (a)	Monte Carlo Simulation Lifetime distribution without Degradation Rate at Denmark	61
5.11 (b)	Monte Carlo Simulation Lifetime distribution with Degradation Rate at Denmark	61
5.12 (a)	Reliability (B ₁₀) Evaluation of PV Inverter at India Component Level	62
5.12 (b)	Reliability (B ₁₀) Evaluation of PV Inverter at India System Level	62
5.13 (a)	Reliability (B ₁₀) Evaluation of PV Inverter at Denmark Component Level	63

5.13 (b)	Reliability (B_{10}) Evaluation of PV Inverter at Denmark System Level	63
5.14	B_{10} Lifetime Comparison Chart	64
5.15	Junction Temperature with different sizing ratios (R_s) at India	65
5.16	Junction Temperature with different sizing ratios (R_s) at Denmark	66
5.17(a)	Average Junction Temperature with different sizing ratios (R_s) at India	66
5.17(b)	Average Junction Temperature with different sizing ratios (R_s) at Denmark	66
5.18 (a)	Rainflow Histogram with sizing ratio $R_s = 1.0$ at India	67
5.18 (b)	Rainflow Histogram with sizing ratio $R_s = 1.2$ at India	67
5.18 (c)	Rainflow Histogram with sizing ratio $R_s = 1.4$ at India	67
5.18 (d)	Rainflow Histogram with sizing ratio $R_s = 1.0$ at Denmark	67
5.18 (e)	Rainflow Histogram with sizing ratio $R_s = 1.2$ at Denmark	67
5.18 (f)	Rainflow Histogram with sizing ratio $R_s = 1.4$ at Denmark	67
5.19 (a)	Monte Carlo Simulation Lifetime distribution with $R_s = 1.0$ at India	69
5.19 (b)	Monte Carlo Simulation Lifetime distribution with $R_s = 1.2$ at India	69
5.19 (c)	Monte Carlo Simulation Lifetime distribution with $R_s = 1.4$ at India	70
5.20 (a)	Monte Carlo Simulation Lifetime distribution with $R_s = 1.0$ at Denmark	70
5.20 (b)	Monte Carlo Simulation Lifetime distribution with $R_s = 1.2$ at Denmark	71
5.20 (c)	Monte Carlo Simulation Lifetime distribution with $R_s = 1.4$ at Denmark	71

5.21 (a)	Reliability (B ₁₀) Evaluation of PV Inverter at India Component Level	72
5.21 (b)	Reliability (B ₁₀) Evaluation of PV Inverter at India System Level	72
5.22 (a)	Reliability (B ₁₀) Evaluation of PV Inverter at Denmark Component Level	73
5.22 (b)	Reliability (B ₁₀) Evaluation of PV Inverter at Denmark System Level	73
5.23	B ₁₀ Lifetime Comparison	74
5.24	Junction Temperature with Bifacial PV Panel at India	75
5.25	Junction Temperature with Bifacial PV Panel at Denmark	75
5.26 (a)	Average Junction Temperature with Bifacial PV Panel at India	76
5.26 (b)	Average Junction Temperature with Bifacial PV Panel at Denmark	76
5.27 (a)	Rain Flow Matrix at India Location	76
5.27 (b)	Rain Flow Matrix at Denmark Location	77
5.28 (a)	Monte Carlo Simulation Lifetime distribution with 0 % More Energy Yield at India	78
5.28 (b)	Monte Carlo Simulation Lifetime distribution with 30 % More Energy Yield at India	78
5.28 (c)	Monte Carlo Simulation Lifetime distribution with 50 % More Energy Yield at India	79
5.29 (a)	Monte Carlo Simulation Lifetime distribution with 0 % More Energy Yield at Denmark	79
5.29 (b)	Monte Carlo Simulation Lifetime distribution with 30 % More Energy Yield at Denmark	80
5.29 (c)	Monte Carlo Simulation Lifetime distribution with 50 % More Energy Yield at Denmark	80

5.30 (a)	Reliability function of PV inverter at India Location Component Level	81
5.30 (b)	Reliability function of PV inverter at India Location System Level	81
5.31 (a)	Reliability function of PV inverter at Denmark Location Component Level	82
5.31 (b)	Reliability function of PV inverter at Denmark Location System Level	82
5.32	B ₁₀ Lifetime Comparison	83
6.1	Hybrid IGBT	85
6.2	One year estimated junction temperature at India Location	86
6.3	One year estimated junction temperature at Denmark Location	86
6.4 (a)	Average Junction Temperature India	87
6.4 (b)	Average Junction Temperature Denmark	87
6.5 (a)	Rain flow Matrix at India Location	87
6.5 (b)	Rain flow Matrix at Denmark Location	88
6.6 (a)	Monte Carlo Simulation Lifetime Distribution of PV inverter at India Location with Conventional Si-IGBT	89
6.6 (b)	Monte Carlo Simulation Lifetime Distribution of PV inverter at India Location with Hybrid Si-SiC IGBT	89
6.7 (a)	Monte Carlo Simulation Lifetime Distribution of PV inverter at Denmark Location with Conventional Si-IGBT	90
6.7 (b)	Monte Carlo Simulation Lifetime Distribution of PV inverter at Denmark Location with Hybrid Si-SiC IGBT	90
6.8 (a)	Reliability function of PV inverter at India Location Component Level	91
6.8 (b)	Reliability function of PV inverter at India Location System Level	91

6.9 (a)	Reliability function of PV inverter at Denmark Location Component Level	92
6.9 (a)	Reliability function of PV inverter at Denmark Location System Level	92
6.10	B ₁₀ Lifetime Comparison	93

LIST OF TABLES

Table. No	Description	Page No.
1.1	Critical Stressors of IGBT	9
1.2	Comparison of Thermal Models	14
1.3	Comparison of Life Time Models	16
2.1	Heatmap Table of Solar Irradiance	29
2.2	Heatmap Table of Ambient Temperature	30
3.1	3-KW grid connected PV inverter parameters	33
4.1	Correlation Range	41
4.2	Correlation Analysis Parameters	42
4.3	Correlation Analysis Parameters	43
4.4	Correlation Analysis Parameters	44
5.1	Bayerer's Lifetime Model Parameters	48
5.2	Lifetime Evaluation for Static Parameters	51
5.3	Lifetime Evaluation for Static Parameters	59
5.4	Lifetime Evaluation for Static Parameters	68
5.5	Lifetime Evaluation for Static Parameters	77
6.1	Lifetime Evaluation for Static Parameters	88

LIST OF APPENDICES

App. No	Description	Page No.
A.1	Derivation for B_x Lifetime Equation	115
A.2	Thermal Parameters of Si-IGBT (IGW30N60H3)	115
A.3	Thermal Parameters of SiC-Diode (C3D20060D)	115
A.4	Cost Comparison of Switches	116
A.5	Algorithm steps for Monte Carlo simulation and obtaining Weibull distribution	116
A.6	Probability Density Function	116

CHAPTER 1

INTRODUCTION AND LITERATURE REVIEW

1.1. Introduction:

Many countries have reached grid parity with solar photovoltaic systems, and many plans are proposed to reach 100 percent utilization of green energy sources by 2050. Furthermore, in the next ten years, the cost of renewables is projected to undercut the cost of fossil fuels [1]. Nevertheless, the PV system is one of the preferable solutions for future energy demand. The factors for the increasing tendency of PV markets are demand for energy increases, government policies towards renewable energy sources, concerns related to the environment, rapid development in PV technologies, an increase in PV installations globally, etc. Global total cumulative PV installed capacity at the end of 2020 is at least about 760.4 GW. Fig. 1.1 shows the global PV cumulative capacity of the top 10 countries. China Leads the market with 253.4 GW, over one-third of overall installed capacity. India is in the Top 10 Countries with 47.4 GW of PV Cumulative Capacity [2].

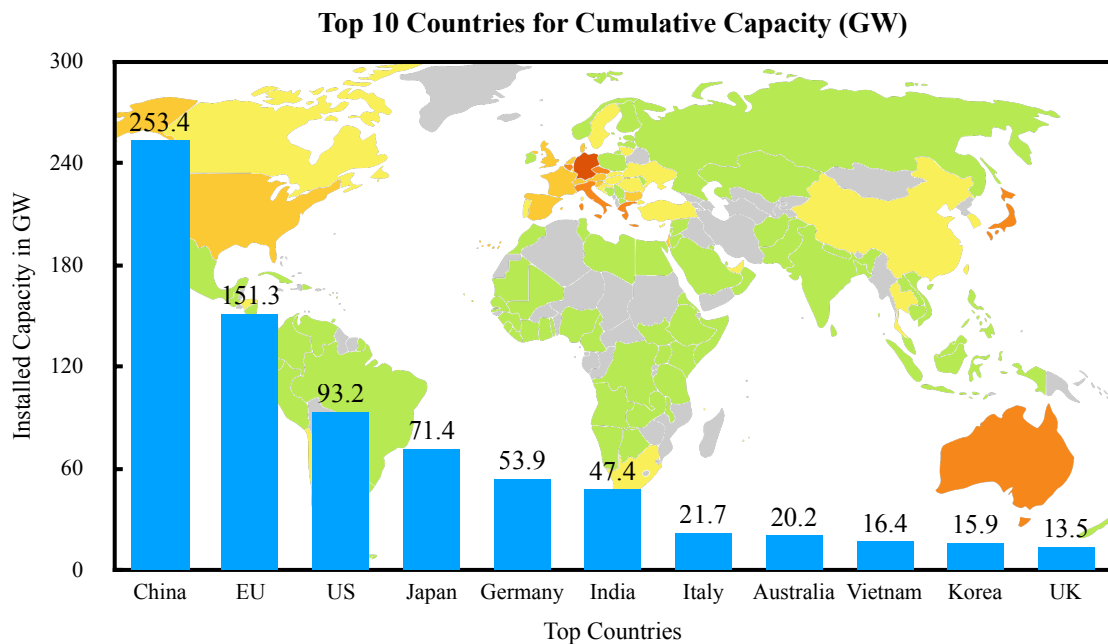


Fig. 1.1. Global PV Cumulative Capacity

About 139.4 GW of PV systems has been commissioned and installed all over the world at end of 2020. Fig. 1.2 shows the global annual PV installed capacity of the top 10 countries. China is at 1st position with 48.2 GW, followed by EU, 19.6 GW, and USA, 19.2 GW. In the European Union, Germany (4.9 GW), Netherlands (3.0 GW) reported with highest installations in the year 2020 followed by Spain, Poland,

Belgium, and France. The US records with 73 % new utility-scale installations in the year 2020. In the top ten countries, six from Asia, two from the EU, and two from America.

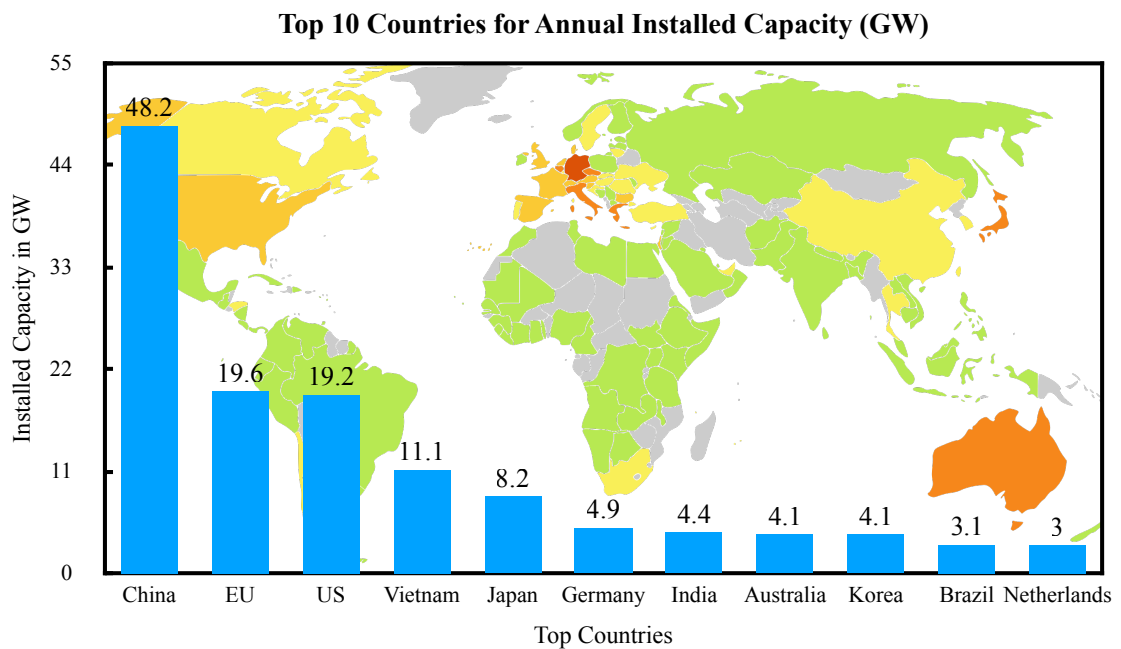


Fig. 1.2. Global Annual PV Installed Capacity

The Highlights of PV Market 2021 are given below

- 3.7 % of global electricity is generated by PV systems.
- Total CO₂ emissions reduced by 877 Mt.
- At least 20 countries installed 1 GW of PV systems.
- At least 14 countries installed 10 GW of cumulative capacity.
- Solar PV per capita 2020 is led by Australia followed by Germany and Japan.

The above statistics clearly show the Photovoltaic Generation systems have a significant demand and share in today's electricity market.

1.1.1. Scope of Solar Energy in India:

Today's India is looking towards renewable energy sources for its power demands. According to the Ministry of New and Renewable Energy (MNRE) [3], the Atmospheric conditions of India can harness enormous solar energy. Annually about 5000 trillion kWh power is incident in the land areas of India. Almost every component receives 4-7 kWh per sq. m per day. Due to this, conversions from solar radiation to heat and from solar radiation to electricity are successfully utilized in India. Photovoltaic Generations are available in both grid connected mode and islanded mode.

It is generously available and meets the energy demands such as power, heating, cooling, etc. in both urban and rural areas of India. Photovoltaic generation is the most secure power and green energy generation of all renewable resources in India. If we harness solar energy efficiently, it meets the whole countries demands. Still, many un-electrified areas are there in India. The Photovoltaic generation systems have the potential to electrify these un-electrified areas.

Ministry of Power, India [4] states that from the past four years there is significant growth in renewable power generation. Annual India's growth in power generation during recent years is shown in the following Fig. 1.3.

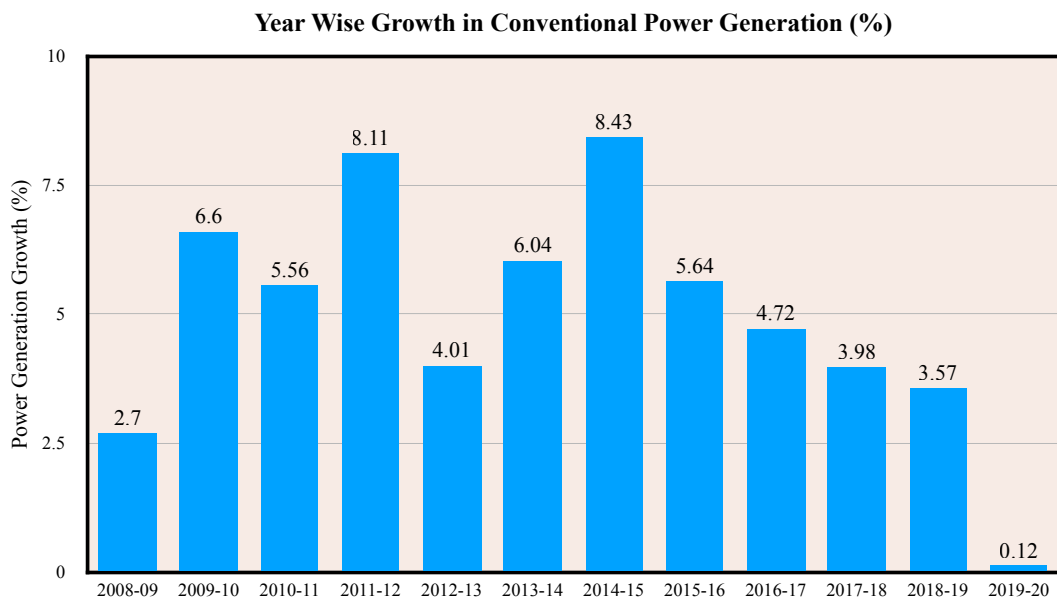


Fig. 1.3. Annual India's growth in Conventional Power Generation

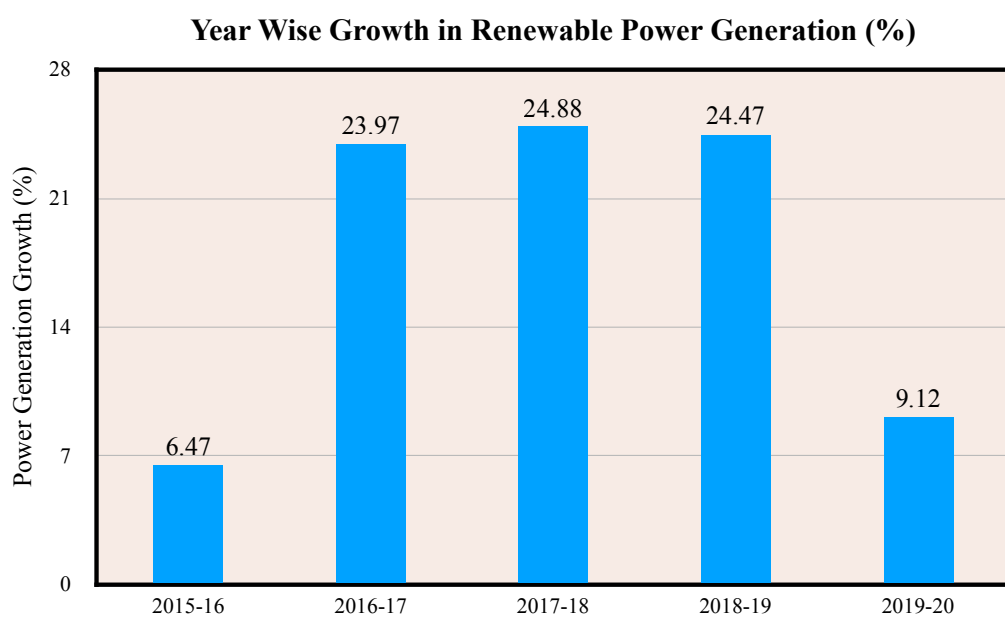


Fig. 1.4. Annual India's growth in Renewable Power Generation

From the Fig. 1.4 statistics, the scope of renewable energy sources is numerously increased in the past four years. The website of the Ministry of New and Renewable Energy (MNRE), reports that renewable energy installed capacity is increased about 226 % in the past 5 years. Solar energy is increased from 2.6 GW to more than 34 GW. Solar power tariff reduced day by day in India and a new record of low solar tariff i.e. Rs: 2.44 /- per unit is recorded in Bhadla, Rajasthan. The government of India brings many policies for the development of renewable energy sources. By 2022 India will become the world’s largest renewable energy, i.e., 175 GW of capacity.

1.2. Reliability in Power Electronic Systems:

Today’s power electronics is one of the enabling technologies for efficient energy conversion in the field of renewable generation, grid interfacing systems, automotive, traction, etc. [5], [6]. Recent advancements push the conversion efficiency to 98 %. Nevertheless, the reliability of power electronics is the major concern to comply with stringent constraints on failure rate, safety, availability, and cost, etc. The scope of the power electronics is defined and categorized into power, electronics, control by N. E. William in 1974 as shown in Fig. 1.5. [7].

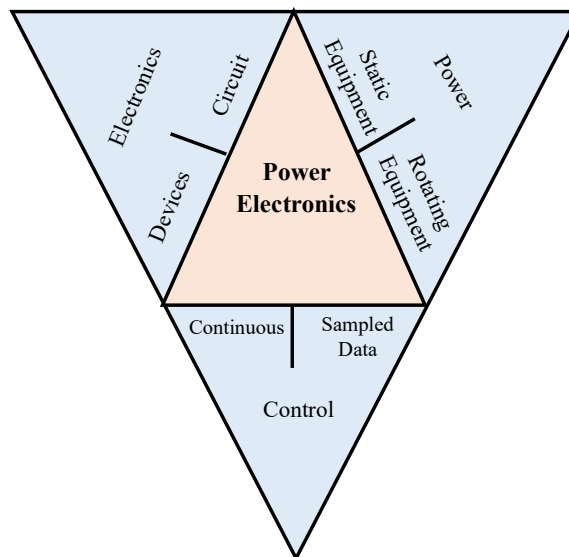


Fig. 1.5. Scope of Power Electronics

The wide range of industrial applications gained the importance of reliable power electronics. “Center for reliable power electronic, Aalborg University, Denmark”, defined the scope of power electronics reliability as shown in Fig. 1.6 [8]. It comprises of three important aspects to be able to concern.

- Control and Monitoring.

- Design and verification.
- Analytical Physics.

Recently, much research in the field of power electronics reliability has been performed in the above aspects such as PoF analysis, Lifetime assessment, Design for Reliability, thermal control, predictions, condition monitoring, etc.

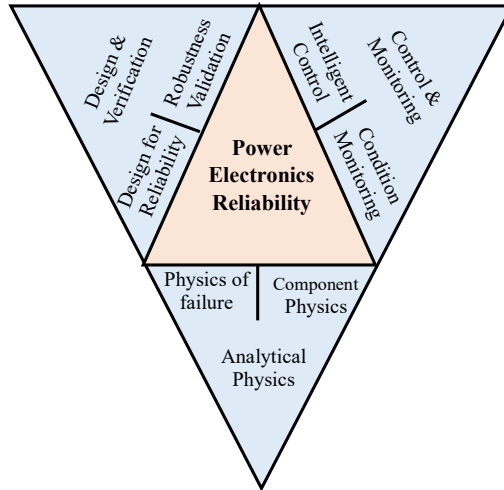


Fig. 1.6. Scope of Power Electronics Reliability

1.3. Power Electronic System Failures and Field Experiences:

According to the field experiences [9]–[11] power electronic systems are the most critical components in terms of lifetime, cost, and failure rate. Field experiences on unscheduled maintenance events and costs of large-scale PV plants are recorded between 2001 to 2006 as shown in Fig. 1.7 and Fig. 1.8 respectively [9].

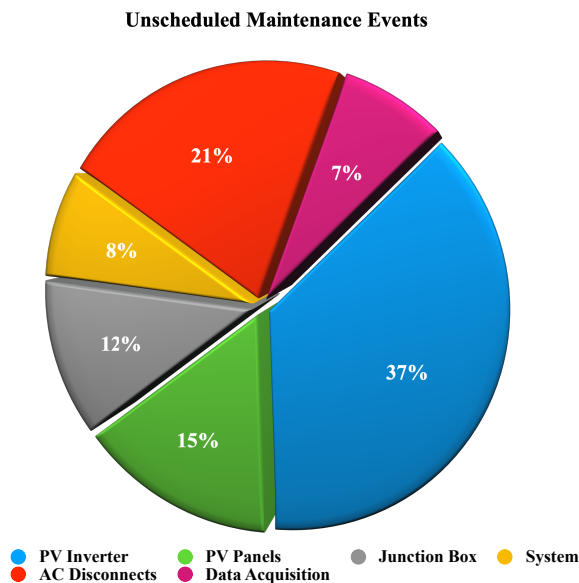


Fig. 1.7. PV Plant Unscheduled Maintenance Events

Unscheduled Maintenance Costs

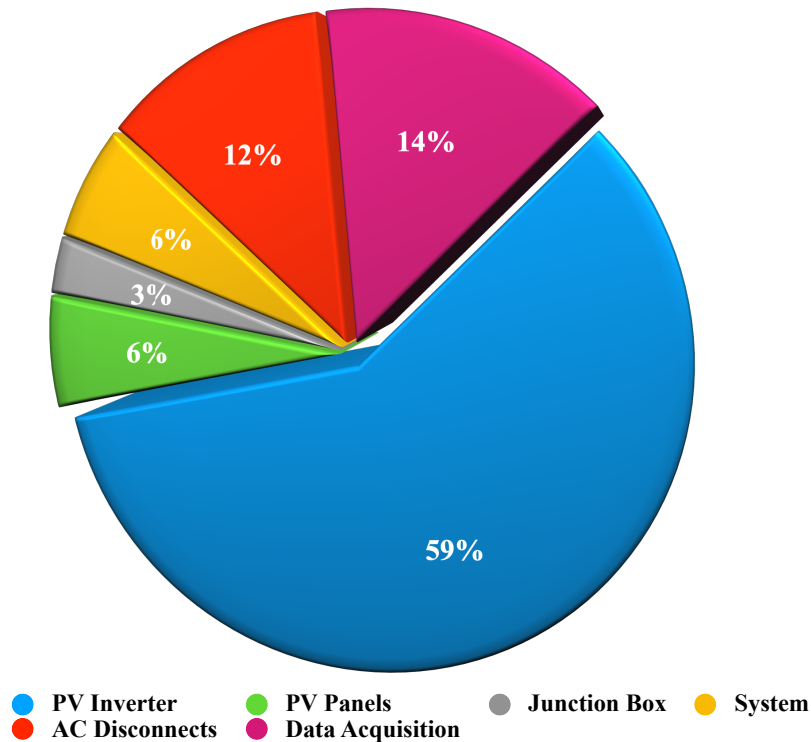


Fig. 1.8. PV Plant Unscheduled Maintenance Costs

A total of 156 events are recorded and categorized as PV inverter, PV panels, junction box, system, AC disconnects, data acquisition. Among the events, PV inverter shares 37 % and the cost associated with it is 59 %. Therefore, the PV inverter is the most crucial component and plays a significant role in terms of reliability concerns.

In the wind system, field experiences for 350 wind turbines from different manufacturers are investigated [11]. Downtime events with a 10-minute average are logged with SCADA, service reports, alarm logs, etc. About 35000 events are considered to determine the failure rate and downtime in subassemblies. The wind system failure rates and downtime events are presented in Fig. 1.9 and Fig. 1.10. It can be seen from the graph that, power converter reported notable failure rates and downtime events with 18 % and 13 % respectively. Hence power converter is also one of the important components for reliability concerns in wind system maintenance. Another study [10] investigated field experiences on 6000 wind turbines in Germany and Denmark for 11 years. This study also derives similar results that power converter with most failure rate events.

Events of Failure Rate

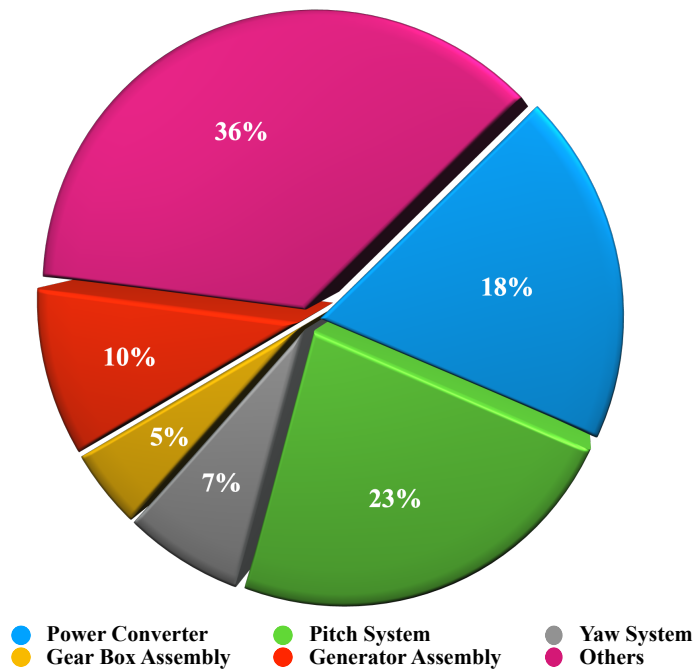


Fig. 1.9. Wind System Failure rate events

Events of Downtime

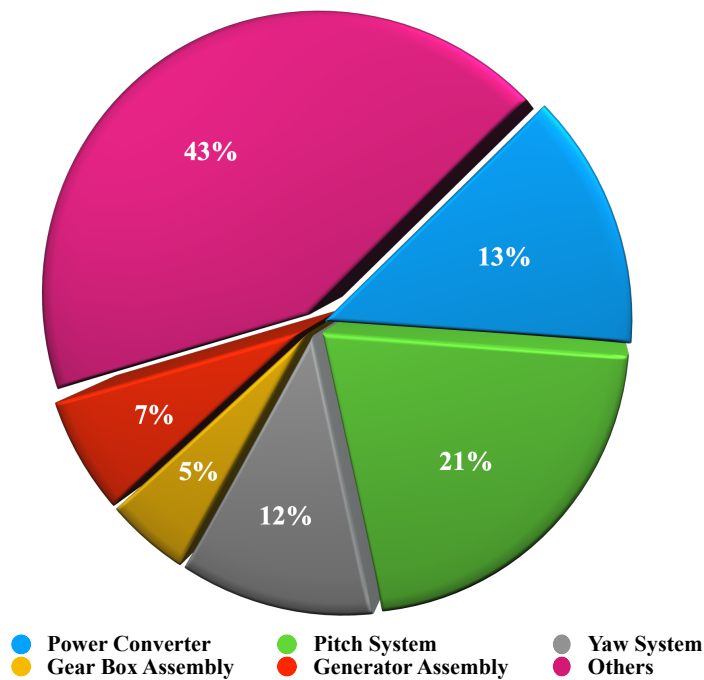


Fig. 1.10. Wind System Down time events

Reports of IEA on “reliability of grid connected PV systems” also presented the power converter with the highest failure rate [12].

1.3.1. Critical Components in PV Inverter:

PV inverter is reported as weakest among all in terms of reliability due to the power semiconductor switches [13]–[20]. Factors such as quality control, adequate design, Electrical component failure, and other manufacturing factors influence the reliability of PV Inverter.

For understanding the factors affecting the reliability of PV Inverter, analysis under critical stress for failure mechanism needs to be investigated. A survey has been taken from the semiconductor manufacturing companies depending on field experiences by [21]. According to the survey majority (31 %) of the maintenance events are associated with power semiconductor switch, i.e. IGBT as shown in Fig. 1.11.

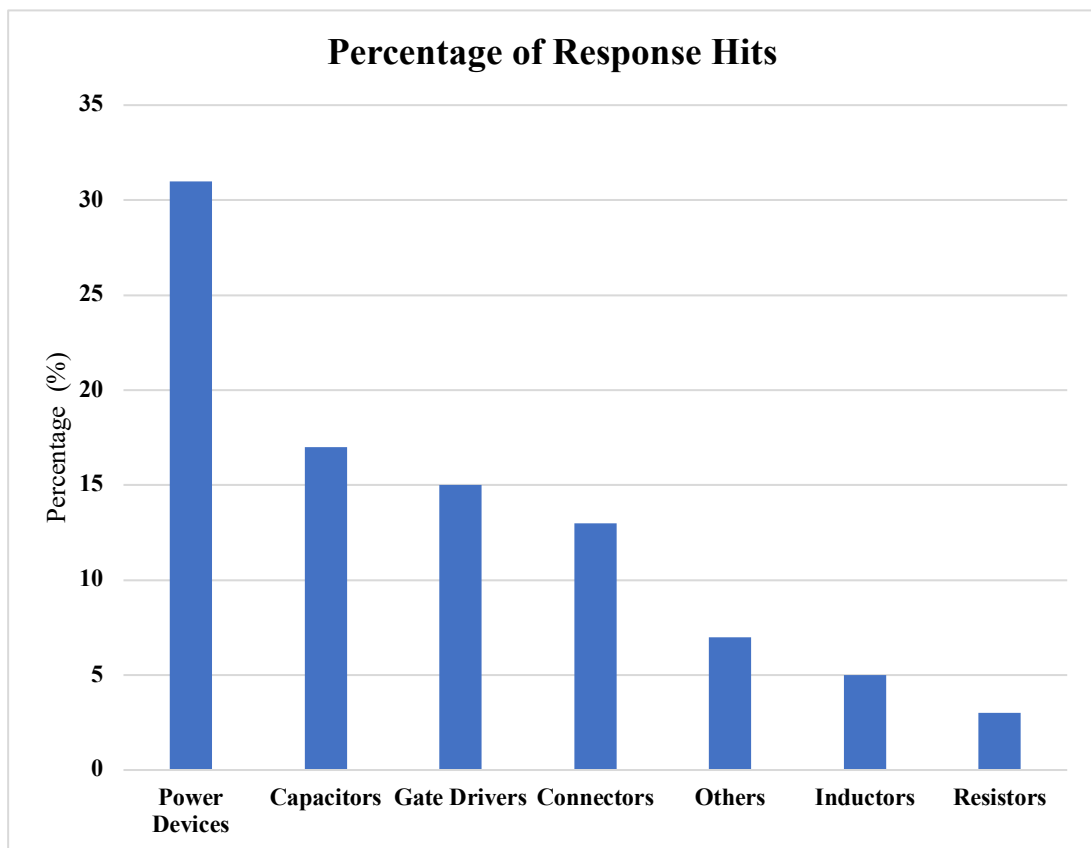


Fig. 1.11. Failure distribution in power converters

Thermal stress is the critical stressor of power semiconductors [8], Various stressors of IGBT are tabulated in the following Table. 1.1.

Table. 1.1. Critical Stressors of IGBT

Types of Load			IGBT		
Climate Condition	Design of the Product	Stressor	Die	Solder joints	Wire-bond
Temperature	IGBT ON/OFF	Temperature swing	High	High	High
	IGBT Thermal control	Average temperature	Medium	Medium	Medium
	IGBT Operating power.	dT/dt	Low	Low	Low
Shock	Mechanical	Mechanical shock	Low		
Humidity/Moisture	IGBT ON/OFF IGBT Thermal control IGBT Operating power.	Relative humidity	Low	Low	Low
Pollution	Enclosure design	Pollution			

Steady-state and cycling temperature affect the failure mechanisms of power semiconductors. In the grid connected PV inverter IGBT is the most unreliable component. Hence it is required to assess the reliability of IGBT to assess the reliability of PV inverter [22] [23] [24].

Fig. 1.12 shows the different layers of IGBT. Due to the thermal cycling during the normal operating conditions, uneven contraction and expansion develop in the layers that lead to shear strains or shear stress. These stresses may lead to a crack down or disconnections will occur. According to [25] there are mainly two types of failures: bond-wire lift-off and die-attach solder fatigue.

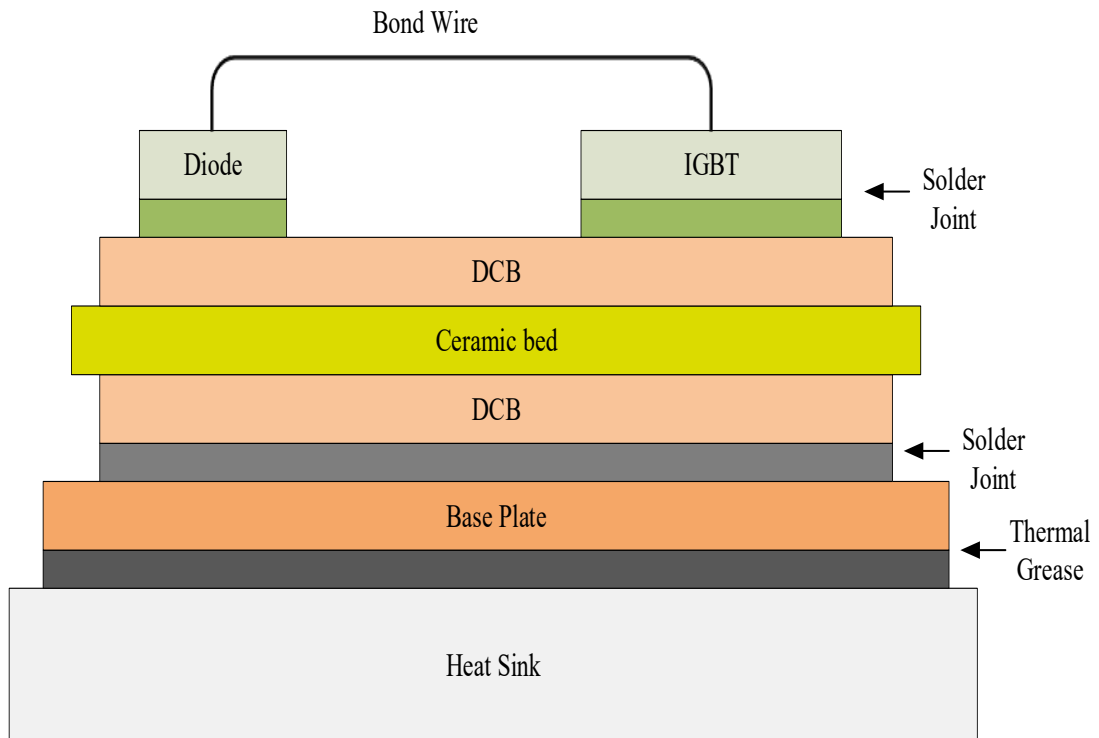


Fig. 1.12 IGBT Cross Section layout

The thermal cycling of IGBT majorly depends on the variations of switching and conduction losses. Due to the thermal cycling when they are in definite number die-attach solder and bond wire failure will occur. Hence the PV inverter fails that affects the reliability [26]–[30].

1.3.2. Need for Reliability Assessment

As India becomes the top PV marketer globally the scope for industries in PV systems increases. Over the past three years, its demand has raised exponentially. Almost many educational organizations, corporates, industries, and domestic households are utilizing grid connected PV systems due to government policies. Hence it is important to anticipate the performance of the PV systems. At the customer end, reliability performance is very important as the long-term utilization impacts the PV system. Generally, manufacturers specify 20 to 25 years of a lifetime for the PV panels and less than 15 years for the PV inverter. The grid connected Inverter costs about 59% of the total cost. Therefore, the reliability of the inverter plays a significant role in the performance assessment. To satisfy the customer needs and for the reliable operation of PV systems, the reliability-oriented performance analysis and improvement methodologies are needed.

1.4. Review of Literature

A detailed review of grid connected PV inverters, reliability analysis, factor affecting, improvement solutions are presented below.

1.4.1. Grid-Connected PV Inverters:

There are several PV inverter configurations are available today.

In [31] reviewed the different PV inverters configurations used for grid integration. The author has mainly classified it into there are four types they are:

1. AC- module inverter,
2. String Inverter,
3. Multi string Inverter.
4. Centralized Inverter,

Fig. 1.13 shows different configurations of PV inverters that are available in the market, i.e. AC-module inverter, string inverter, multi-string inverter, centralized inverter. From all these configurations, NPC, T-type, and H-bridge are used for both high power applications and residential applications for kW to LV range.

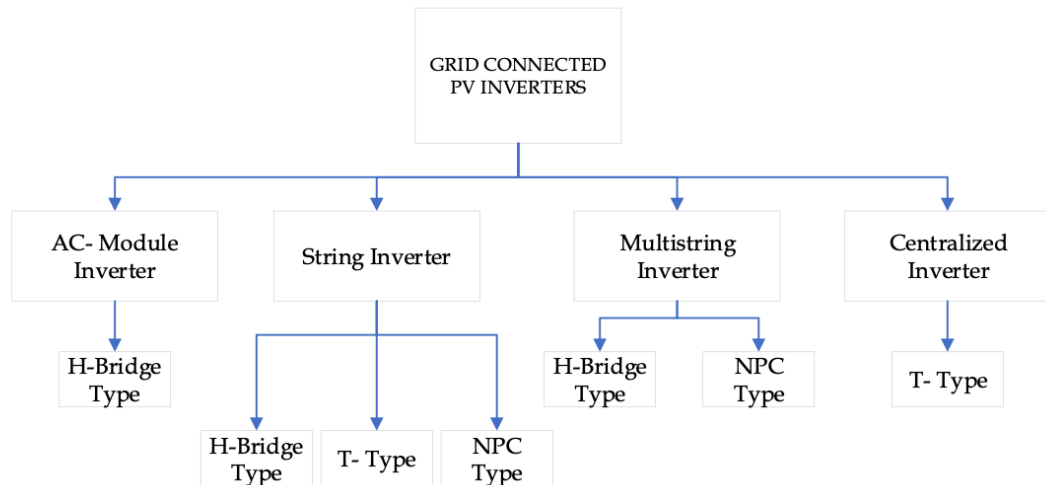


Fig. 1.13 Different configurations of Grid Connected PV Inverters

AC- module inverter is used for the small-scale applications, i.e. < 350 W range, string, and multi-string inverters are used for medium-scale applications, i.e. < 10 KW and < 500 KW respectively, Centralized inverter are used for the large-scale applications, i.e. < 850 KW range. The unit cost for the string inverters is high as it is apt only for low-power applications. The efficiency of the central inverter is higher i.e.,

about 98.6 %, but there are several disadvantages: it needs blocking diodes, Poor MPPT performance, only single MPPT, flexibility. Whereas in the case of Multi string inverter separate MPPT systems are there for each string. Related research is also carried out in [5], [32]–[35].

In [36] proposes “Three-phase cascaded H-bridge (CHB) converter and multiple string dc-dc converters” to compensate power imbalances between the cells. This can withstand the increase in capacity, also improve power quality. Different methodologies for cascaded Multilevel Inverters are carried out in [37]–[39].

In [40] proposes Asymmetric CMLI with Reduced leakage current methodology for the single-stage PV systems. The conventional two-stage configuration (DC/DC to DC/AC) lowers the efficiency and reliability of the PV system. To over these problems, In [41] proposes a Modular cascaded H-bridge multilevel photovoltaic (PV) inverter for single-phase/three-phase grid-connected applications. The CHB Inverter system has many advantages as it has high power conversion efficiency, feasibility for multiple sources, etc.

1.4.2. Reliability Analysis of Grid Connected PV Inverter:

Reliability analysis of PV inverter consists of several stages as shown in Fig. 1.14. A detailed review of each stage is presented here.

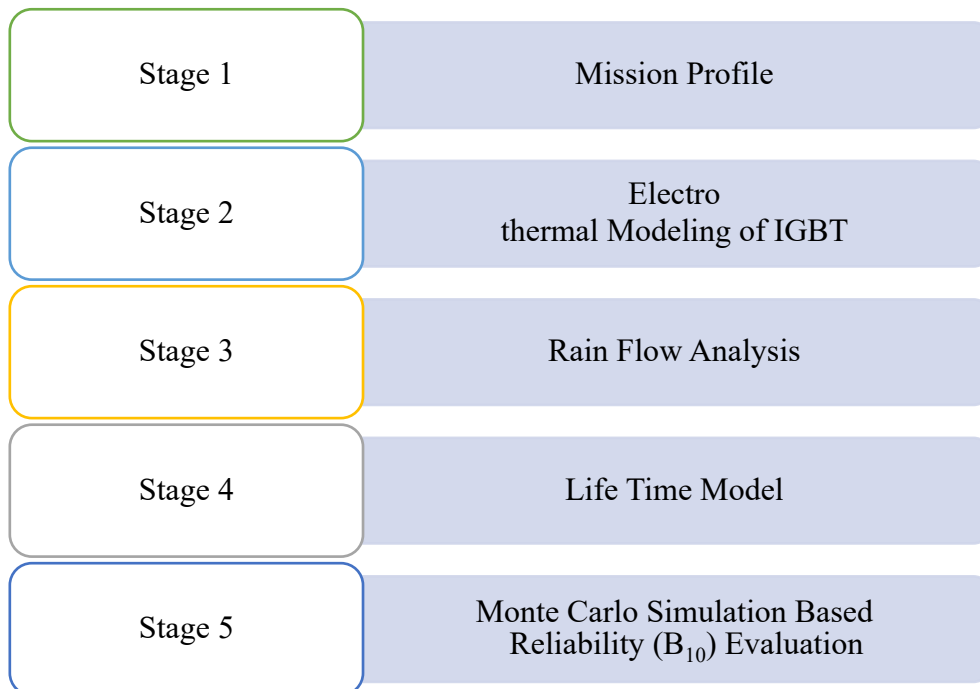


Fig. 1.14. Stages of Reliability Analysis

1.4.2.1. Mission Profile:

Mission profile oriented reliability analysis is becoming more popular for real-time assessment [42]–[45]. The Performance of the PV Systems is affected by environmental aspects such as Solar Irradiance and Ambient Temperature called as Mission Profile [46]. Hence for real-time reliability assessment one year Mission Profile data is logged at “Padmasri B V Raju Institute of Technology, Narsapur, Medak District, Telangana, India” and Alborg, Denmark.

1.4.2.2. Electro Thermal Modeling of IGBT:

The thermal cycling in IGBT generates heat and affects the components. Hence it is important to consider the temperature factor in reliability assessment. The device characteristics change with the temperature change. A thermal runaway will occur if the temperature exceeds the rated limit. Several cooling methods i.e. air, liquid, and heat sinks are designed in the power converters for thermal management. To anticipate the thermal profile of IGBT Electro Thermal Modelling is needed.

In [47] proposes the modeling of Foster and the Cauer Thermal models. The Foster model is also called a Partial-fraction circuit or Pi Model. It is the simplest model and it is commonly used by manufacturers. The Cauer model is also called a Continued-fraction circuit, T-model, or ladder network. It is less complex commonly used by researchers. Related research work is carried in [48]–[52].

Another commonly used thermal model is the finite element model. In [53] proposes FEM Model. FEM is time-consuming also it requires large computation time and memory. Thermal model using the finite element method also proposed by [54]–[56].

In [57] proposes modified Elmore thermal model, it requires individual layer dimensions, This model is more accurate and complex with the combination of FEM and two RC parallel circuits. Related works are also presented in [58].

In [59] proposes the FEM+ Multi exponential thermal model for IGBT. It is complex and Less time-consuming. It is the combination of FEM and RC parallel (usually 4) circuits. It is more accurate. Related models are also discussed in [60]–[62].

In [63] proposes Fourier thermal model. It is a thermal diffusion-based model which is complex and consumption time is high.

In [64] developed Hefner’s thermal model based on the finite difference method. The computation complexity analysis is complex for this model.

The comparison of the different thermal models is tabulated in the following Table. 1.3.

Table. 1.2. Comparison of Thermal Models

Author's	Thermal Method	Complexity in Calculation & Evaluation	Remarks
Schütze, T. et al. [47]	Foster Thermal Model	Simplest	Commonly used by manufacturers
Schütze, T. et al. [47]	Cauer Thermal Model	Less complex	Commonly used
R.B.B. Ovando et al. [53]	FEM Thermal Model	Less complex, but time consuming	Large computation time and memory
M. Ciappa et al. [57]	Modified Elmore Thermal Model	Complex, Less time consuming	Combines FEM and two RC parallel circuits
M. Musallam et al. [59]	FEM+ Multi exponential Thermal Model	Complex, Less time consuming	Combines FEM and RC parallel (usually 4) circuits.
T. Bryant et al. [63]	Fourier Thermal Model	Complex	Thermal diffusion based; computation time high
A. R. Hefner et al. [64]	Hefner's Thermal model	Complex	Finite difference method
Z. Hu et al. [65]	Adaptive Thermal Equivalent Circuit Model	Complex, Less Time Consuming	Practical Method

In [65] proposed an adaptive thermal equivalent circuit model for the IGBT to monitor the real-time health of the IGBT. This method is accurate for the calculation of the junction temperature of IGBT. In [66] proposed a simplified thermal model for

IGBT by considering Power loss profiles of MLI. In [67] proposed an improved cauer thermal model. Also, the studies [68]–[70] carried in the thermal modeling of IGBT.

From all the above thermal models foster thermal is the simplest model, mainly it is used by the manufacturers. Hence to realize the practical IGBT foster thermal model is selected. The loss profile is taken from the Manufacturer's data sheet. From this thermal model junction temperature corresponding to the yearly mission profile is calculated.

1.4.2.3. Rain Flow Analysis:

Rain Flow is a cycle counting analysis to analyze the fatigue data. This algorithm was first proposed by “Matsuishi and Endo” in 1968. In the reliability analysis rain flow counting algorithm is used to analyze the junction temperature variations and to extract the Number of Cycles n_i , Cycle Period t_{on} , Mean Junction Temperature T_{jm} , Cycle Amplitude ΔT_j [71].

1.4.2.4. Life Time model:

There are several lifetime models are used for power semiconductors. These are mainly categorized into two types.

- Physical models
- Analytical models.

Based on the thermo-mechanical aspects life time models are designed considering the failure mechanisms and temperature profiles. A physical model based on the knowledge of stress/strain deformation and failure mechanisms and to be known priory. By conducting the simulations and experiments, stress/strain deformation and failure mechanisms can be known.

Analytical models depend on the Number of cycles to failure (N_f). In [72] Proposed the Coffin-Manson, Coffin Manson Arrhenius models. These models are widely used. In this model, the number of cycles to failure depends on junction temperature (ΔT_j) and mean temperature (T_m). Even though this model is simple it is not accurate because it doesn't consider other parameters such as cooling, heating times and cycle frequencies.

In [73] proposed Norris Landzberg model. This model considers cycle frequency including junction temperature (ΔT_j) and mean temperature (T_m). This model

doesn't consider cooling and heating times. In [74] proposed Bayerer's Model. This Model is also called a multi-parameter model, large power cycling data is considered. Therefore, Bayerer's Model is the accurate model in the Analytical Models. Comparison of Analytical models is tabulated in Table. 1.4.

Table. 1.3. Comparison of Life Time Models

Author's Name	Analytical Model	Number of cycles to failure (N_f)	Parameters
S. S. Manson et al. [72]	Coffin-Manson	$N_f = a(\Delta T_j)^{-n}$	Junction Temperature (ΔT_j)
S. S. Manson et al. [72]	Coffin Manson Arrhenius	$N_f = a(\Delta T_j)^{-n} \cdot e^{\frac{E_a}{k \cdot T_m}}$	Junction Temperature (ΔT_j), Mean temperature (T_m)
K. C. Norris et al. [73]	Norris Landzberg model	$N_f = a \cdot f^{-n_2} (\Delta T_j)^{n_1} \cdot e^{\frac{E_a}{k \cdot T_{max}}}$	Junction Temperature (ΔT_j), Mean temperature (T_m), Frequency (f)
R. Bayerer et al. [74]	Bayerer's Model	$N_f = A(\Delta T_j)^{\beta_1} \cdot e^{\frac{\beta_2}{(T_j + 273K)}} \cdot t_{on}^{\beta_3} \cdot I^{\beta_4} \cdot V^{\beta_5} \cdot D^{\beta_6}$	Heating time(t_{on}), Applied DC current(I), Diameter of the bond wire (D), blocking voltage(V)

In [75] proposed Gaussian process for the life estimation of discrete IGBT. This lifetime estimation is characterized based on-state collector-emitter voltage drop. In [76] presented cost and life cycle analysis for PV inverter. Studies on life time estimation are carried in [77]–[81]. In this work, Bayerer’s model is used.

1.4.2.5. Monte Carlo Simulation Based Reliability (B_{10}) Evaluation

Monte Carlo Simulation is first introduced by D. B. Hertz in 1964 for finance problems. It is used to generate ‘n’ samples with uncertainties. In the reliability analysis of PV inverter researchers use this simulation to generate the lifetime samples with uncertainties [82], [83]. In this work samples are generated using normal probability distribution as per Eq. a.2. Lifetime is calculated for all the generated samples and fitted in a Weibull distribution. Finally, B_{10} lifetime is calculated.

1.4.3. Factors affects the Reliability of PV Inverter:

The reliability of PV inverters depends on several factors. Factors that impact the reliability performance of PV inverters are shown in Fig. 1.15.

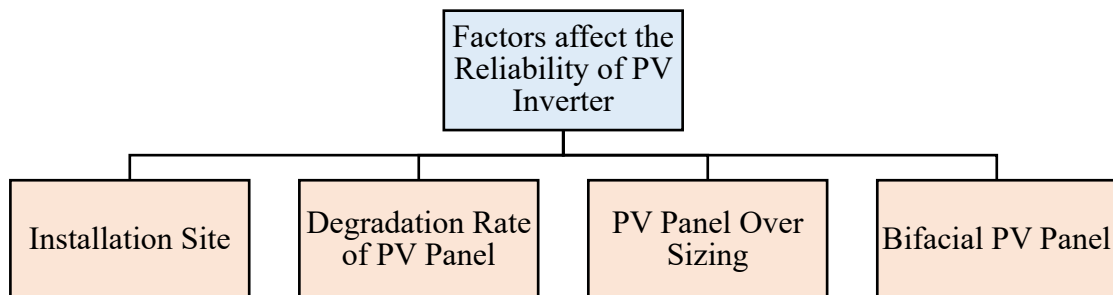


Fig. 1.15. Factors affects the Reliability of PV Inverter

1.4.3.1. Installation Site:

Environmental conditions vary from location to location. Regions near the equator receive relatively high average solar irradiance and average ambient temperature all over the year. Similarly, regions far from the equator receive relatively low average solar irradiance and average ambient temperature all over the year. Nevertheless, the performance of PV inverters is affected by environmental conditions. Comparative reliability analysis of PV inverter between installation sites of Denmark (Relatively Cold) and Arizona (Relatively Hot) is presented in [84]. Installation site with relatively cold location exhibits higher reliability than relatively hot location.

1.4.3.2. Degradation Rate of PV Panel:

Degradation rate impacts the long-term operation of PV panels, leading to a decrease in power output. A report “All India Survey of PV Module Degradation: 2013” by NCPRE, IIT Bombay [85], presented the degradation study at different locations of India. The impact of the degradation rate of PV panels on inverter reliability is presented in [86]. It reduces the thermal loading on the inverter hence an increase in reliability reported.

1.4.3.3. PV Panel Oversizing:

To reduce the cost of PV energy, panel oversizing is the common approach for more energy yield in low irradiance locations. This increases the inverter loading and negative impact on reliability performance. Impact of PV panel oversizing on inverter lifetime and reliability presented in [87].

1.4.3.4. Bifacial PV Panel:

Recent advancements in PV panel technology concern to energy yield is the Bifacial PV panel. As the name implies it, can harvest energy from both sides i.e., front and rear sides of the panel as shown in Fig. 1.16, this leads to increased energy yield. Hence this technology attracted the PV industries in recent years.

Bifacial PV manufacturers Trina solar, LONGi, LG, etc., claims up to 30% of more energy yield. About twenty countries already installed the bifacial PV panels by the end of August 2019. The total installed bifacial PV panel capacity is 8.53 GW, and it is forecasted about 21 GW to be installed by 2024. The global annual bifacial installed capacity is shown in Fig. 1.17 [88].

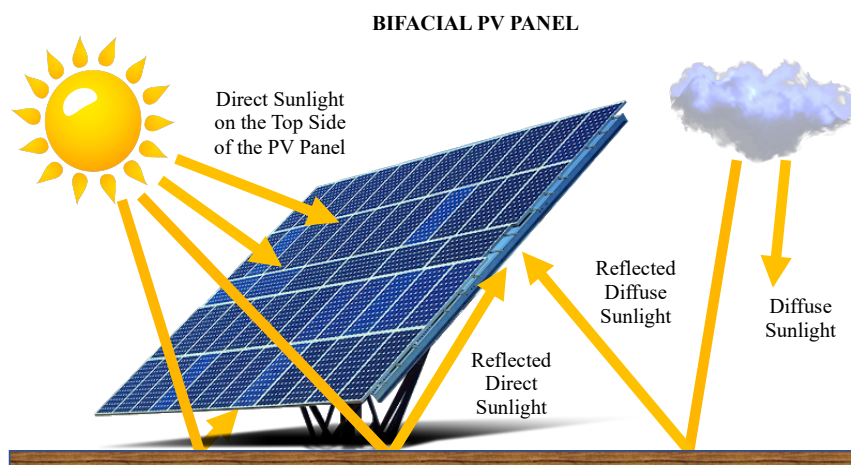


Fig. 1.16. Bifacial PV Panel

Fig. 1.18 shows the top five countries with the bifacial installed capacity. China leads with 6282 MW followed by USA, Brazil, Egypt, and Australia. About 100 MW is installed in Taiwan, Mexico, Oman and 10–35 MW have been built in European countries.

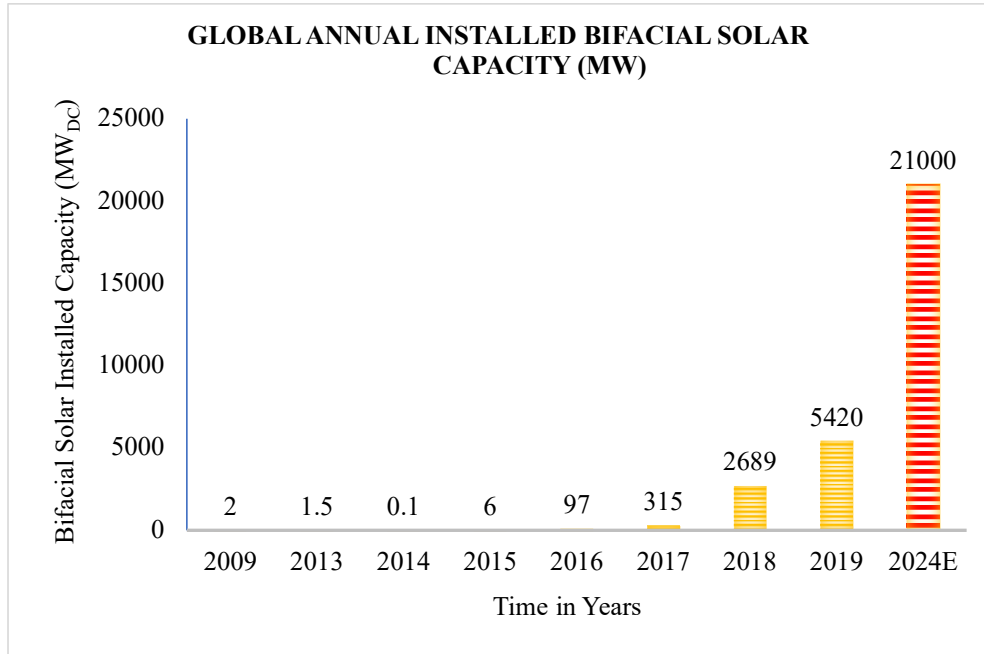


Fig. 1.17. Global annual installed bifacial solar capacity

A survey on the potential of Bifacial PV Panel in global perspective is presented in [89]. Metrological study with single light source characterization is presented in [90]. A model to estimate the rear solar irradiance is presented in [91].

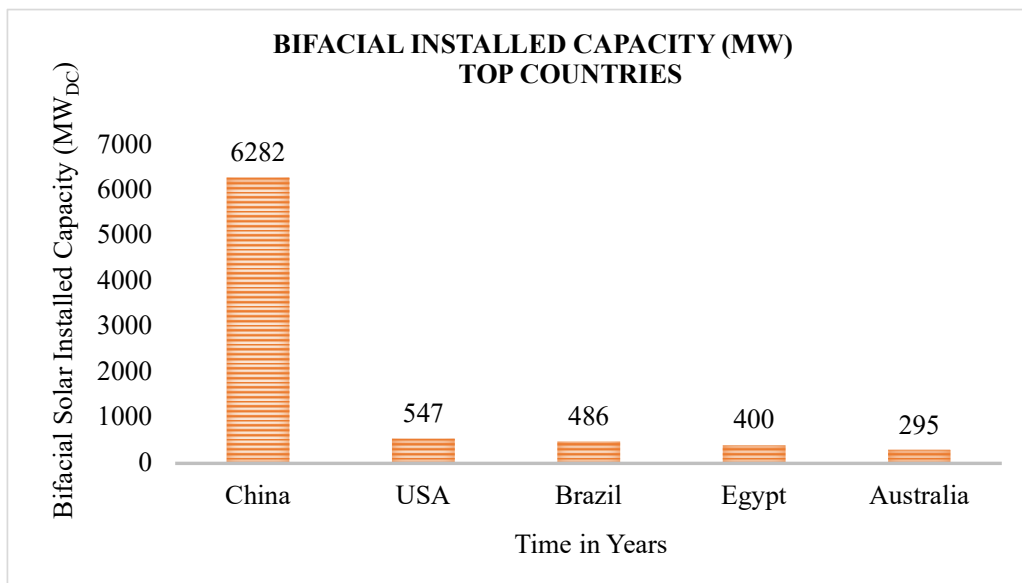


Fig. 1.18. Top five countries with the highest bifacial solar installed capacity

The performance analysis of Bifacial PV panel considering horizontal and inclined sun trackers in several locations of china is compared with monofacial PV Panel [92]. Also, comparative analysis of floating type panels is performed [93] and an experimental model for both panels is implemented [94]. Comparative study between vertical bifacial and tilted monofacial system for agrivoltaics application is presented in [95]. Bifacial PV system is presented in [96] to overcome the issues caused by duck curves in monofacial PV system.

Meanwhile, PV manufacturers focused on improving the design for highly reliable power electronics conversion systems [5]. Bifacial PV panel inevitably affects the loading performance of PV inverter, as it operates nearly the rated power for a longer duration. This leads to an increase in thermal stress on power electronic components.

1.4.4. Reliability Improvement of PV Inverters:

Today's PV energy conversion systems (i.e., Inverter) requires power electronics device with low failure rates, to provides the high reliability. Conventional Si-based power electronics switches reached their theoretical limits and are not capable to address current power needs. Significant advancements are made in Si IGBTs but in the case of Si diodes, these advancements are not up to the mark, also restrict the performance of power electronic converters [97]. In [98], SiC-based power electronic switches are provided with a wide band gap that performs superior compared to conventional Si-based devices. The notable advantages of SiC-based devices are low switching losses, high switching speed and blocking voltage, etc., hence the performance of the system will be improved. Nevertheless, the cost of SiC devices is a major concern. Hence, it is not economical to replace all the devices in the PV inverter with SiC devices. To overcome this issue hybrid application of Si/SiC-based devices has been proposed in many studies [99]–[104].

An active gate-controlled technique is designed in [100] to improve the efficiency of the hybrid-Si/SiC-based inverter. The design of a hybrid module with Si IGBT and SiC MOSFET is discussed in [101]. In [102], the application of a hybrid module i.e. Si/SBD for the Current source ZCSI based DC-DC converter has been presented. In [105], a model presented with a T_j controller to reduce the converter losses. In [106], the author proposed a design of a hybrid three-level NPC inverter. It's consists of four Si-IGBTs and two SiC MOSFETs for reliability improvement, also this paper addressed the cost limit constraints of SiC based devices. Application of hybrid

Si/SiC power module in half-bridge traction inverter is presented in [107]. A comparative study between Si and SiC based devices for ANPC inverters is presented in [108]. Performance comparison studies of the DC-DC converter in electric vehicles are presented in [103] considering hybrid Si/SiC power modules. In [109] author presented optimal gate control for T_j balance and power loss minimization considering hybrid Si/SiC power modules. Related work also presented in [104], [110]–[113], [114] still there is the gap in reliability analysis of hybrid Si/SiC power modules to design high reliable inverter.

1.5. Research Gaps and Objectives:

From the state of the art literature, the following are research gaps identified.

- Reliability analysis of PV inverter needs to be assessed under variable mission profile conditions and uncertainties.
- Junction Temperature estimation for yearly mission profile.
- Validation is required of estimated junction temperature.
- The factor that impacts the reliability of PV inverter needs to be assessed.
- Reliability improvement solution for PV inverter.

From the above motivation, the main objective of this research proposal is to assess and improve the Reliability of grid connected PV Inverters. In this regard, the objectives of this research are as follows

1. Real Time Mission Profile data of one year to be logged and Pre-Processed for Reliability Assessment of Grid Connected PV Inverter at Indian Locations. Along with this Mission profile data at Denmark Location is considered for comparison.
2. Development of Electro-Thermal Model of IGBT in PV Inverter for the calculation of Junction Temperature for One-year Mission profile at both India and Denmark locations.
3. Validation for the Calculated Junction Temperature by finding correlation between the calculated junction temperature with the case temperature.
4. Identifying the factors such as Panel Degradation rate, PV Panel Over Sizing that effects the Reliability performance of the Grid Connected PV Inverters.

5. Improvement solutions to ensure the Reliability performance of the Grid Connected PV Inverter

1.6. Proposed Methodology:

The reliability analysis of grid connected PV inverter and improvement solutions are proposed in this work. Real time yearly mission profile data (Solar Irradiance and Ambient Temperature) is considered. Solar irradiance is measured using Pyranometer and Ambient temperature is measured using an RTD device. The measured parameters are logged with the help of CR3000 data logger at “Padmasri B V Raju Institute of Technology, Narsapur, Medak, Telangana, India”. In addition to this mission profile data at Denmark location is considered where Denmark has cold weather conditions and India has Hot weather conditions. A test case of a single-phase 3-kW grid connected PV inverter is considered and simulated in the PLECS platform. Full bridge configuration is adopted, It consists of four 600V, 30A IGW30N60H3 IGBT's. The thermal profile of the IGW30N60H3 IGBT's is taken from the Infineon manufacturer data sheet for a realistic approach. Foster Electro Thermal Model is implemented to estimate junction temperature. Since junction temperature calculation is indirect method validation is needed. The validation is made by correlating the junction temperature of the PV inverter with the case temperature, solar irradiance and ambient temperature. Along with the Mission Profile, the case temperature of the PV inverter is logged. Positive correlation gives the validation of Junction Temperature.

The variations of the estimated junction temperature follow irregular profiles as per the mission profile. Hence a cycle counting algorithm is needed to anticipate the variations. Rainflow counting algorithm is used to analyze the variations. From the rainflow algorithm No. of Cycles n_i , Mean Junction Temperature T_{jm} , Cycle Amplitude ΔT is calculated. Lifetime is evaluated using the miner's rule. In the obtained lifetime, all the parameters are constant i.e., all the devices should fail at the same rate but practically this is not feasible, so to overcome this the variation of 5 % is considered and 10000 samples are generated using Monte Carlo simulation. All the generated samples are fitted in two parameter Weibull distribution and reliability function at both component level and system level is obtained. From the reliability function, B_{10} lifetime is calculated.

The next part of this proposal is to analyze the factors that affect the reliability performance of PV Inverter. In this work factors such as Installation site, Degradation

rate of PV panel, PV Panel Over Sizing, Bifacial PV Panels are considered to analyze the impact. Finally, Improvement solutions to ensure the Reliability performance of the Grid Connected PV Inverter. A hybrid Si/SiC switch is proposed for reliability improvement of PV inverter. The hybrid Switch consists of Si-IGBT (IGW30N60H3) and SiC- diode (C3D20060D) and its effectiveness are analyzed by comparing it with conventional Si-IGBT. The proposed methodology block diagram is presented in Fig. 1.19.

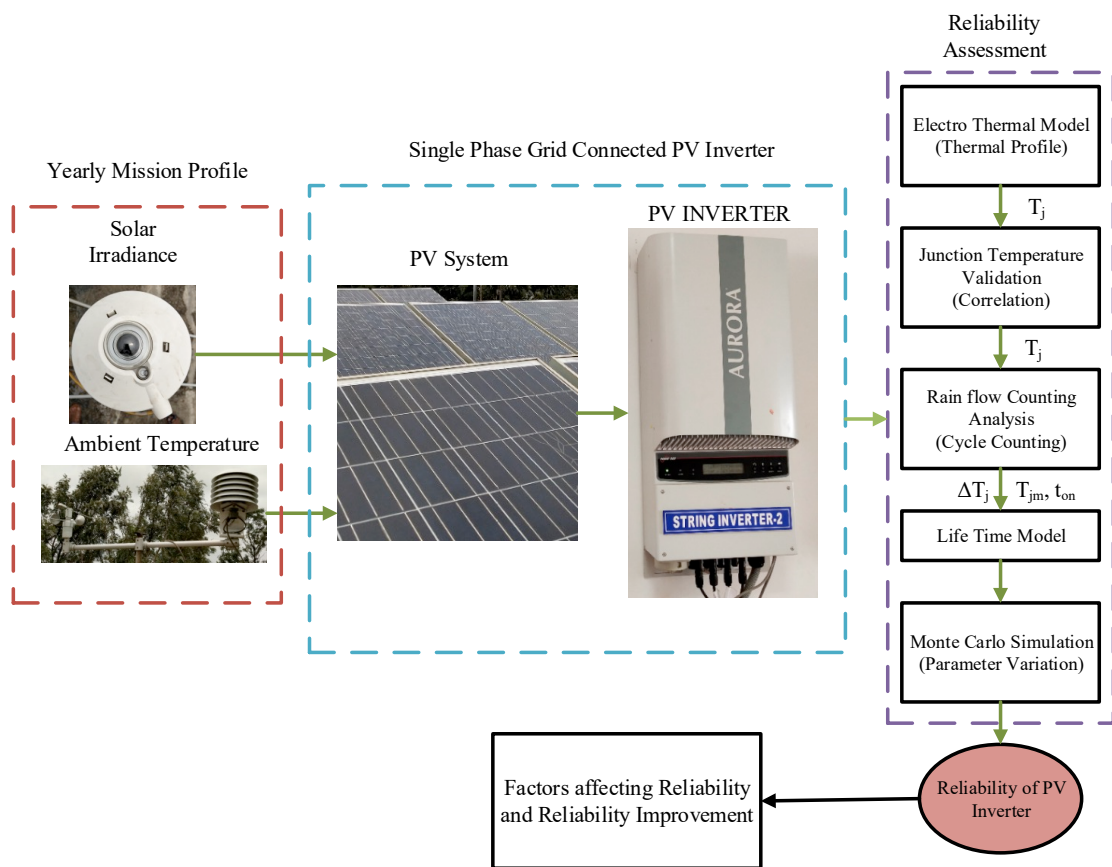


Fig. 1.19. Proposed Methodology Block Diagram

1.11. Organization of the thesis:

The rest of the thesis is organized as follows

Chapter 2: In this chapter, Logging and Pre-Processing of Real Time Mission Profile data i.e., Solar Irradiance and Ambient Temperature of one year at both India and Denmark Locations are presented. Month wise mission profile heat map tables are presented.

Chapter 3: This chapter deals with Electro-Thermal Model of IGBT to estimate the Junction Temperature for One-year Mission profile at both India and Denmark locations.

Chapter 4: This chapter deals with Validation for the Calculated Junction Temperature by finding the correlation between the calculated junction temperature with the case temperature, solar irradiance, and ambient temperature.

Chapter 5: This chapter deals with Identifying the factors such as Panel Degradation rate, PV Panel Over Sizing that affect the Reliability performance of the Grid Connected PV Inverters.

Chapter 6: This chapter deals with Improvement solutions to ensure the Reliability performance of the Grid Connected PV Inverter.

Chapter 7: This chapter deals with the conclusion and future scope.

CHAPTER 2

MISSION PROFILE DATA LOGGING

2.1. Mission Profile:

In real time conditions, the PV inverter is exposed to thermal variations that are influenced by non-uniform mission profile. This impacts the reliability performance of PV inverters. Hence to account for these factors, mission profile data of the real field is considered [45]. In this work solar irradiance and ambient temperature are considered as mission profile and logged for one year with one minute sample is at India and Denmark Locations.

2.2. Mission Profile at India Location:

Mission profile data at India location is collected from INDNOR solar station, installed at “B V Raju Institute of Technology, Narsapur, Medak, Telangana”, India, where Latitude is 17.7394° N and Longitude is 78.2846° E. CMP11 Pyranometer is used to measure solar irradiance as shown in Fig. 2.1, RTD device is used to measure ambient temperature as shown in Fig. 2.2, CR3000 data logger is used to log mission profile as shown in Fig. 2.3. RS485 cable is used as a communication cable and interfaced to CPU via RS232 cable.



Fig. 2.1 CMP11 Pyranometer



Fig. 2.2 RTD Device



Fig. 2.3 CR3000 Data Logger

The schematic of experimentation is presented in Fig. 2.4. The CR3000 data logger logs solar irradiance in W/m^2 and ambient temperature in $^{\circ}\text{C}$.

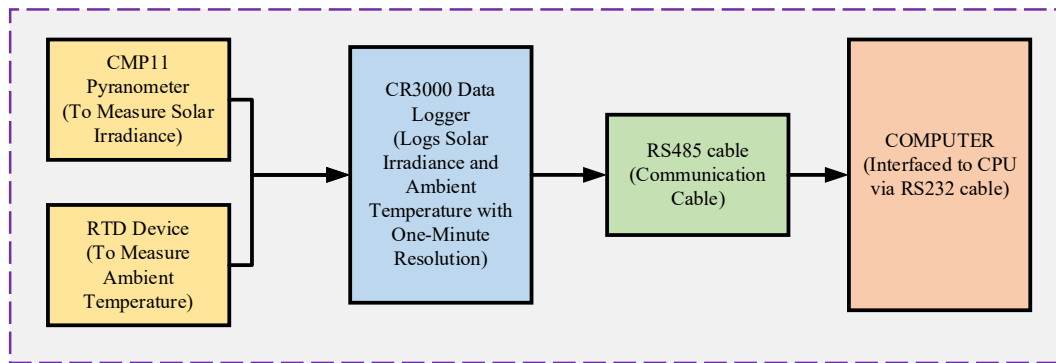


Fig. 2.4 Schematic of experimentation

One-year mission profile data from 01-September-2018 to 31-August-2019 is logged and shown in the following Fig: 2.5.

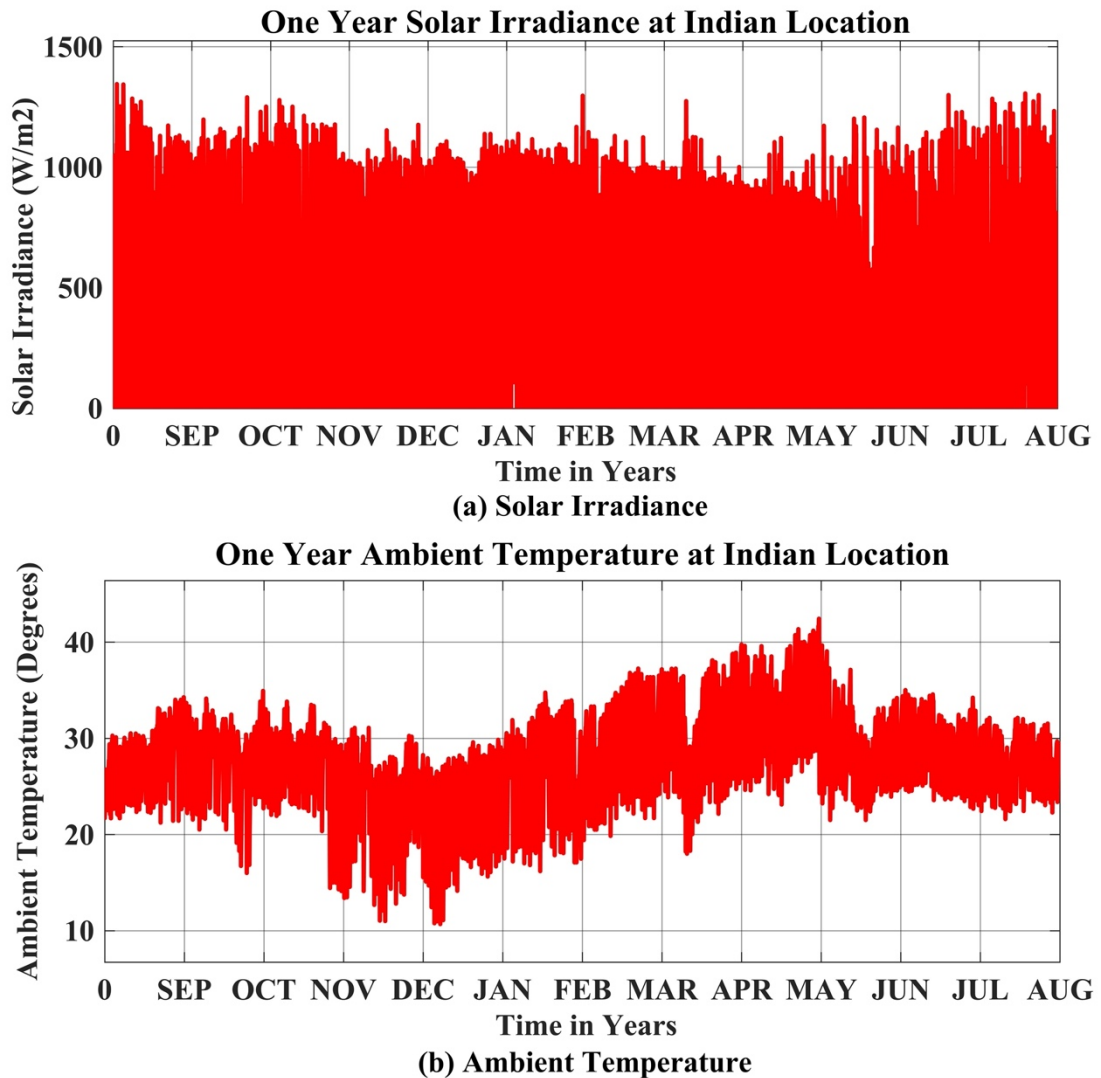


Fig. 2.5. One Year Mission Profile Data at India Location

The maximum ambient temperature in India is recorded from March to June similarly low ambient temperature in India is recorded from November to February. Solar irradiance and ambient temperature are continuously varying all over the year.

2.3. Mission Profile at Denmark Location:

The real time mission profile data i.e. solar irradiance and ambient temperature logs for one-year form [115] at Denmark from 01-September-2018 to 31-August-2019 as shown in Fig. 2.6 where Latitude is 57.0488° N and Longitude is 9.9217° E.

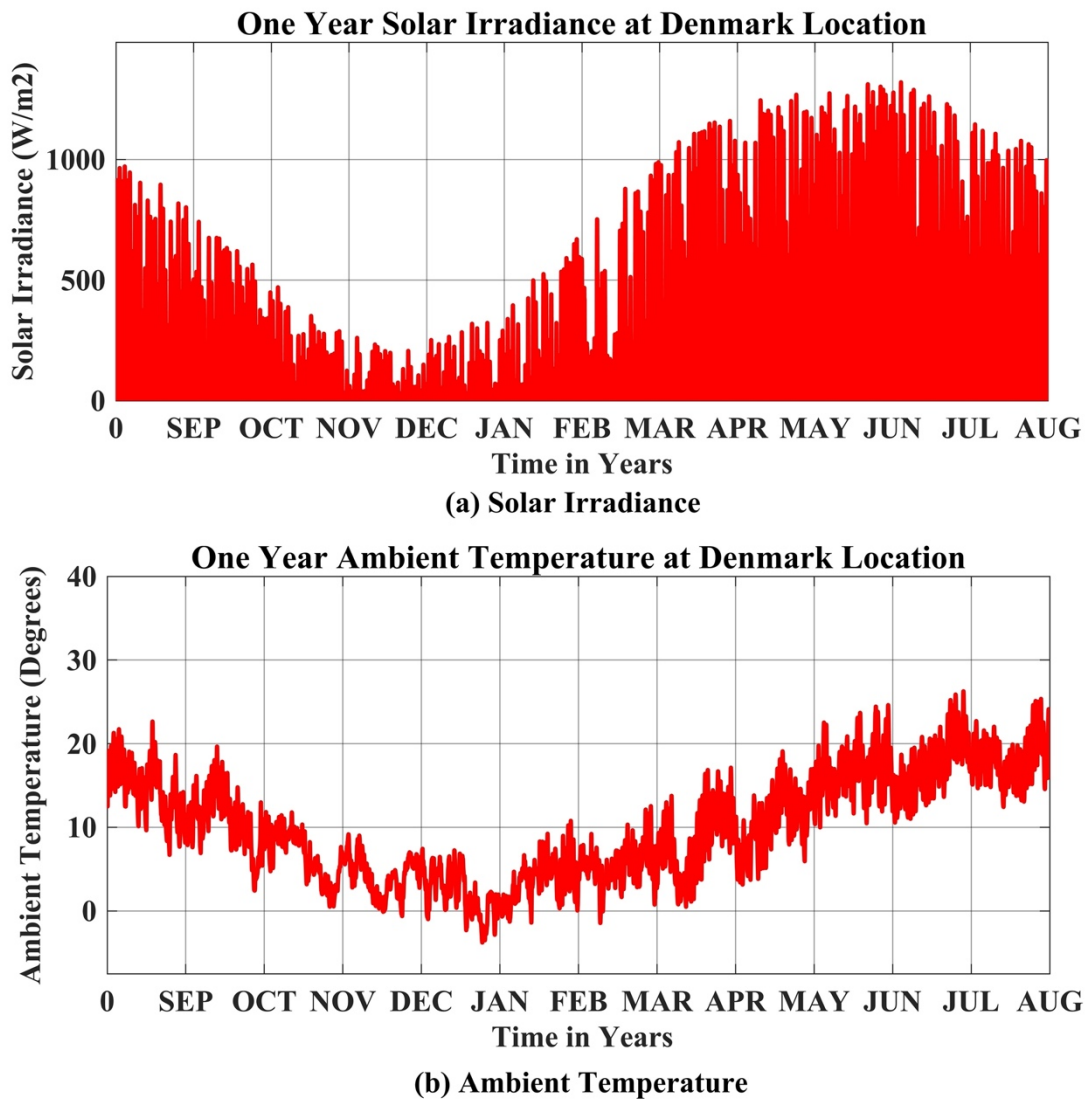


Fig. 2.6 One Year Mission Profile Data at Denmark Location

The maximum ambient temperature in Denmark is recorded from May to August similarly low ambient temperature in Denmark is recorded from November to

February. Solar irradiance and ambient temperature are continuously varying all over the year.

2.4. Mission Profile Comparison:

For the mission profile comparison, a month-wise heatmap table of solar irradiance (Wh/m²) and ambient temperature (°C) at both India and Denmark locations from September – 2018 to August - 2019 are tabulated in Table. 2.1 and Table. 2.2 respectively.

Table. 2.1 Heatmap Table of Solar Irradiance.

Country/ Month	Solar Irradiance (Wh/m ²)	
	India	Denmark
SEP	165053	100054
OCT	186766.1	61622.69
NOV	164028.1	24233.29
DEC	144757.6	10711.25
JAN	165846.2	16247.97
FEB	172830.1	36188.28
MAR	215120.5	71213.96
APR	213292.3	149069.7
MAY	215131.3	176171.3
JUN	145693.6	198472.5
JUL	148344.1	191219.2
AUG	146975.4	152064.2

Red = High, Yellow = Medium, Green = Low

From the Table. 2.1, at India location solar irradiance maximum is recorded in March, April, May and in the remaining months, moderate values are recorded.

At Denmark location solar irradiance maximum is recorded in June, August and minimum are recorded in September, October, November, December, January, February, March.

Table. 2.2 Heatmap Table of Ambient Temperature

Country/ Month	Ambient Temperature (°C)	
	India	Denmark
SEP	25.81	14.79
OCT	25.44	10.78
NOV	24.51	6.43
DEC	21.75	4.17
JAN	21.14	1.95
FEB	25.08	3.66
MAR	29.84	5.32
APR	32.71	7.95
MAY	34.68	10.5
JUN	30.51	16.77
JUL	27.14	17.34
AUG	25.76	18.03

Red = High, Yellow = Medium, Green = Low

From the Table. 2.2, at India location ambient temperature maximum is recorded in March, April, May and in the remaining months, moderate values are recorded.

At Denmark location ambient temperature maximum is recorded in June, August and minimum are recorded in September, October, November, December, January, February, March.

The heatmap Table. 2.1 and 2.2 showcase that solar irradiance and ambient temperature vary from time to time and location to location, thereby the reliability performance of PV inverter also varies.

2.5. Chapter Summary:

In this chapter mission profile is logged for one year with one minute resolution at India and Denmark locations. Using heat map tables month wise solar irradiance and ambient temperature are presented.

CHAPTER 3

ELECTRO THERMAL MODELING OF IGBT

3.1. Electro Thermal Modelling of IGBT:

The variations of temperature (thermal cycling) at the junction layers of IGBT lead to the failure of the device. Environmental conditions are not constant; hence mission profile always varies with respect to time, which leads to the temperature variations in the IGBT. In contrast, to assess the reliability of IGBT, the temperature at the junction layers needs to be estimated [43]. As the junction temperature cannot be estimated directly, an electro thermal model of IGBT is required for estimation. The detailed literature review is presented in Chapter. 1. In this work foster electro thermal model is implemented on a test case of a 3-kW grid connected PV inverter.

3.2. Test Case:

A test case of single phase 3-kW grid connected PV inverter is considered and simulated in PLECS platform as shown in Fig. 3.1. Full bridge configuration is adopted, It consists of four 600V, 30A IGW30N60H3 IGBT's. The thermal profile of the IGW30N60H3 IGBT's is taken from the Infineon manufacturer data sheet [116]. The test case parameters are tabulated in Table. 3.1.

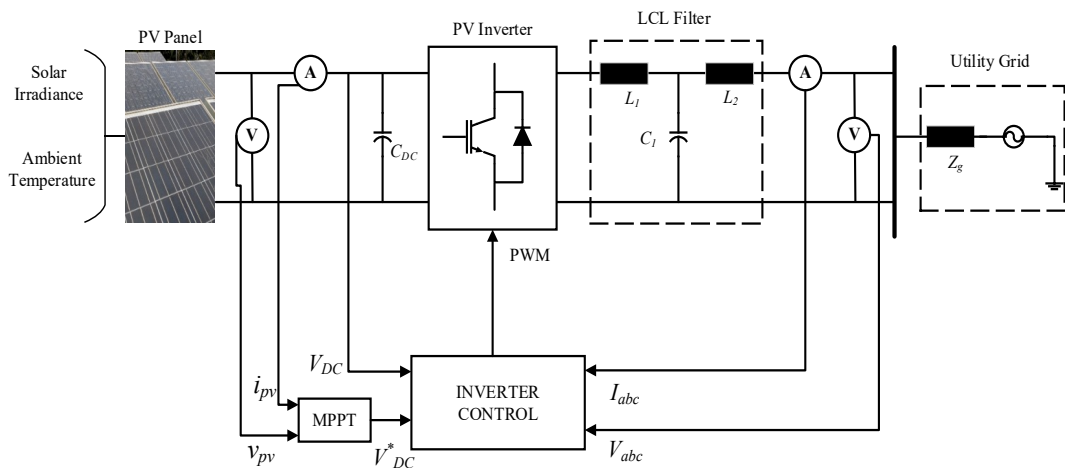


Fig. 3.1. Single phase 3-kW grid connected PV inverter

Table. 3.1. 3-kW grid connected PV inverter parameters

Name		Specification
PV panel model		BP365
PV inverter rated power		3-kW
Grid voltage		230 V
Grid frequency		50 Hz
Dc link capacitance		1.5e-3 F
IGBT make		Infineon
IGBT model		IGW30N60H3
IGBT Voltage rating		600 V
IGBT Current rating		30 A
IGBT min T_j		25 ⁰ C
IGBT max T_j		175 ⁰ C
LCL Filter	L ₁	2e-3 H
	L ₂	3e-3 H
	C ₁	4.7e-6 F

In the grid connected PV system, BP365 65 W PV module is considered [117]. It comprises two parallel strings, each string consists of 22 modules and it provides 380 V V_{DC} to the inverter. The inverter is connected to 230 V_{rms}, 50 Hz single phase grid via LCL filter.

The control methodology comprises MPPT controller, voltage controller, and current controller. The MPPT controller ensures the maximum power from the PV panel to do this incremental conduction algorithm is implemented. The voltage controller regulates the PV voltage to do this type 2 controller is implemented. The current controller controls the modulation index for injecting the required current into the grid to do this PR controller with 50 Hz resonant frequency is implemented. Finally, a unipolar modulation scheme with a 25 kHz switching frequency is deployed.

3.3 IGBT Thermal Flow:

The heat dissipated at the junction layers of IGBT flows to the case or base plate (T_c). From case (T_c) to heat sink (T_h) and then from heat sink (T_h) to ambient (T_a). The thermal flow in IGBT is shown in Fig. 3.2.

Thermal Flow of IGBT

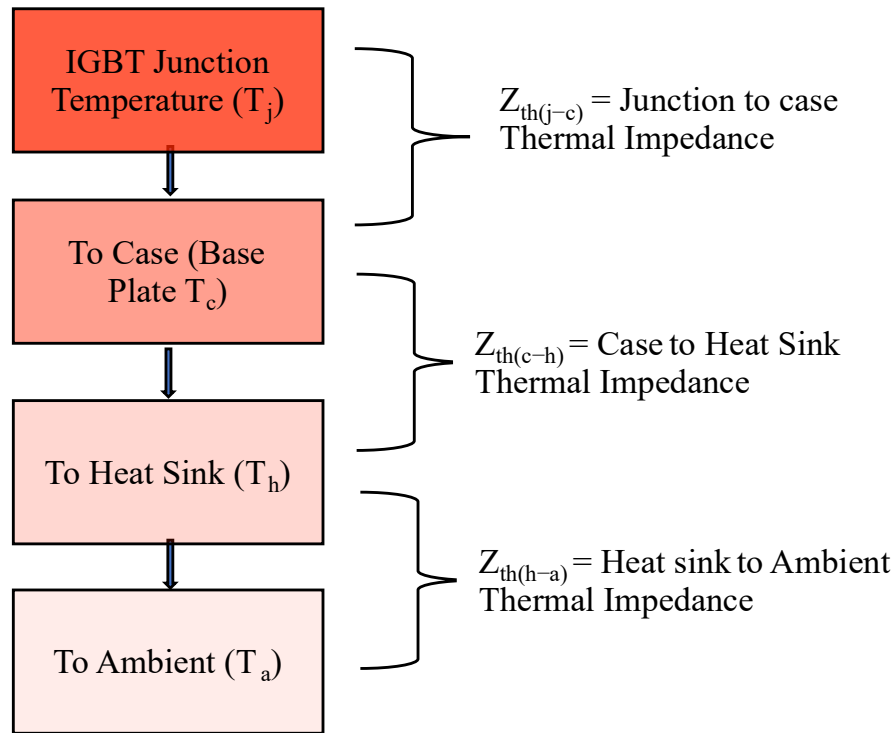


Fig. 3.2. Thermal Flow of IGBT

To estimate the junction temperature the following are required.

- Total power losses (P_T) of IGBT.
- Thermal impedances (Z_{th}) of IGBT.
- Ambient temperature (T_a).

The total power losses can be obtained from the manufacturer's data sheet. Thermal impedances such as junction to case thermal impedance $Z_{th(j-c)}$, case to heat sink thermal impedance $Z_{th(c-h)}$ and heat sink to ambient thermal impedance $Z_{th(h-a)}$ can be calculated using the foster electro thermal model. Ambient temperature can be obtained from mission profile data.

3.4. Instantaneous Junction Temperature

The Mathematical expression for T_j at any instant is shown in Eq. 3.1.

$$T_j = Z_{th(j-c)} * P_T + T_C \quad 3.1$$

where

- $Z_{th(j-c)}$ = Thermal Impedance of Junction to case
- P_T = Total Power Loss
- T_c = Case Temperature

The Mathematical expression for Case Temperature (T_c) is shown in Eq. 3.2.

$$T_C = T_a + (Z_{th(c-h)} + Z_{th(h-a)}) * P_T \quad 3.2$$

Where

- T_a = Ambient Temperature
- $Z_{th(c-h)}$ = Thermal Impedance of Case to Heat Sink.
- $Z_{th(h-a)}$ = Thermal Impedance of Heat sink to Ambient.

The power loss in the IGBT is due to heat dissipation. Majorly there are two types of power losses they are

- Conduction Losses (P_c)
- Switching Losses (P_s)

The total loss of IGBT is calculated using Eq. 3.3.

$$P_T = P_S + P_C \quad 3.3$$

The Switching loss is calculated using Eq. 3.4.

$$P_S = (E_{on} + E_{off}) \times f \quad 3.4$$

where

- f = Fundamental switching frequency,
- E_{on} = Turn-on loss
- E_{off} = Turn-off loss.

Fig. 3.3 shows Turn on losses, Fig. 3.4 shows Turn off losses where the Maximum Junction temperature (T_j) is 175° and Minimum Junction temperature (T_j) is 25°

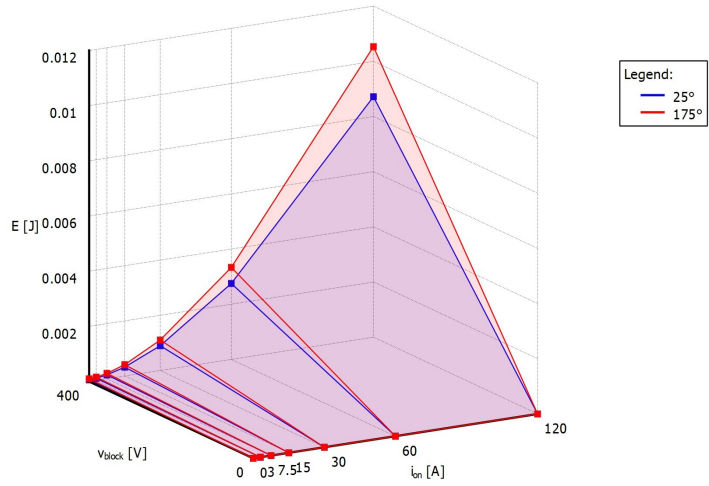


Fig. 3.3. IGBT Turn on Losses

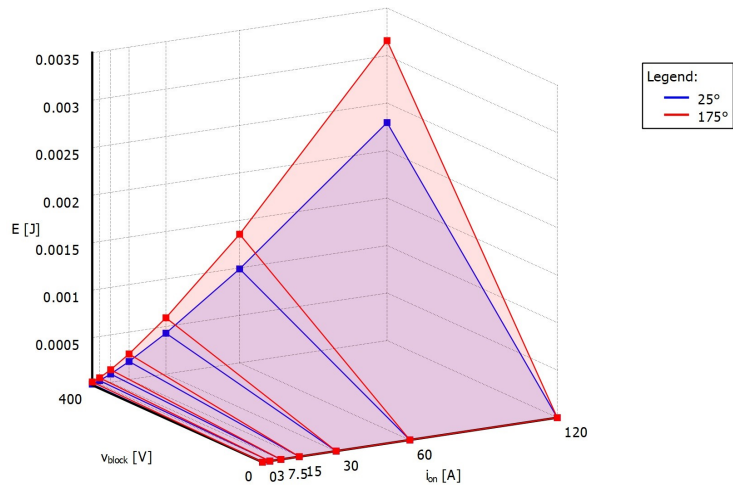


Fig. 3.4. IGBT Turn off Losses

The conduction losses of the IGW30N60H3 IGBT show in Fig. 3.5.

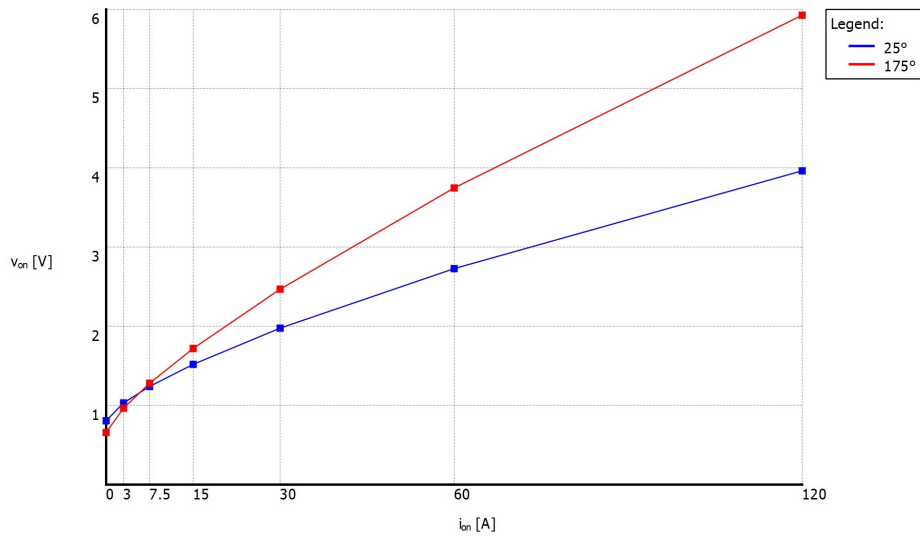


Fig. 3.5. IGBT Conduction Losses

3.5. Foster Electro Thermal Modelling of IGBT:

The Foster model is considered for the electro thermal modeling of IGBT. The thermal equivalent parameters can be acquired from the device manufacturer datasheet. It is implemented on a test case of a 3-kW PV inverter as shown in Fig. 3.6.

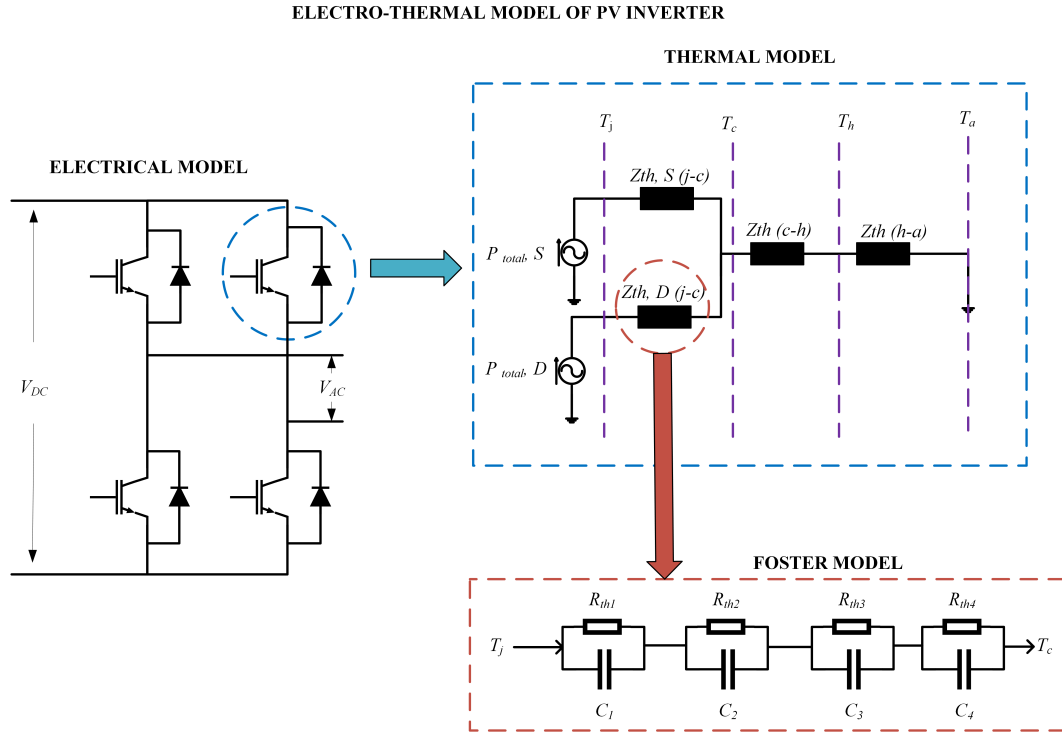


Fig. 3.6. Foster Electro Thermal Model of PV Inverter

The parameters of Foster Electro Thermal Model are presented in Fig. 3.7.

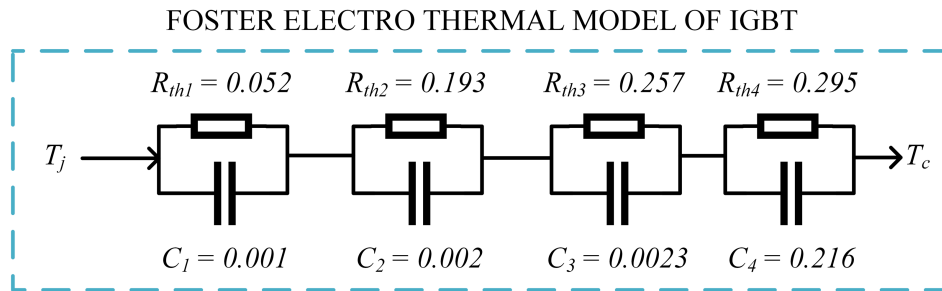


Fig. 3.7. Parameter of Foster Electro Thermal Model

Foster thermal model parameters represent the thermal impedance that directly influences the junction temperature as given in Eq. 3.1. Thermal impedances such as junction to case thermal impedance $Z_{th(j-c)}$, case to heat sink thermal impedance $Z_{th(c-h)}$, and heat sink to ambient thermal impedance $Z_{th(h-a)}$ are obtained using this model.

3.6. Junction Temperature Calculated from Yearly Mission Profile

The junction temperature of 600V/30A IGBT is calculated using foster electro thermal model corresponding to the yearly mission profile. Junction Temperature at India and Denmark locations are shown in Fig. 3.8 and Fig. 3.9 respectively.

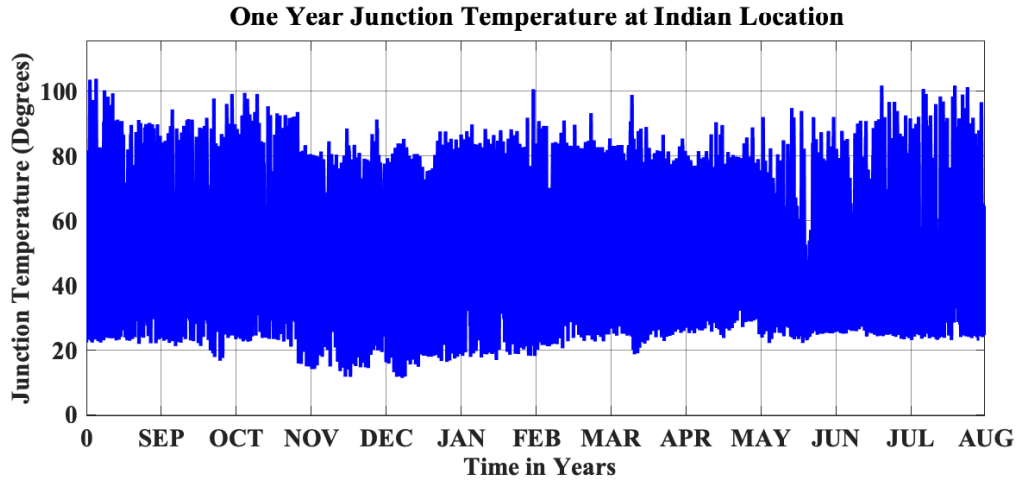


Fig. 3.8 One year Junction Temperature at India Location

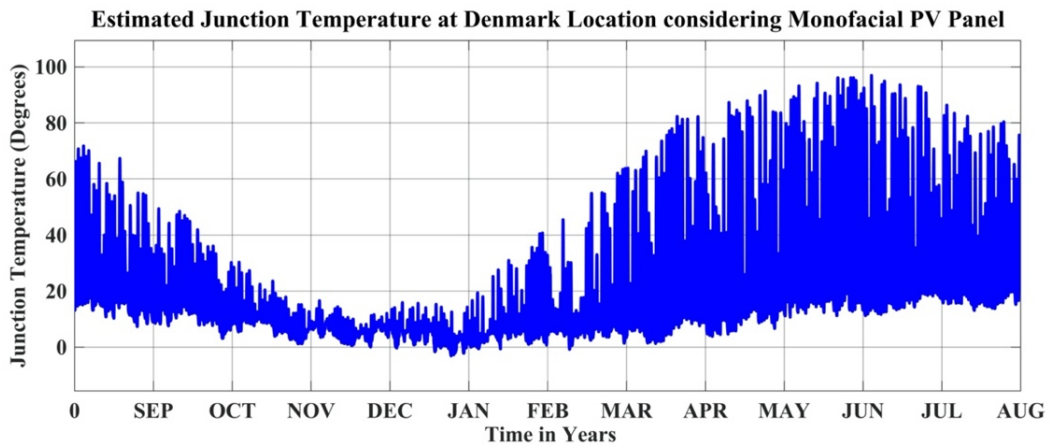


Fig. 3.9 One year Junction Temperature at Denmark Location

Mean Junction Temperature ($^{\circ}\text{C}$) at India location is 55.66°C and, at Denmark location is 16.37°C . Junction Temperature Mean Difference ($^{\circ}\text{C}$) between both locations is 39.29°C . There is a significant amount of Mean Difference between India and Denmark locations. This scenario leads to reliability performance deviation between India and Denmark.

3.7. Chapter Summary:

In this chapter Foster Electro Thermal Model is implemented on a test case of full-bridge 3-kW PV inverter with four 600V, 30A IGW30N60H3 IGBT's to estimation of Junction Temperature. Finally, The yearly mission profile is translated to junction temperature at both locations.

CHAPTER 4

VALIDATION OF ESTIMATED JUNCTION TEMPERATURE

4.1. Validation of Estimated Junction Temperature:

As the junction temperature is calculated by the indirect method, the calculation method needs to be validated. The validation is made by correlating the junction temperature of the PV inverter with the case temperature, solar irradiance, and ambient temperature. Along with the mission profile, the case temperature of the PV inverter is logged at Hyderabad, Telangana, India as shown in Fig. 4.1.

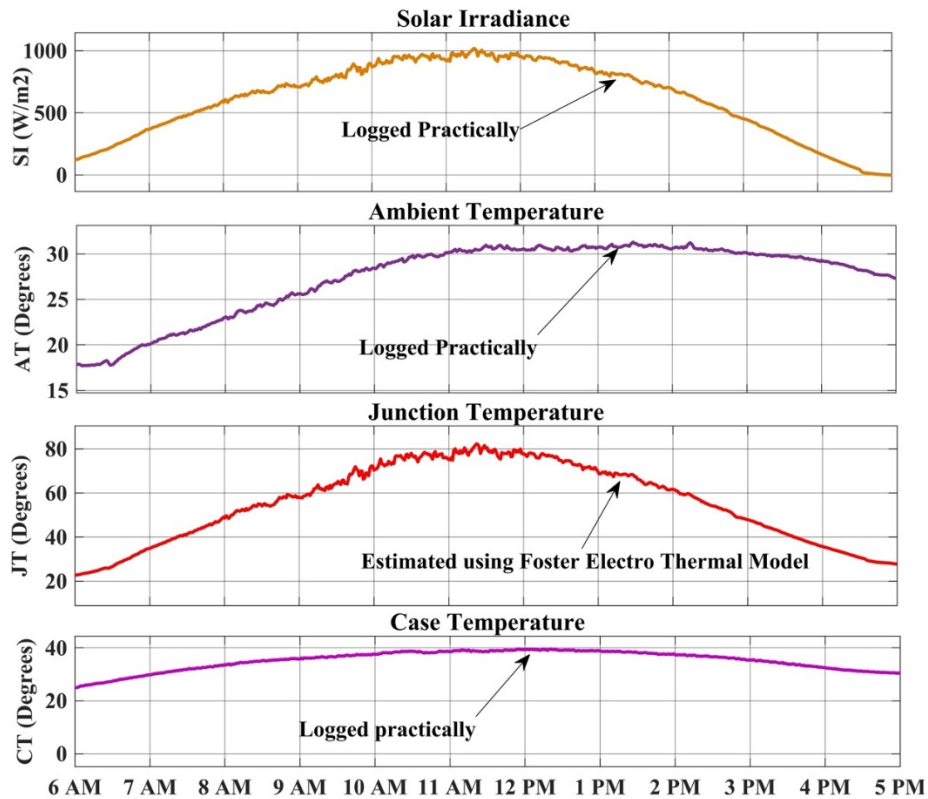


Fig: 4.1 Correlation Variables

4.2. Correlation Analysis:

The measure of association or correlation, are statistics for determining the strength of association between two variables. The degree of association between two variables is measured by correlation. The coefficient of correlation, developed by Karl Pearson, is a numerical measure of the degree of association between two variables [118] as shown in Eq. 4.1.

$$r = \frac{\sum(x_i - \bar{x})(y_i - \bar{y})}{\sqrt{\sum(x_i - \bar{x})^2 \sum(y_i - \bar{y})^2}} \quad (4.1)$$

where

r = Pearson's correlation coefficient

x_i = values of the x-variable in a sample

\bar{x} = mean of the values of the x-variable

y_i = values of the y-variable in a sample

\bar{y} = mean of the values of the y-variable

The coefficient of correlation lies between +1 and -1, shown in Table. 4.1.

Table. 4.1 Correlation Range

-1	0	1
Negative Correlation	No Correlation	Positive Correlation
A correlation coefficient of -1 means that for every positive increase in one variable, there is a negative decrease of a fixed proportion in the other.	Zero means that for every increase, there isn't a positive or negative increase	A correlation coefficient of 1 means that for every positive increase in one variable, there is a positive increase of a fixed proportion in the other.

4.3. Correlation Analysis between Junction Temperature and Case Temperature:

Junction temperature and case temperature from 6:00 AM to 5:12 PM on 01-01-2019 with one-minute resolution are considered for correlation analysis. The degree of association between these two variables is evaluated by Karl Pearson correlation analysis.

4.3.1. Hypothesis Statement:

The hypothesis for the correlation analysis is defined below

- H0 = Between the variable's junction temperature and case temperature No correlation exists.

- H1: Between the variable's junction temperature and case temperature correlation exists.

4.3.2. Correlation Analysis Parameters:

Bivariate Karl Pearson correlation analysis is implemented using SPSS to find the degree of association between junction temperature and case temperature, correlation coefficient is tabulated in Table: 4.2.

Table: 4.2 Correlation Coefficients

Correlations			
		Junction Temperature	Case Temperature
Junction Temperature	Coefficient of Correlation	1	.935**
	P-Value		.000
	Samples	672	672
Case Temperature	Coefficient of Correlation	.935**	1
	P-Value	.000	
	Samples	672	672
***. Correlation is significant at the 0.01 level (2-tailed)."			

4.3.3. Hypothesis Conclusion:

As the p-value is less than 0.05($p < 0.05$, 1.037E-303), hence we reject the null hypothesis of no correlation (H_0) and conclude that a significant correlation exists between the junction temperature and case temperature. $R = + 0.934938$ i.e., Strong positive association. Hence there is a strong association between junction temperature and case temperature.

4.4. Correlation analysis between Junction Temperature and Solar Irradiance

Junction temperature and solar irradiance from 6:00 AM to 5:12 PM on 01-01-2019 with one-minute resolution are considered for correlation analysis. The degree of association between these two variables is evaluated by Karl Pearson correlation analysis.

4.4.1. Hypothesis Statement:

The hypothesis for the correlation analysis is defined below

- H0 = Between the variable's junction temperature and solar irradiance No correlation exists.
- H1: Between the variable's junction temperature and solar irradiance correlation exists.

4.4.2. Correlation Analysis Parameters:

Bivariate Karl Pearson correlation analysis is implemented using SPSS to find the degree of association between junction temperature and solar irradiance, correlation coefficient is tabulated in Table: 4.3.

Table. 4.3 Correlation Coefficients.

Correlations			
		Junction Temperature	Solar Irradiance
Junction Temperature	Coefficient of Correlation	1	.978**
	P-Value		.000
	Samples	672	672
Solar Irradiance	Coefficient of Correlation	.978**	1
	P-Value	.000	
	Samples	672	672
“**”. Correlation is significant at the 0.01 level (2-tailed).”			

4.4.3. Hypothesis Conclusion:

As the p-value is less than 0.05 ($p < 0.05$, 0), hence we reject the null hypothesis of no correlation (H0) and conclude that a significant correlation exists between the junction temperature and solar irradiance. $R = + 0.978430$ i.e., Strong positive association. Hence there is a strong association between junction temperature and solar irradiance.

4.5. Correlation analysis between Junction and Ambient Temperature

Junction temperature and ambient temperature from 6:00 AM to 5:12 PM on 01-01-2019 with one-minute resolution are considered for correlation analysis. The degree of association between these two variables is evaluated by Karl Pearson correlation analysis.

4.5.1. Hypothesis Statement:

The hypothesis for the correlation analysis is shown below

- H0 = Between the variable's junction temperature and ambient temperature No correlation exists.
- H1: Between the variable's junction temperature and ambient temperature correlation exists

4.5.2. Correlation Analysis Parameters:

Bivariate Karl Pearson correlation analysis is implemented using SPSS to find the degree of association between junction temperature and ambient temperature, correlation coefficient is tabulated in Table: 4.4.

Table. 4.4. Correlation Coefficients.

Correlations			
		Junction Temperature	Ambient Temperature
Junction Temperature	Coefficient of Correlation	1	.730**
	P-Value		.000
	Samples	672	672
Ambient Temperature	Coefficient of Correlation	.730**	1
	P-Value	.000	
	Samples	672	672
“**”. Correlation is significant at the 0.01 level (2-tailed).”			

4.5.3. Hypothesis Conclusion:

As the p-value is less than 0.05 ($p < 0.05$, $6.5062E-113$), hence we reject the null hypothesis of no correlation (H_0) and conclude that a significant correlation exists between the junction temperature and ambient temperature. $R = + 0.730140$ i.e., positive association. Hence there is an association between junction temperature and ambient temperature.

In all three cases, estimate junction temperature exhibits a positive association with case temperature, solar irradiance, and ambient temperature, hence it is validated.

4.6. Chapter Summary:

In this chapter the validation of estimated junction temperature is made by correlating with the case temperature, solar irradiance, and ambient temperature. In all the cases positive correlation is recorded. In the correlation analysis between junction temperature and case temperature, correlation coefficient $R = 0.934938$ i.e., Strong positive association. In the correlation analysis between junction temperature and solar irradiance, correlation coefficient $R = 0.978430$ i.e., strong positive association. In the correlation analysis between junction and ambient temperature, correlation coefficient $R = 0.730140$ i.e., positive association, and hence it is validated.

CHAPTER 5

RELIABILITY ANALYSIS OF PV INVERTER

5.1 Reliability analysis of PV Inverter Methodology:

The critical component of the PV inverter needs to be identified. From the literature review, IGBT is identified as a critical component (Presented in Chapter 1). Hence it is needed to anticipate the reliability of IGBT in PV inverter. The first reliability of IGBT is analyzed i.e., component level and then system level reliability is analyzed by combining all the individual components using series reliability block diagram approach. The flow chart for reliability analysis of PV inverter flow chart is shown in Fig. 5.1.

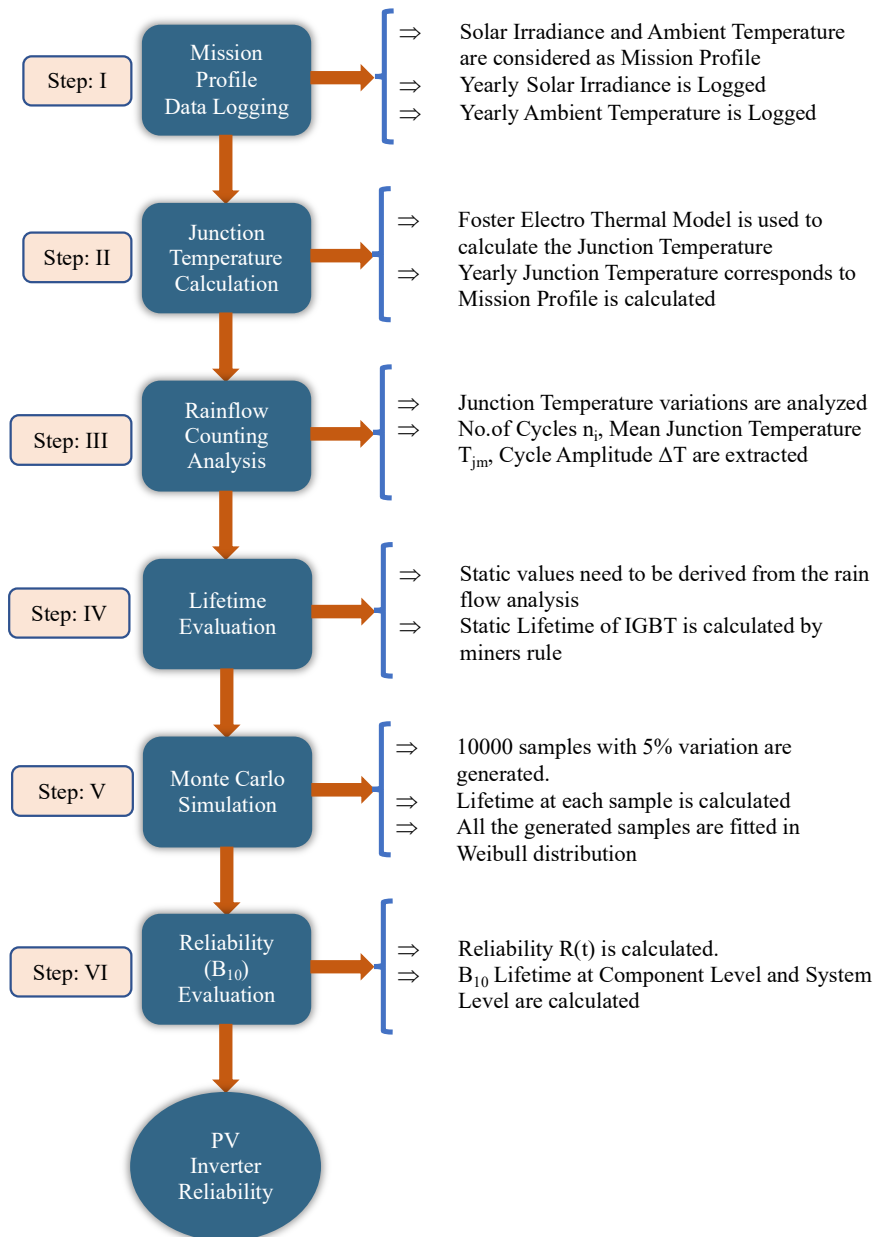


Fig. 5.1 Reliability Analysis Flowchart

Step: I Mission Profile:

Environmental factors such as Solar Irradiance and Ambient Temperature also called a mission profile affect the reliability performance of PV inverter. Hence, real time yearly mission profile data is logged (Described in Chapter 2).

Step: II Junction Temperature Calculation:

The junction temperature of IGBT corresponds to the yearly mission profile is calculated using foster electro thermal model at India and Denmark locations (Described in Chapter 3).

Step: III Rain Flow Counting Analysis:

The variations of the estimated junction temperature follow irregular profiles as per the mission profile. Hence a cycle counting algorithm is needed to anticipate the variations. Rainflow counting algorithm is used to analyze the variations. From the rainflow algorithm No.of Cycles n_i , Mean Junction Temperature T_{jm} , Cycle Amplitude ΔT are calculated [77].

Step: IV Life Time Evaluation:

A lifetime of IGBT is calculated by miner's rule [119] as shown in Eq. 5.1

$$Life\ Time\ (LT) = \frac{1}{Life\ Consumption\ (LC)} \quad (5.1)$$

Life Consumption of IGBT is as shown in Eq. 5.2

$$Life\ Consumption\ (LC) = \sum \frac{No.\ of\ Cycles\ (n_i)}{No.\ of\ Cycle\ to\ failure\ (N_{fi})} \quad (5.2)$$

Where

- No.of Cycles n_i from rainflow counting algorithm.
- No.of Cycles to failure N_{fi} can be calculated by bayerer's [74] lifetime model is as shown in Eq. 5.3.

$$N_f = A(\Delta T_j)^{\beta_1} \cdot e^{\frac{\beta_2}{(T_j + 273K)}} \cdot t_{on}^{\beta_3} \cdot I^{\beta_4} \cdot V^{\beta_5} \cdot D^{\beta_6} \quad (5.3)$$

The parameter of the above equation is tabulated in Table. 5.1.

Table. 5.1. Bayerer's Lifetime Model Parameters

Parameter	Value
Technology Factor (A)	9.34E+14
Coefficient (β_1)	-4.416
Coefficient (β_2)	1285
Coefficient (β_3)	-0.463
Coefficient (β_4)	-0.716
Coefficient (β_5)	-0.761
Coefficient (β_6)	-0.5
Current per bond foot (I)	3-23 A
Voltage class (V)	6-33 V
Bond wire diameter	75-500 μm

Step: V Monte Carlo Simulation:

In the above lifetime model, all the parameters are constant i.e., all the devices should fail at the same rate but practically this is not feasible, so to overcome this the variation of 5 % is considered and 10000 samples are generated using Monte Carlo simulation [82].

Step: VI Reliability (B_{10}) Evaluation:

All the generated samples are fitted in Weibull distribution to calculate the reliability function as given below [120]

For component level reliability function is as shown in Eq. 5.4

$$R_i(t) = e^{-\left(\frac{t}{\alpha}\right)^\gamma} \tag{5.4}$$

where α is Scale Parameter

γ is Shape Parameter

In Eq. 5.4, the shape parameter γ is obtained from Weibull distribution and the Scale Parameter α is a characteristic lifetime where 63.2 % of the population have failed.

For system-level reliability function is as shown in Eq. 5.5

$$R_{total}(t) = \prod_{i=1}^n R_i(t) \quad (5.5)$$

where $R_i(t)$ individual component reliability.

Finally, B_{10} lifetime (Probability to fail 10 % of the population) can be calculated using Eq. 5.6

$$B_x = \left[\ln \left(\frac{100}{100-x} \right) \times (\alpha)^\gamma \right]^{\frac{1}{\gamma}} \quad (5.6)$$

were

x is percentage of population

α is Scale Parameter

γ is Shape Parameter.

5.2 Reliability Analysis of PV inverter:

The reliability analysis of PV inverter is performed at both India and Denmark locations to account for the impact of the Installation site.

5.2.1 Rain flow Counting Analysis:

The variations of junction temperature calculated at India and Denmark locations are analyzed using rain flow counting algorithm. From the rain flow counting algorithm No.of Cycles n_i , Mean Junction Temperature T_{jm} , Cycle Amplitude ΔT are calculated at both locations as shown in Fig. 5.2.

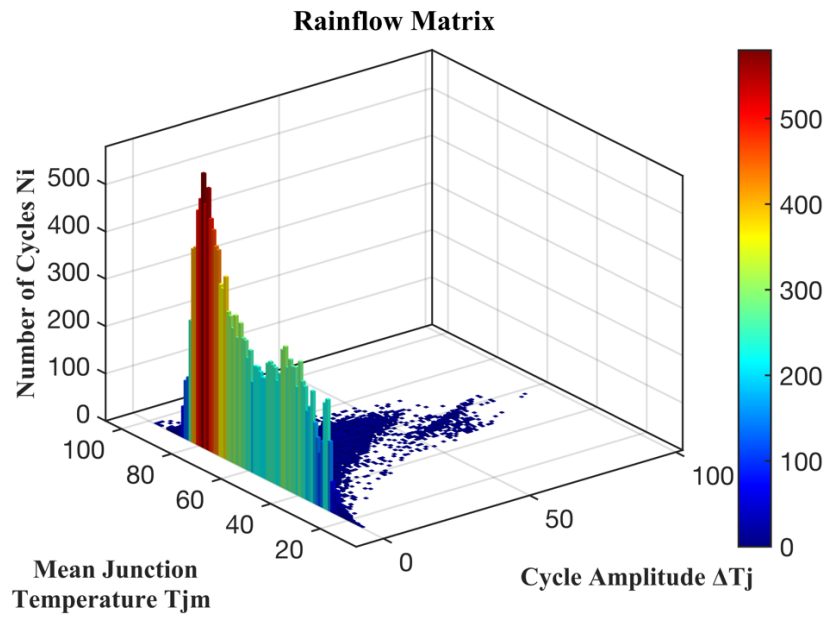


Fig. 5.2(a). Rain flow Matrix India Location

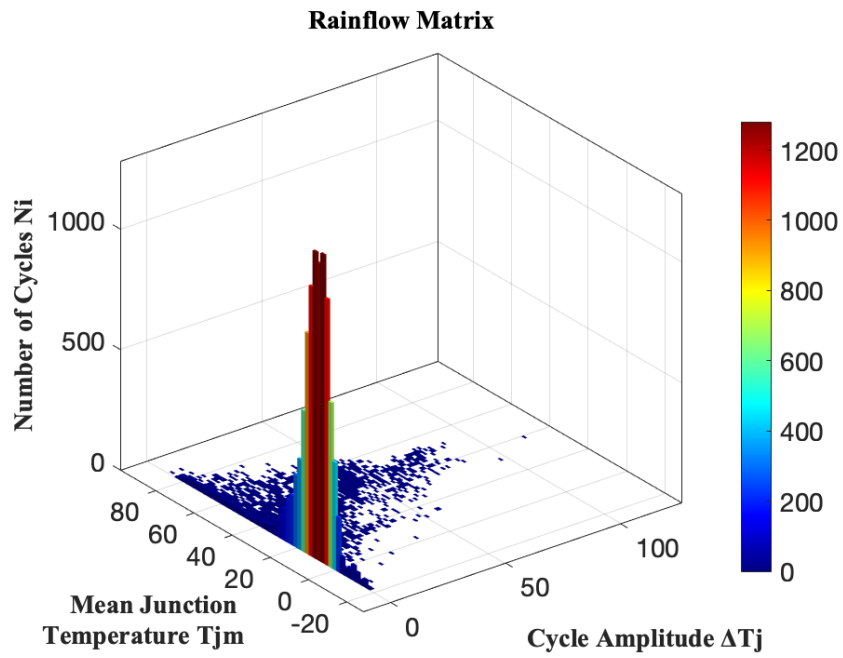


Fig. 5.2(b). Rain flow Matrix Denmark Location

5.2.2. Life Time Evaluation:

For the lifetime evaluation, static values (mean values) need to be derived from the rain flow analysis. The static values at the India location are T_{jm} is 59.77°C , ΔT_j is 5.95°C . Similarly, at Denmark location are T_{jm} is 19.23°C , ΔT_j is 4.69°C . The lifetime corresponds to the static values that are calculated with Eq. 5.1 and are tabulated in the following Table. 5.2.

Table. 5.2. Lifetime Evaluation for Static Parameters

Country	Mean Junction Temperature (T_{jm})	Cycle Amplitude (ΔT_j)	Life Consumption (LC)	Lifetime in Years (LT)
India	59.77°C	5.95°C	0.02201564	45.42
Denmark	19.23°C	4.69°C	0.01115268	89.66

As the temperature at the India location is relatively high, the lifetime is 45.42 years, where at the Denmark location temperature is relatively low, the lifetime is 89.66 years. Hence this shows that lifetime varies from location to location based on climatic conditions. The lifetime of PV inverter is reported more in cold climatic conditions.

5.2.3. Monte Carlo Simulation based Reliability (B_{10}) Evaluation.

Using Monte Carlo simulation population size of 10000 are generated and the lifetime at each sample is calculated with 5 % variation using Eq. 5.1. The 10000 population are fitted with Weibull distribution as shown in Fig. 5.3.

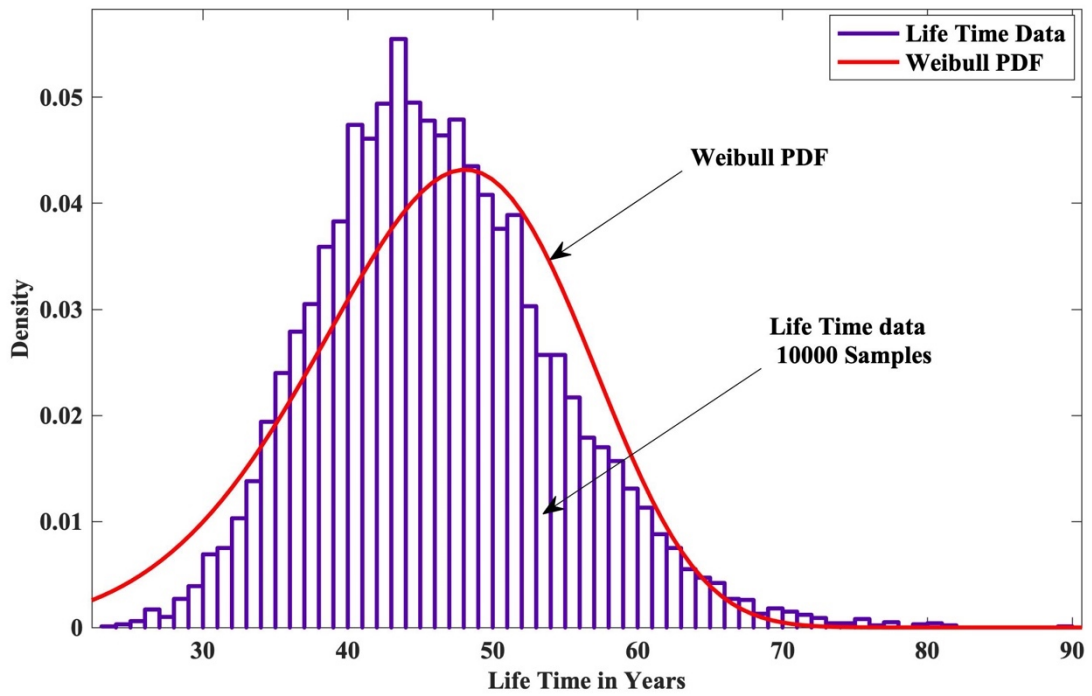


Fig. 5.3(a) Monte Carlo Simulation Lifetime Distribution at India Location

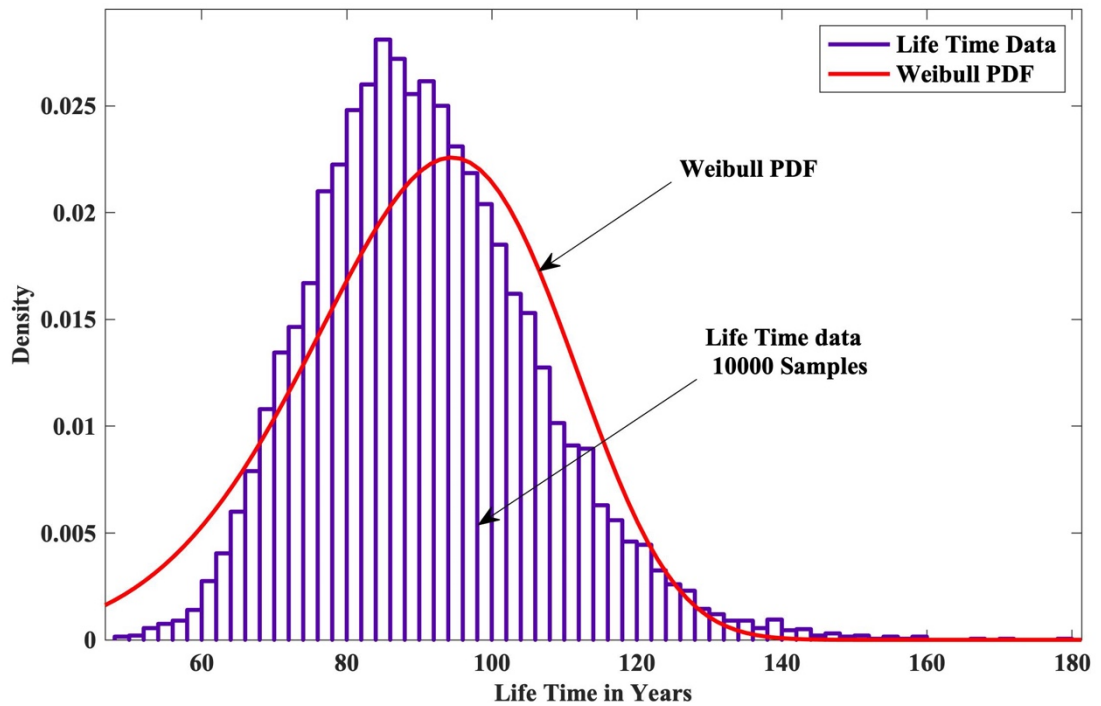


Fig. 5.3(b) Monte Carlo Simulation Lifetime Distribution at Denmark Location

The reliability function $R(t)$ is calculated using two parameter Weibull distribution. Component level reliability is calculated using Eq. 5.4, system level reliability is calculated using Eq. 5.5, B_{10} lifetime is calculated using Eq. 5.6. $R(t)$ at India and Denmark locations are as shown in Fig. 5.4 and Fig. 5.5 respectively.

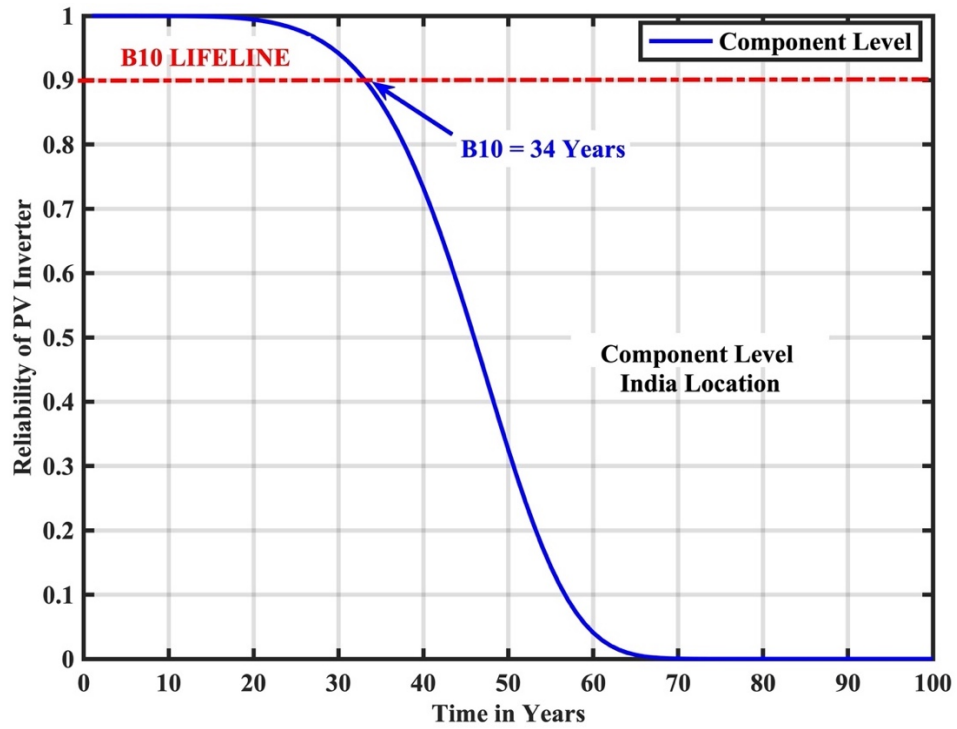


Fig. 5.4(a). Reliability (B_{10}) Evaluation of PV Inverter at India Location Component Level

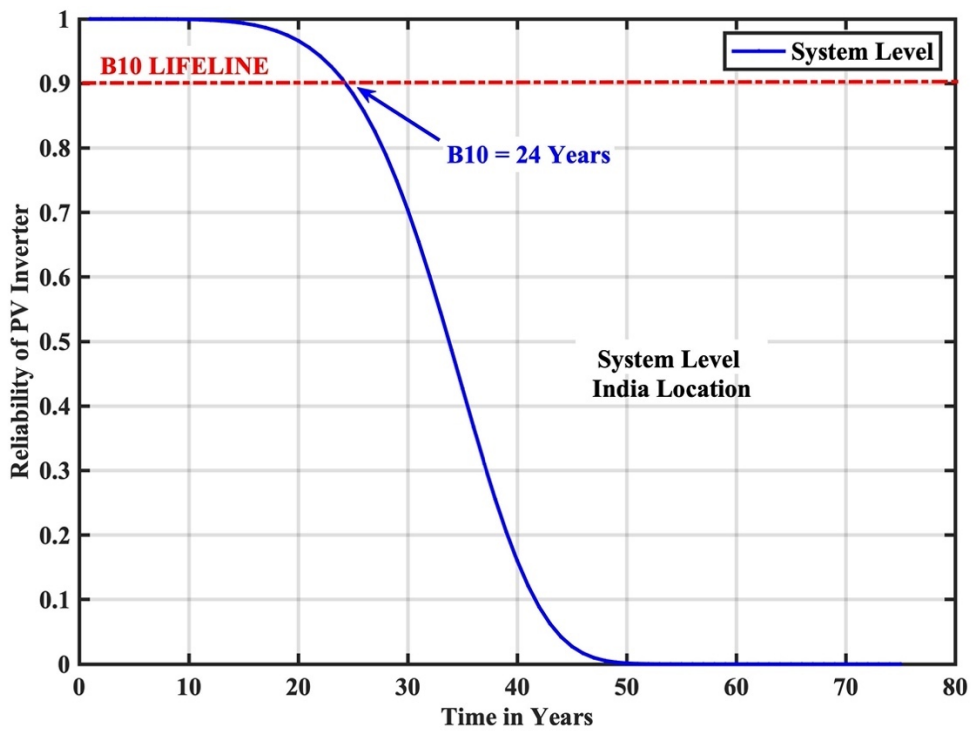


Fig. 5.4(b). Reliability (B_{10}) Evaluation of PV Inverter at India Location System Level

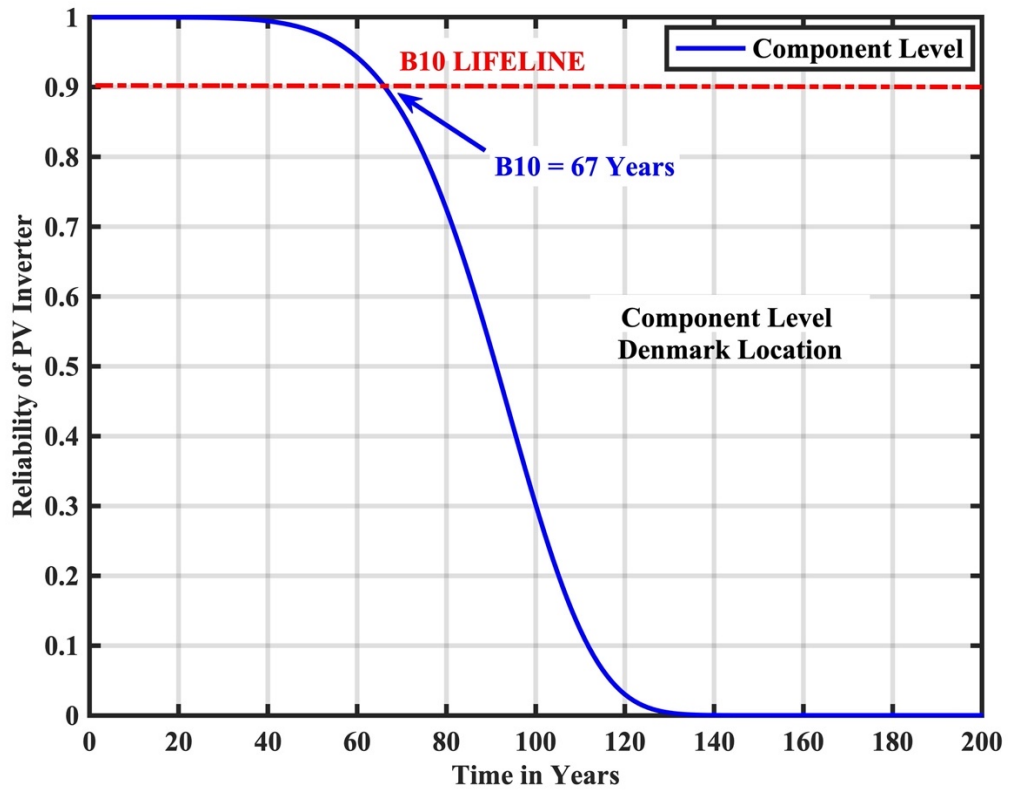


Fig. 5.5(a). Reliability (B_{10}) Evaluation of PV Inverter at Denmark Location
Component Level

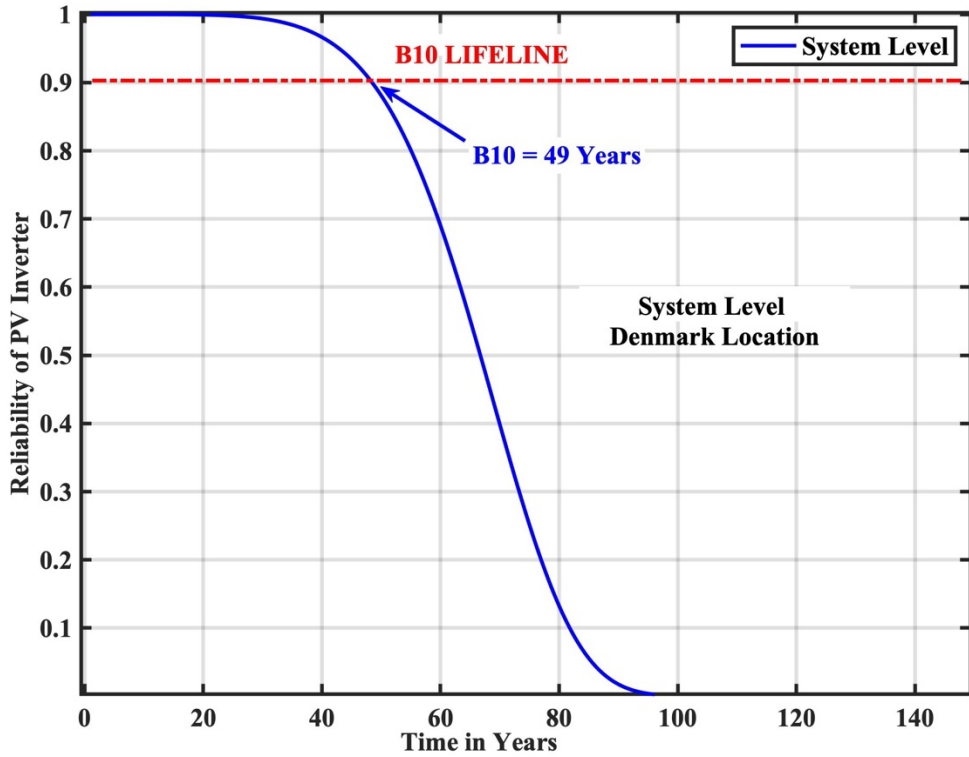


Fig. 5.5(b). Reliability (B_{10}) Evaluation of PV Inverter at Denmark Location
System Level

Installation site has a significant impact, reliability varies from location to location based on climatic conditions. The reliability of PV inverter is reported more in cold climatic conditions i.e., higher B10 life time is recorded at Denmark location (relatively cold) when compared to India (relatively hot)

5.2.4 B₁₀ Lifetime Comparison:

The B₁₀ lifetime recorded in India where climatic conditions are relatively hot is 34 years (Component Level) and 24 years (System Level). Similarly, the B₁₀ lifetime recorded in Denmark where climatic conditions are relatively cold is 67 years (Component Level) and 49 years (System Level). B₁₀ lifetime comparison bar chart is shown in Fig. 5.6. This scenario clearly shows that B₁₀ lifetime varies with respect to geographical locations and environmental conditions. Reliability is higher in relatively cold locations than in relatively hot locations.

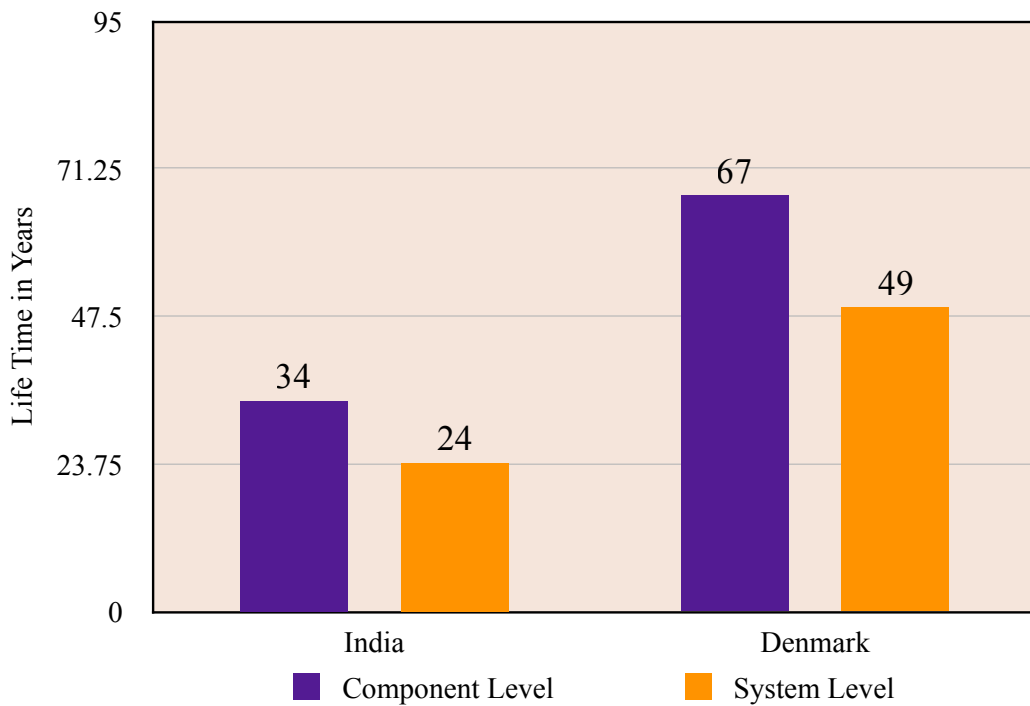


Fig. 5.6. B₁₀ Lifetime Comparison Chart

5.3. Factors Effecting The Reliability Of PV Inverter:

Various factors affect the reliability of the PV inverter. In this work, the following factors are considered for reliability analysis.

- Impact of Degradation Rate on PV Inverter Reliability
- Impact of PV Panel Oversizing on PV Inverter Reliability
- Impact of Bifacial PV Panel on PV Inverter Reliability

In all these cases impact of the installation site is presented by considering India and Denmark locations.

5.3.1. Impact of Degradation Rate on PV Inverter Reliability:

The PV panel performance will degrade yearly and deteriorate the power output. Hence during the reliability analysis degradation rate is considered. The overall degradation rate per year can be calculated as follows.

$$\% P_{DR} = \frac{(P_{Np} - P_p)}{P_{Np} * Age} * 100 \quad \% / Year \quad (5.7)$$

Where

P_{DR} = PV Power Degradation Rate

P_{Np} = PV Nameplate power at STC

P_p = PV present value power a STC

To analyze the impact of degradation rate on PV inverter reliability a degradation rate of 1.93 % per year for five years of operation is considered at India Location, 0.15 % per year for five years of operation is considered at Denmark Location.

5.3.1.1. Junction Temperature considering Degradation Rate:

The yearly mission profile is translated to Junction Temperature using foster electro thermal model. Junction Temperature with and without panel degradation rate at India and Denmark Location is shown in Fig. 5.7(a) and Fig. 5.7(b) respectively.

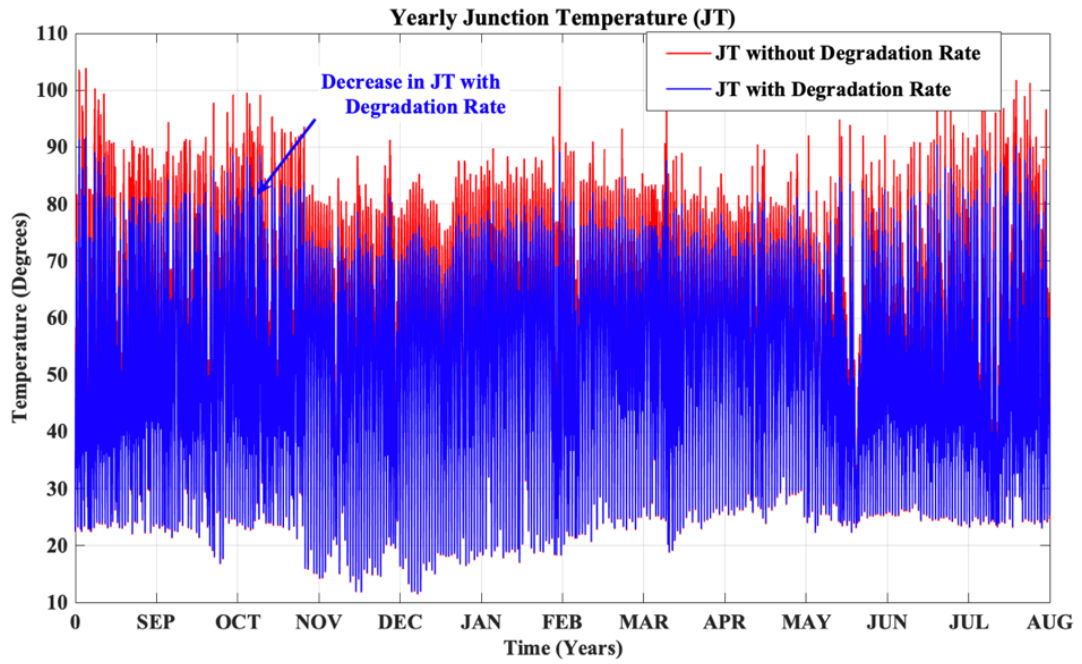


Fig. 5.7(a). Junction Temperature with and without Degradation Rate at India Location

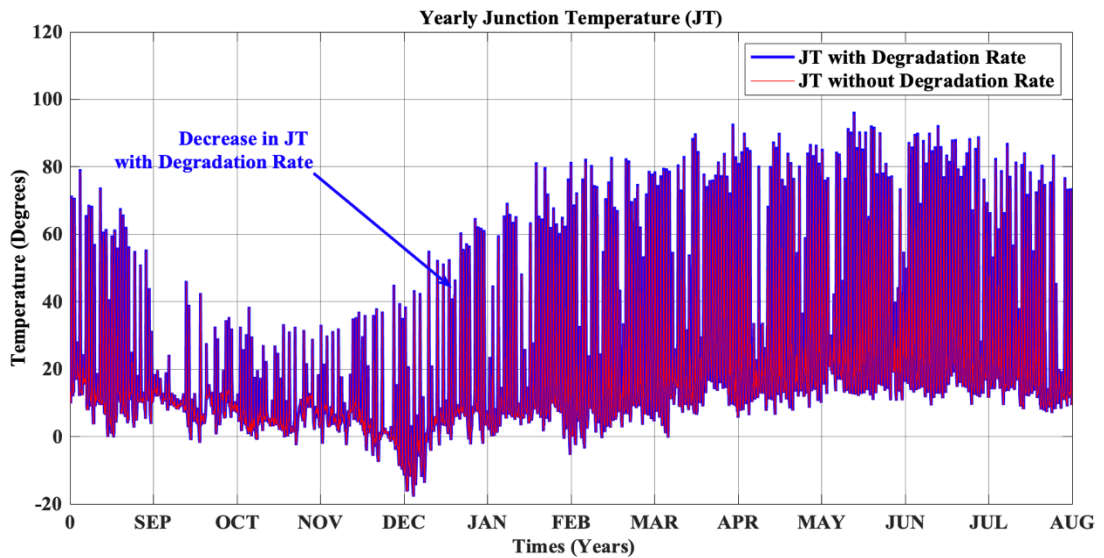


Fig. 5.7(b). Junction Temperature with and without Degradation Rate at Denmark Location.

The junction temperature by considering the degradation rate shows the decreasing trend at both locations. The average values of calculated junction temperature at both locations are compared and presented in Fig. 5.8. In India, it is decreased from 55.66°C to 52.18°C . Similarly, at the Denmark location, it is decreased from 16.38°C to 15.73°C

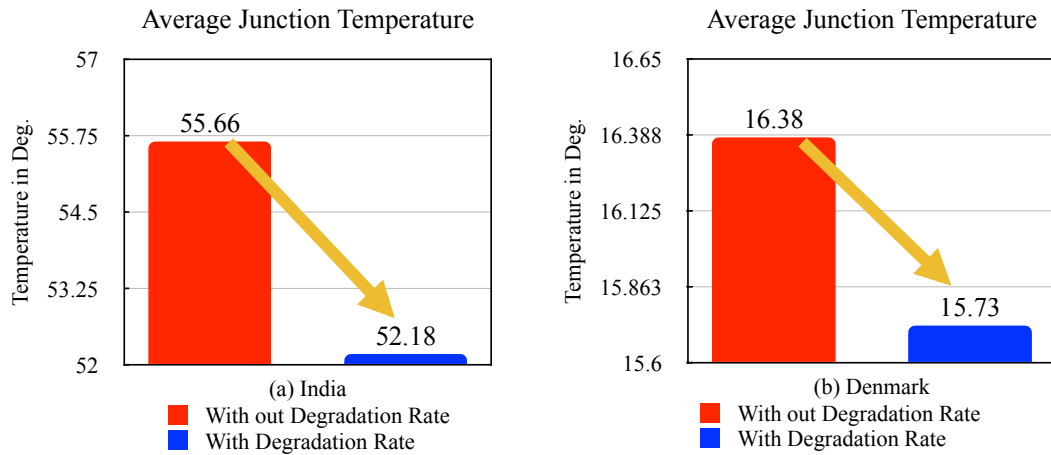


Fig. 5.8 Average Junction Temperature (a) India (b) Denmark

5.3.1.2. Rainflow Analysis:

Junction Temperature variations are analyzed using rainflow counting algorithm and N_i , T_{jm} , ΔT are calculated. Rainflow histogram with and without degradation rate at India and Denmark Location is shown in Fig. 5.9.

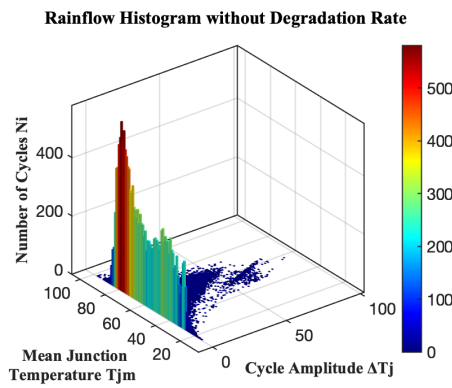


Fig. 5.9 (a). Rainflow Histogram without Degradation Rate at India

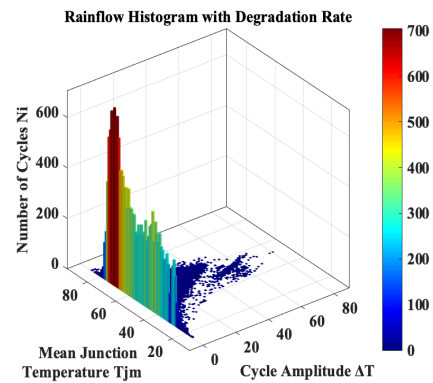


Fig. 5.9 (b). Rainflow Histogram with Degradation Rate at India

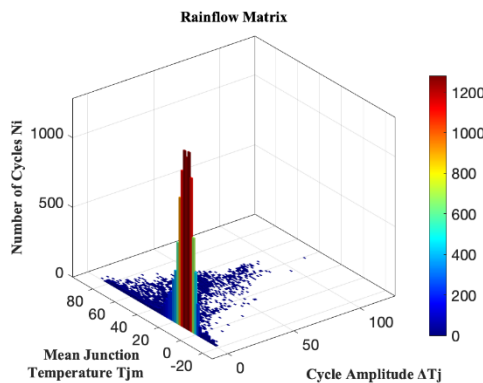


Fig. 5.9 (c). Rainflow Histogram without Degradation Rate at Denmark

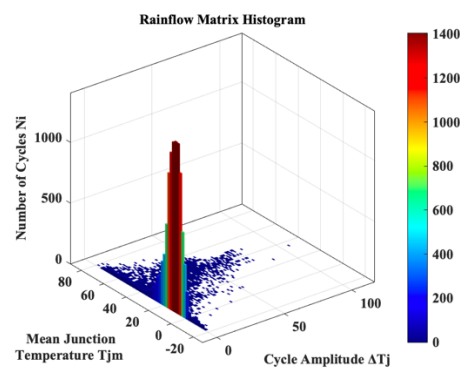


Fig. 5.9 (d). Rainflow Histogram with Degradation Rate at Denmark

5.3.1.3. Life Time Evaluation:

For the lifetime evaluation, static values (mean values) need to be derived from the rain flow analysis. The lifetime corresponds to the static values that are calculated with Eq. 5.1 and are tabulated in the following Table. 5.3.

Table. 5.3. Lifetime Evaluation for Static Parameters

Country		Mean Junction Temperature (T_{jm})	Cycle Amplitude (ΔT_j)	Life Consumption (LC)	Lifetime in Years (LT)
India	Without Degradation Rate	59.77 °C	5.95 °C	0.02201564	45.42
	With Degradation Rate	55.58 °C	4.97 °C	0.00959831	104.18
Denmark	Without Degradation Rate	19.23 °C	4.69 °C	0.01115268	89.66
	With Degradation Rate	19.17 °C	4.63 °C	0.01059962	94.34

At both locations with degradation rate increased lifetime is recorded. At the India location, lifetime increased from 45.42 to 104.18 years, at Denmark location lifetime increased from 89.66 to 94.34 years. Since at India degradation rate is more increased lifetime is observed than Denmark location.

5.3.1.4. Monte Carlo Simulation based Reliability (B_{10}) Evaluation:

Monte Carlo simulation is used to generate 10000 samples with 5 % variation. The lifetime for each sample is calculated with and without degradation rate using Eq. 5.1. All the samples are fitted in two parameter Weibull distribution. The Monte Carlo

simulation lifetime distribution at India and Denmark locations are shown in Fig. 5.10 and Fig. 5.11 respectively.

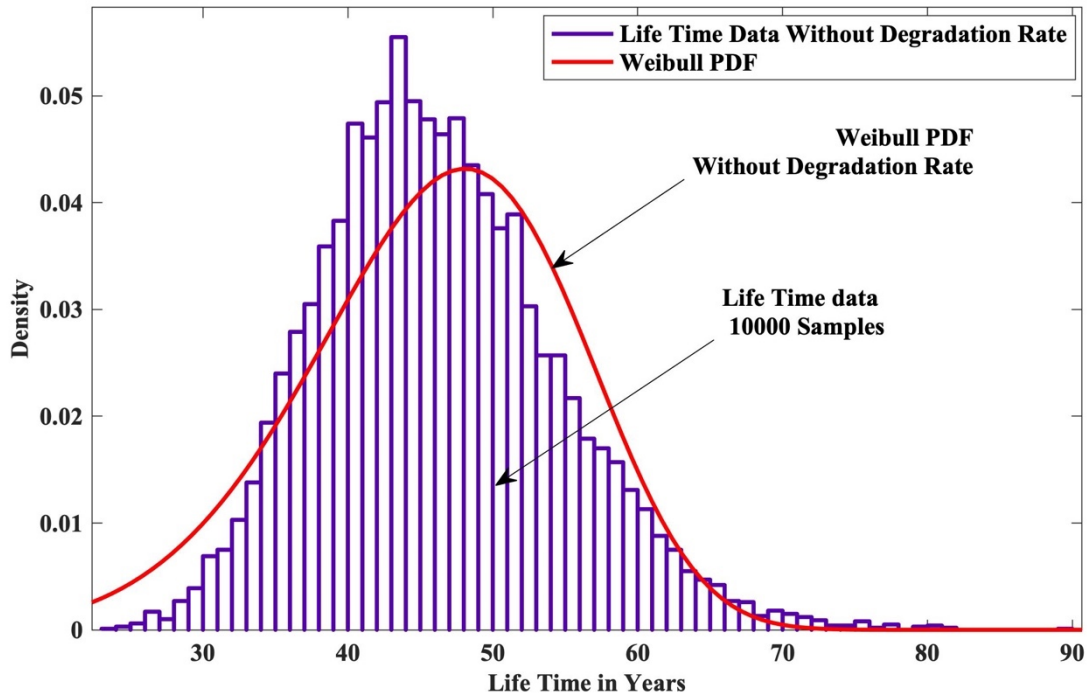


Fig. 5.10(a). Monte Carlo Simulation Lifetime distribution without Degradation Rate at India

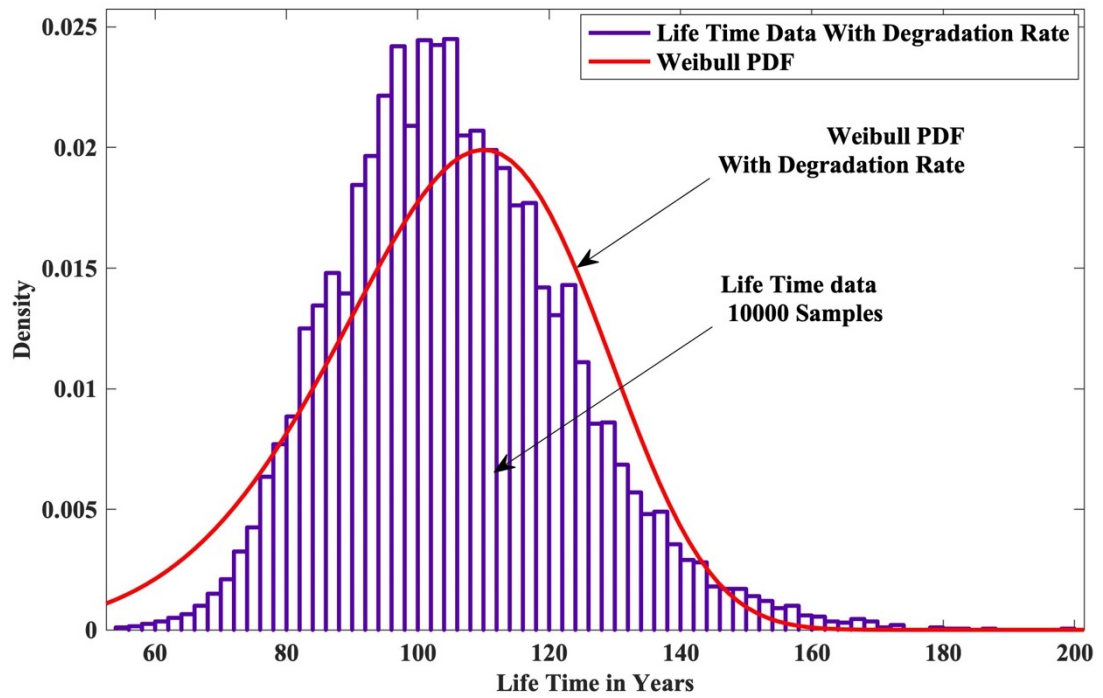


Fig. 5.10(b). Monte Carlo Simulation Lifetime distribution with Degradation Rate at India

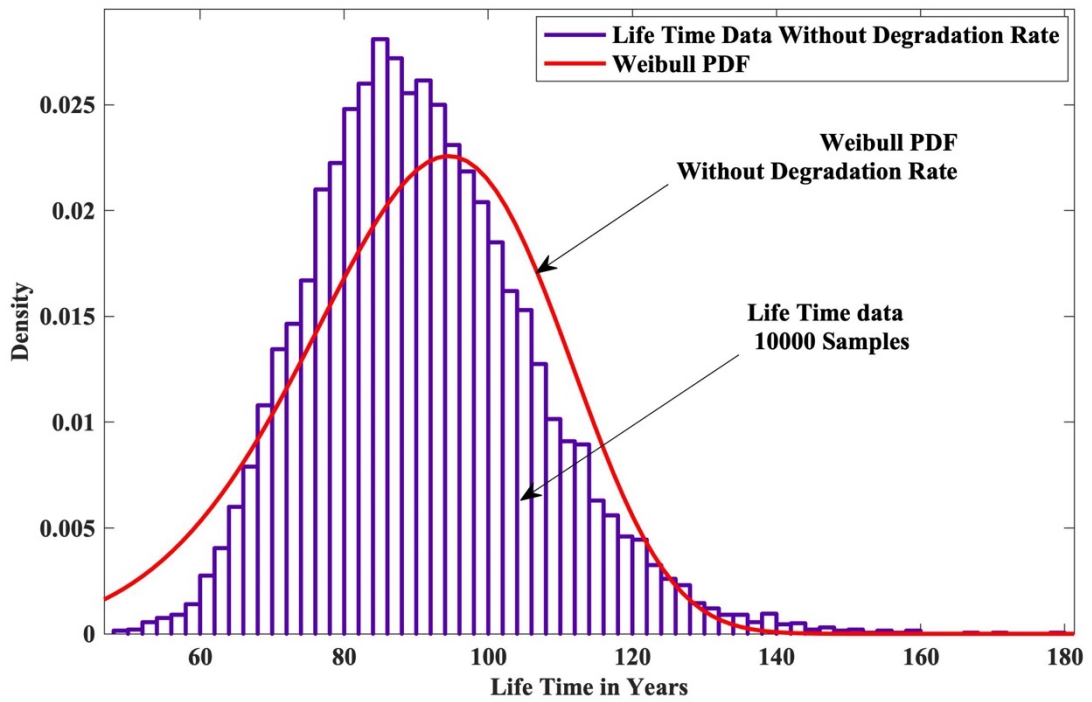


Fig. 5.11(a). Monte Carlo Simulation Lifetime distribution without Degradation Rate at Denmark

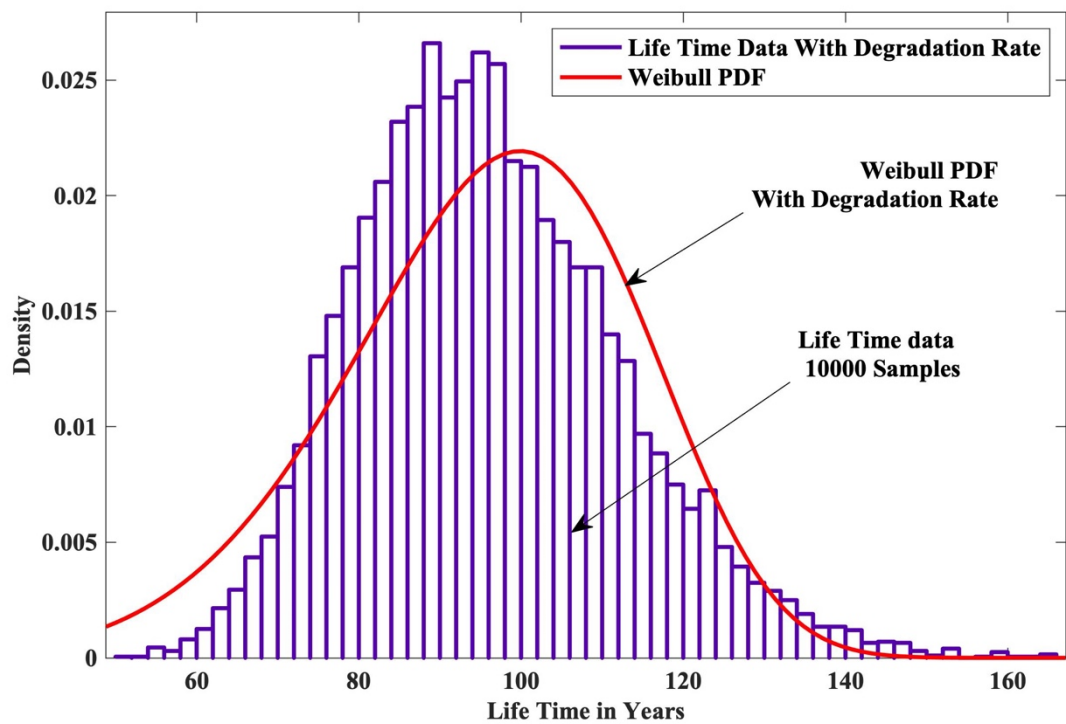


Fig. 5.11(b). Monte Carlo Simulation Lifetime distribution with Degradation Rate at Denmark

The reliability function $R(t)$ is calculated using two parameter Weibull distribution. Component level reliability is calculated using Eq. 5.4, system level reliability is calculated using Eq. 5.5, B_{10} lifetime is calculated using Eq. 5.6. $R(t)$ at India and Denmark locations are as shown in Fig. Fig. 5.12 and Fig. 5.13 respectively.

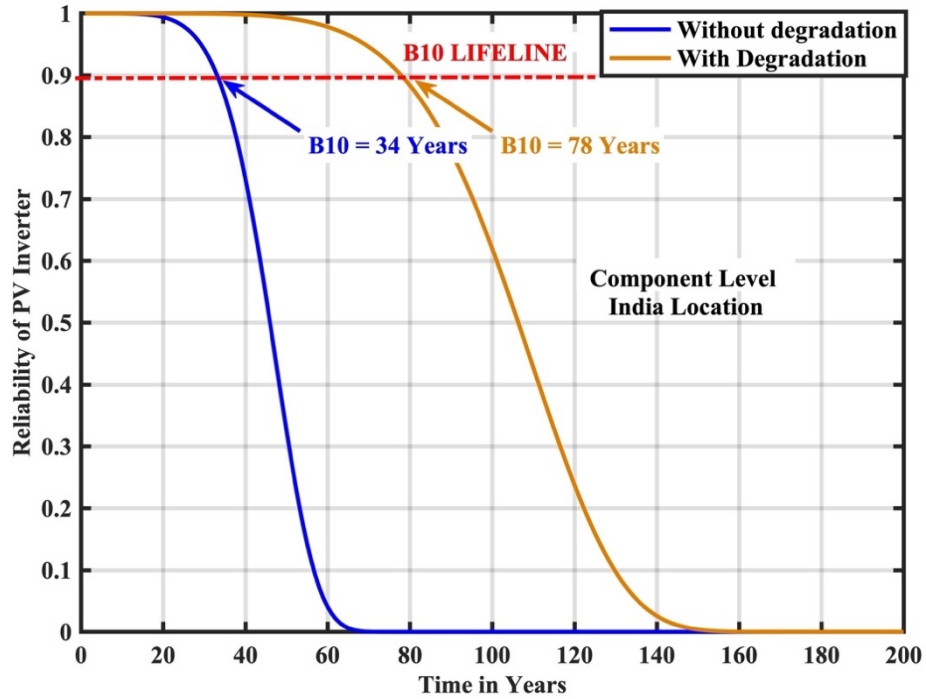


Fig. 5.12(a) Reliability (B_{10}) Evaluation of PV Inverter at India Component Level

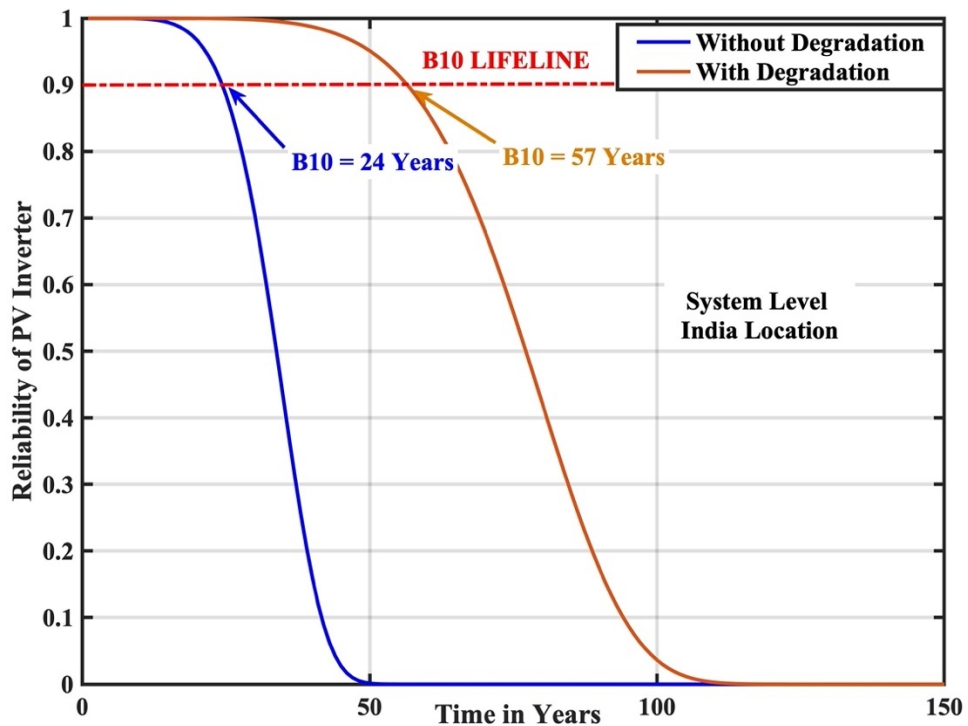


Fig. 5.12(b) Reliability (B_{10}) Evaluation of PV Inverter at India System Level

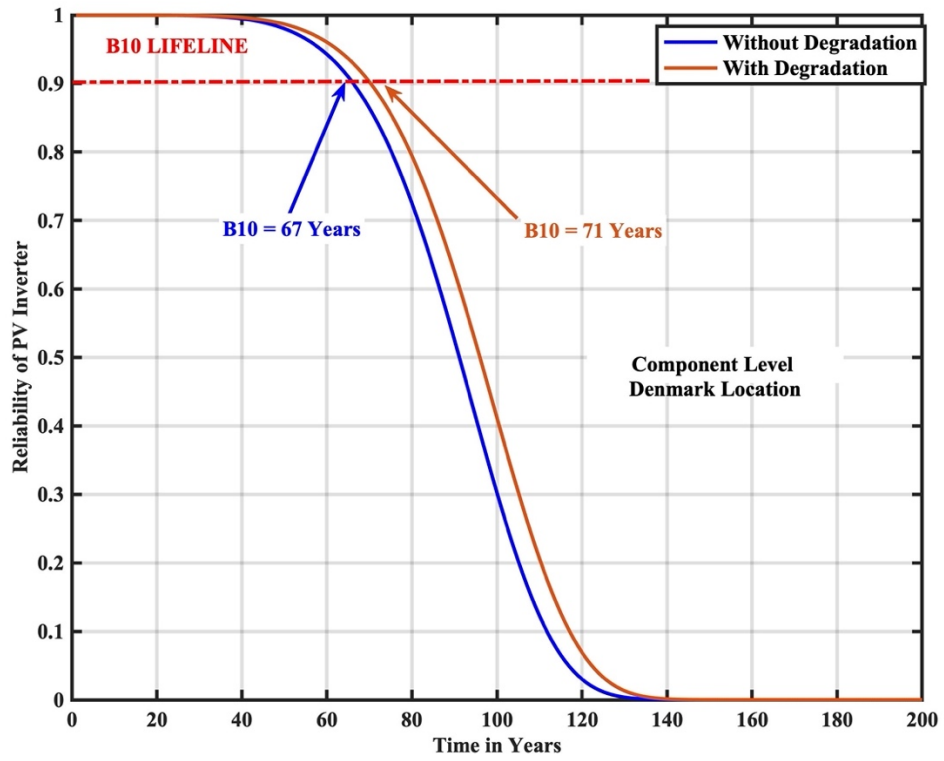


Fig. 5.13(a). Reliability (B_{10}) Evaluation of PV Inverter at Denmark Component Level

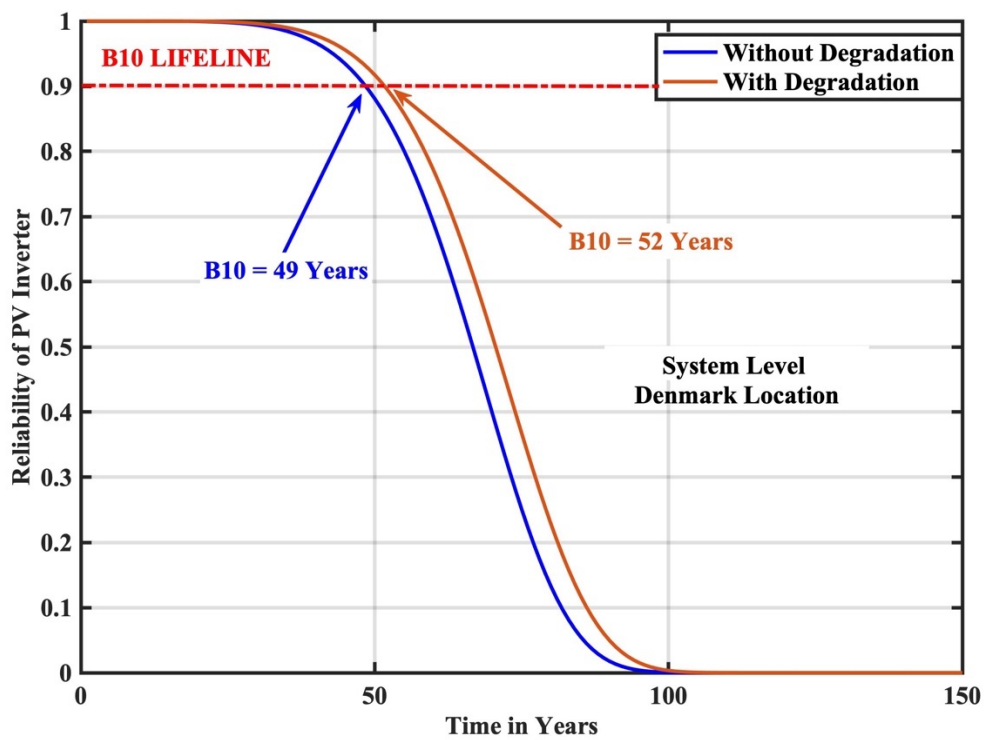


Fig. 5.13(b). Reliability (B_{10}) Evaluation of PV Inverter at Denmark System Level

From the reliability curves, it is observed that B_{10} lifetime has a significant impact when the PV panel degradation rate is considered. B_{10} lifetime increases at both locations.

At the India component level reliability (B_{10}) is 78 years, system level reliability (B_{10}) is 57 years. Similarly, at the Denmark component level reliability (B_{10}) is 71 years, system level reliability (B_{10}) is 52 years.

5.3.1.5. B_{10} Lifetime Comparison:

The degradation rate on PV inverter reliability has a significant impact at both locations. An increase in B_{10} lifetime is recorded at both locations, comparative analysis at the component level and system level are shown in Fig. 5.14. In India B_{10} lifetime at component level increased from 34 to 78 years, at system level increased from 24 to 57 years. Similarly, in Denmark B_{10} lifetime at component level increased from 67 to 71 years, at system level increased from 49 to 52 years.

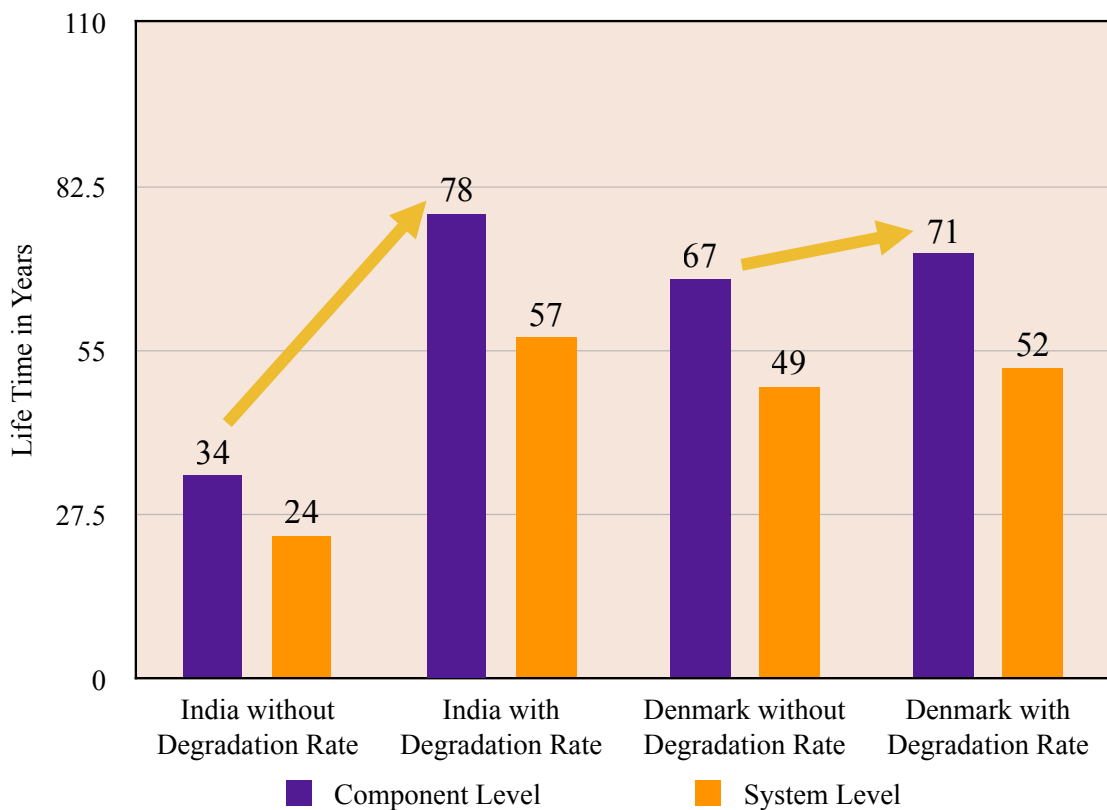


Fig. 5.14. B_{10} Lifetime Comparison Chart

5.3.2. Impact of PV Panel Oversizing on PV Inverter Reliability:

PV panel sizing ratio (R_s) is defined as the ratio between PV panel rated power at STC to PV inverter rated power.

$$R_s = \frac{PV_{Panel\ Rated\ Power}}{PV_{Inverter\ Rated\ Power}} \quad (5.8)$$

If $R_s > 1$ then the PV panel is said to be oversized. Oversizing of PV panels is implemented in the areas of low irradiance to harness more power.

To analyze the impact of PV Panel Oversizing on PV inverter panel sizing ratio $R_s = 1.0, 1.2, 1.4$ are considered.

5.3.2.1 Junction Temperature considering PV Panel Oversizing:

The yearly mission profile is translated to junction temperature using foster electro thermal model. Junction temperature considering for $R_s = 1.0, 1.2, 1.4$ at India and Denmark location are shown in Fig. 5.15 and Fig. 5.16 respectively.

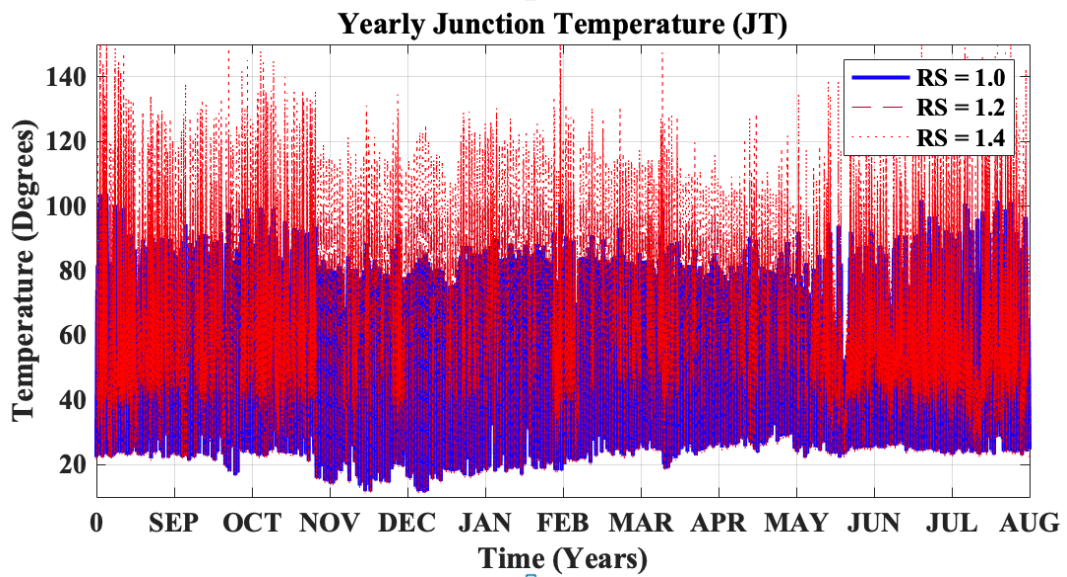


Fig. 5.15. Junction Temperature with different sizing ratios (R_s) at India.

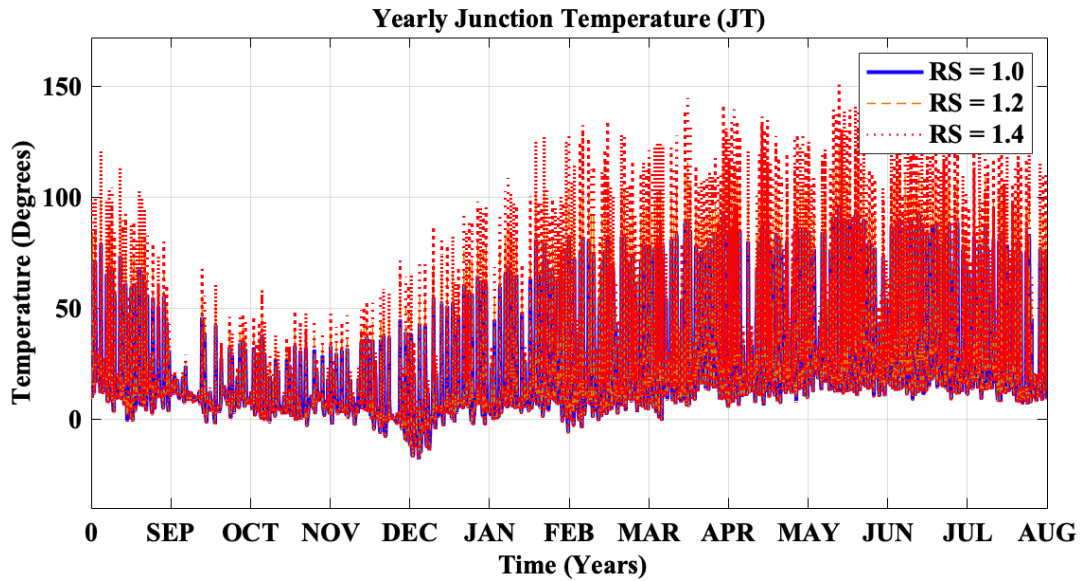


Fig. 5.16. Junction Temperature with different sizing ratios (R_s) at Denmark.

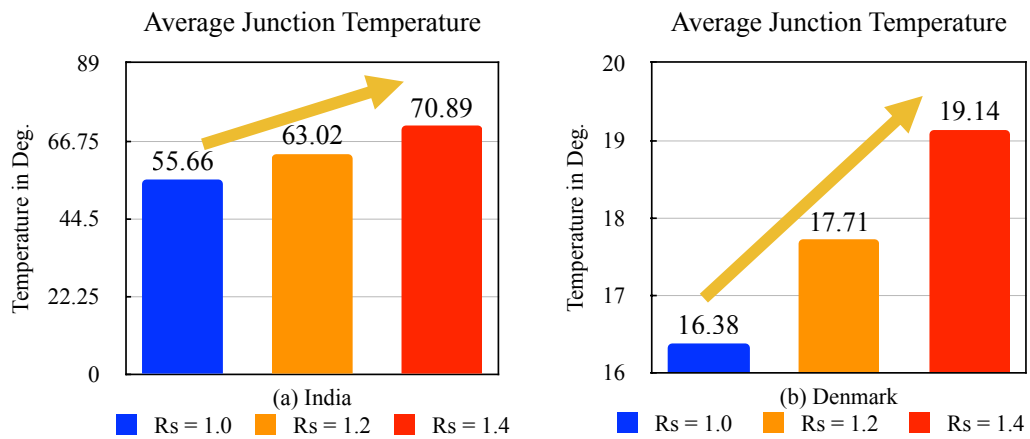


Fig. 5.17. Average Junction Temperature with different sizing ratios (R_s)

The junction temperature by considering PV panel over sizing shows the increasing trend at both locations. The average values of calculated junction temperature at both locations are compared and presented in Fig. 5.17. In India, it is increased from 55.66 °C to 70.89 °C. Similarly, at the Denmark location, it is increased from 16.38 °C to 19.14 °C.

5.3.2.2 Rainflow Analysis:

Junction temperature variations are analyzed using rainflow counting algorithm and N_i , T_{jm} , ΔT are calculated. Rainflow histogram for different R_s at India and Denmark locations are shown in Fig. 5.18.

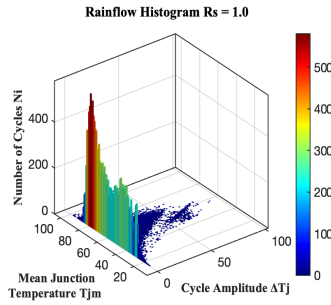


Fig. 5.18 (a). Rainflow Histogram with sizing ratio $R_s = 1.0$ at India

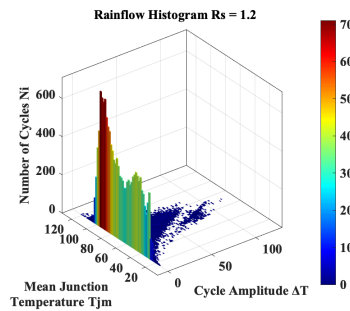


Fig. 5.18 (b). Rainflow Histogram with sizing ratio $R_s = 1.2$ at India

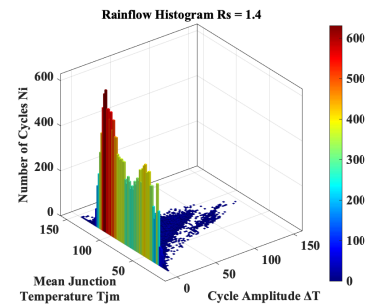


Fig. 5.18 (c). Rainflow Histogram with sizing ratio $R_s = 1.4$ at India

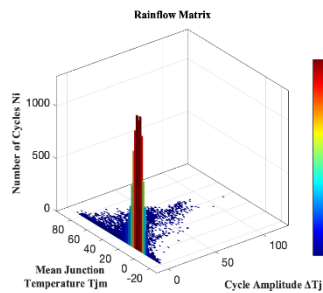


Fig. 5.18 (d). Rainflow Histogram with sizing ratio $R_s = 1.0$ at Denmark

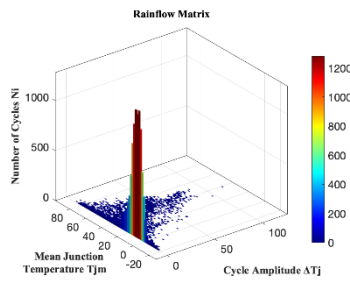


Fig. 5.18 (e). Rainflow Histogram with sizing ratio $R_s = 1.2$ at Denmark

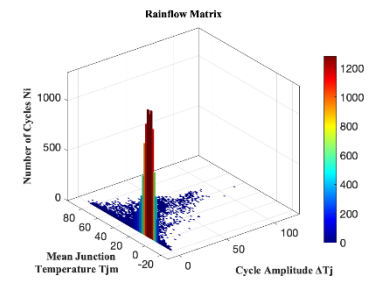


Fig. 5.18 (f). Rainflow Histogram with sizing ratio $R_s = 1.4$ at Denmark

5.3.2.3. Life Time Evaluation:

For the lifetime evaluation, static values (mean values) need to be derived from the rain flow analysis. The lifetime corresponds to the static values that are calculated with Eq. 5.1 and are tabulated in the following Table. 5.4.

At both locations with PV panel oversizing decreased lifetime is recorded. At the India location, lifetime decreased from 45.42 to 3.59 years, at Denmark location lifetime decreased from 89.66 to 10.05 years.

Table. 5.4. Lifetime Evaluation for Static Parameters

Country		Mean Junction Temperature (T_{jm})	Cycle Amplitude (ΔT_j)	Life Consumption (LC)	Lifetime in Years (LT)
India	Over Sizing Ratio $R_s = 1.0$	59.77 °C	5.95 °C	0.02201564	45.42
	Over Sizing Ratio $R_s = 1.2$	68.45 °C	7.95 °C	0.08697831	11.49
	Over Sizing Ratio $R_s = 1.4$	77.84 °C	10.12 °C	0.27791115	3.59
Denmark	Over Sizing Ratio $R_s = 1.0$	19.23 °C	4.69 °C	0.01115268	89.66
	Over Sizing Ratio $R_s = 1.2$	21.03 °C	6.08 °C	0.03622299	27.60
	Over Sizing Ratio $R_s = 1.4$	23.02 °C	7.59 °C	0.09944222	10.05

5.3.2.4. Monte Carlo Simulation based Reliability (B_{10}) Evaluation:

Monte Carlo simulation is used to generate 10000 samples with 5 % variation. The lifetime for each sample is calculated for different R_s using Eq. 5.1. All the samples are fitted in two parameter Weibull distribution. The lifetime distribution at India and Denmark locations are shown in Fig. 5.19 and Fig. 5.20 respectively.

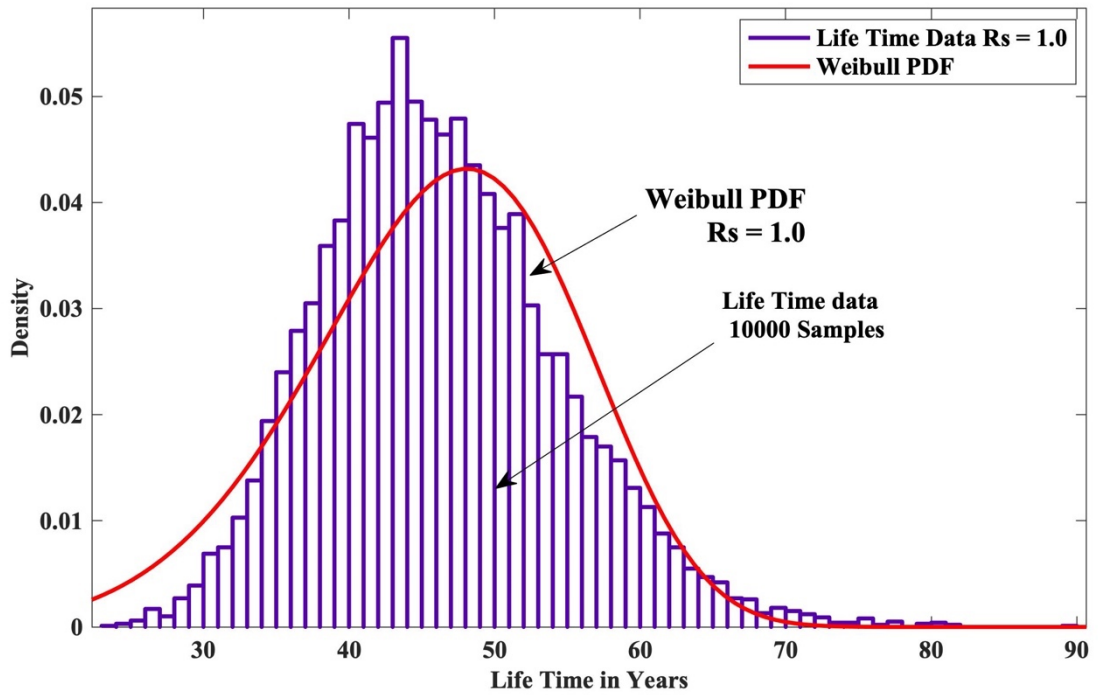


Fig. 5.19(a). Monte Carlo Simulation Lifetime distribution with $R_s = 1.0$ at India

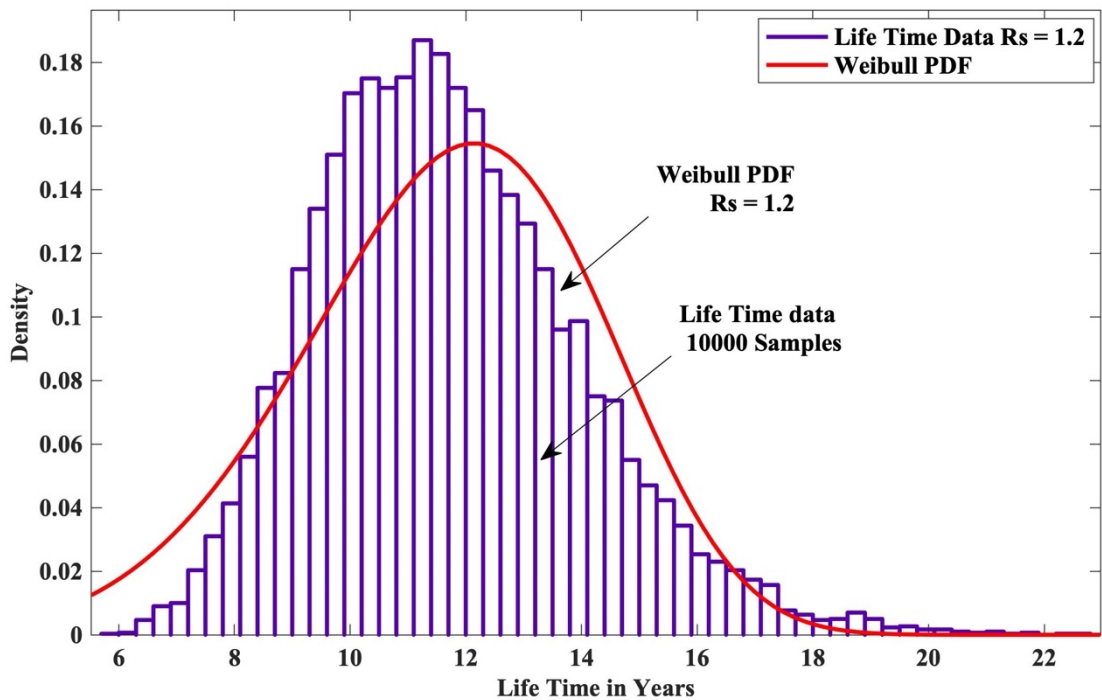


Fig. 5.19(b). Monte Carlo Simulation Lifetime distribution with $R_s = 1.2$ at India

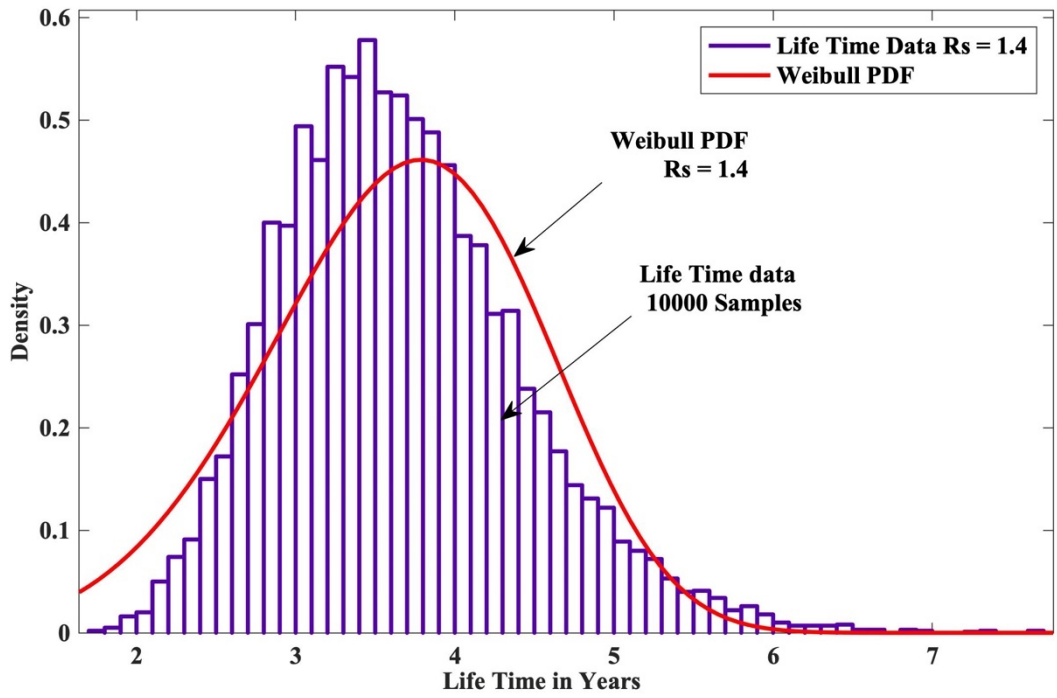


Fig. 5.19(c). Monte Carlo Simulation Lifetime distribution with $R_s = 1.4$ at India

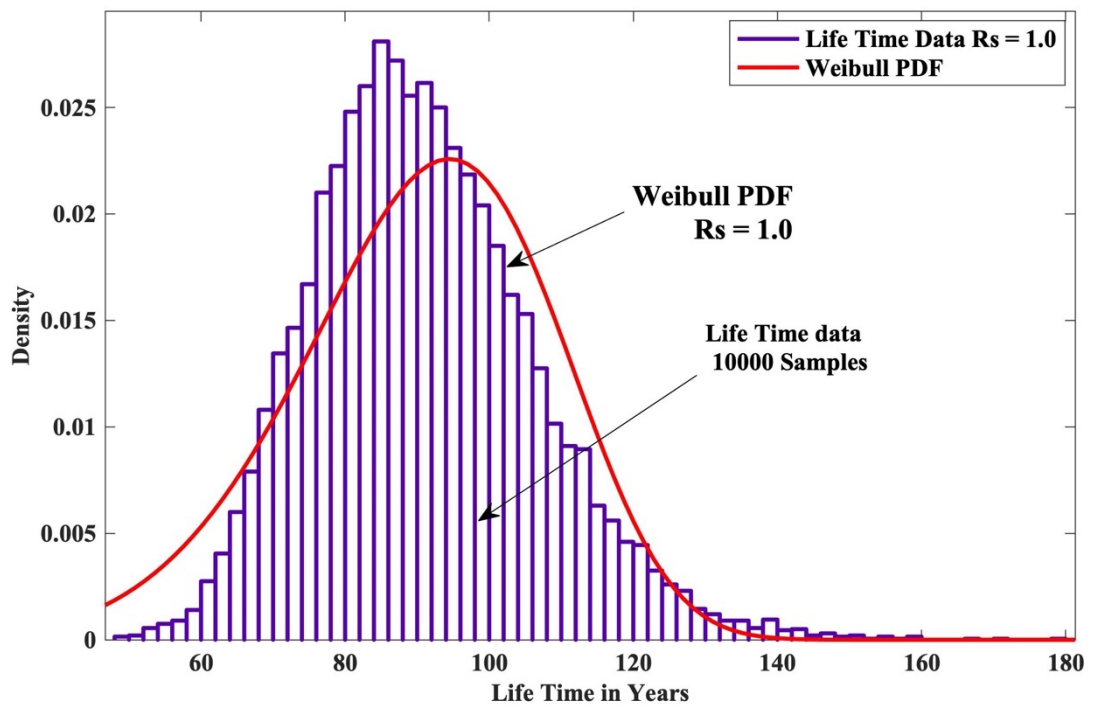


Fig. 5.20(a). Monte Carlo Simulation Lifetime distribution with $R_s = 1.0$ at Denmark

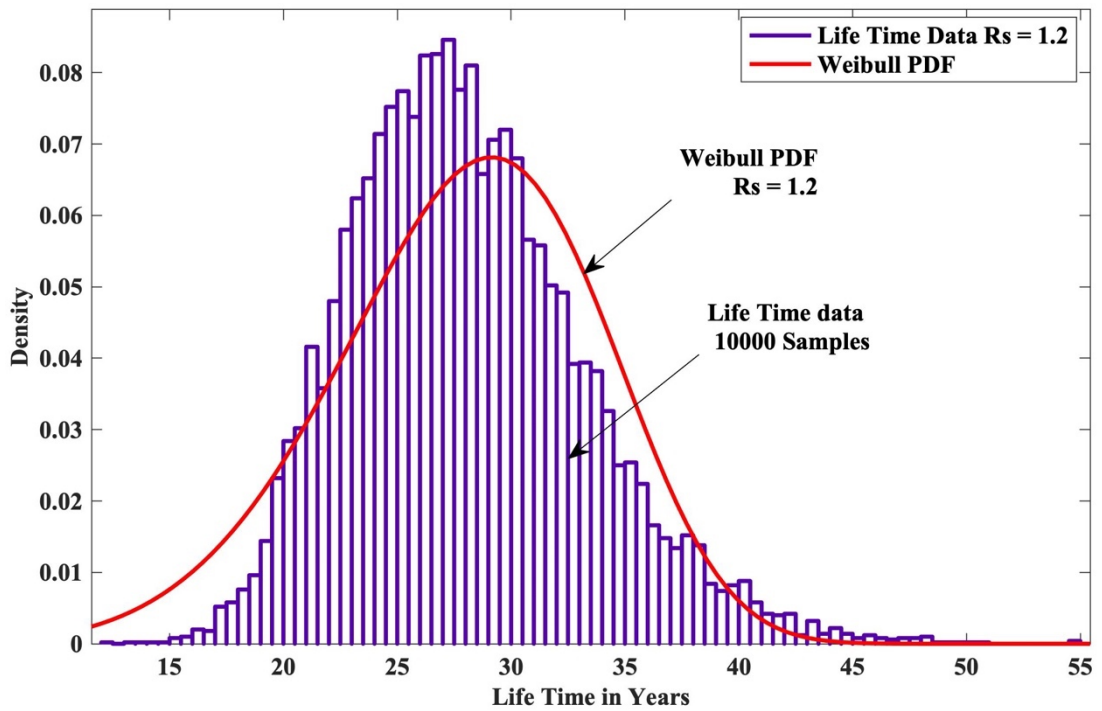


Fig. 5.20(b). Monte Carlo Simulation Lifetime distribution with $R_s = 1.2$ at Denmark

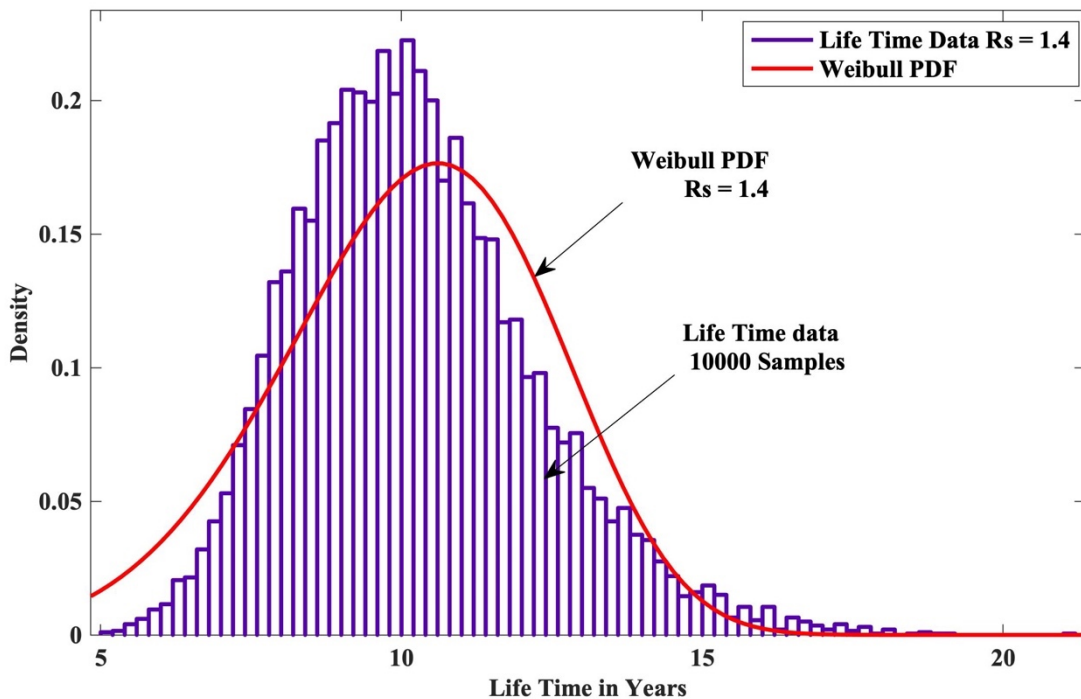


Fig. 5.20(c). Monte Carlo Simulation Lifetime distribution with $R_s = 1.4$ at Denmark

The reliability function $R(t)$ is calculated using two parameter Weibull distribution. Component level reliability is calculated using Eq. 5.4, system level reliability is calculated using Eq. 5.5, B_{10} lifetime is calculated using Eq. 5.6. $R(t)$ at India and Denmark locations are as shown in Fig. 5.21 and Fig. 5.22 respectively.

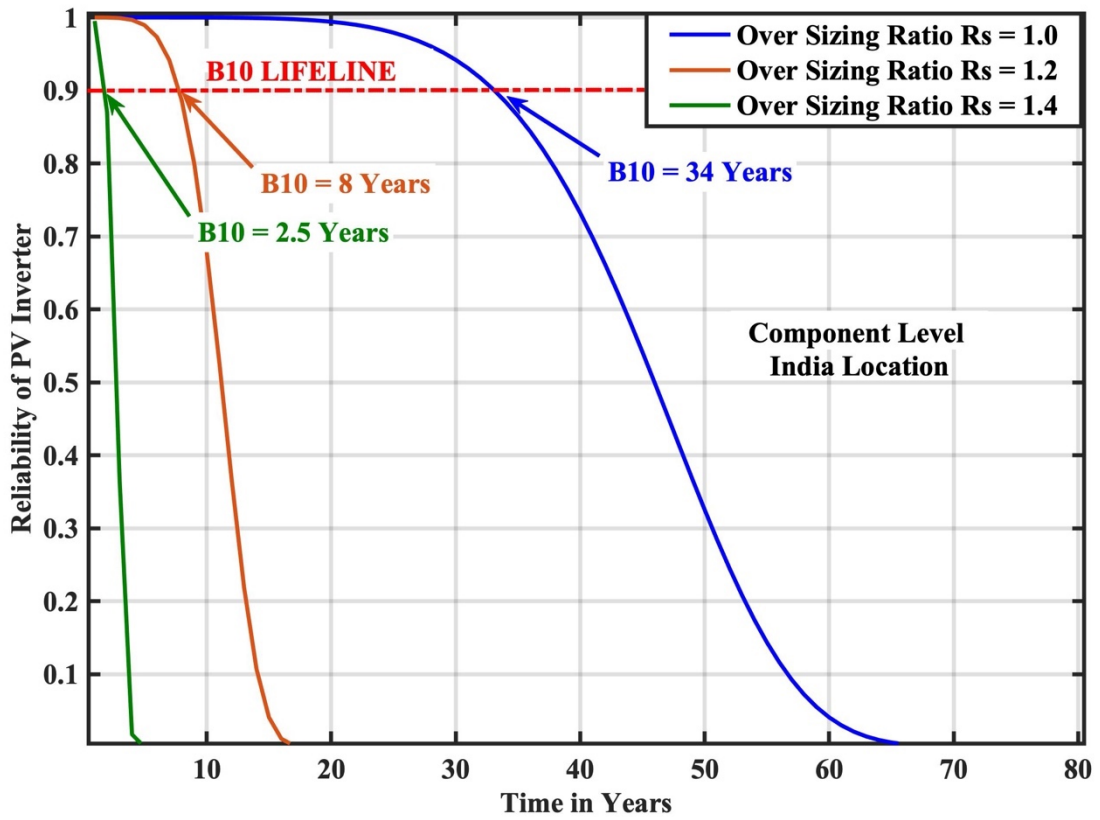


Fig. 5.21(a). Reliability (B_{10}) Evaluation of PV Inverter at India Component Level

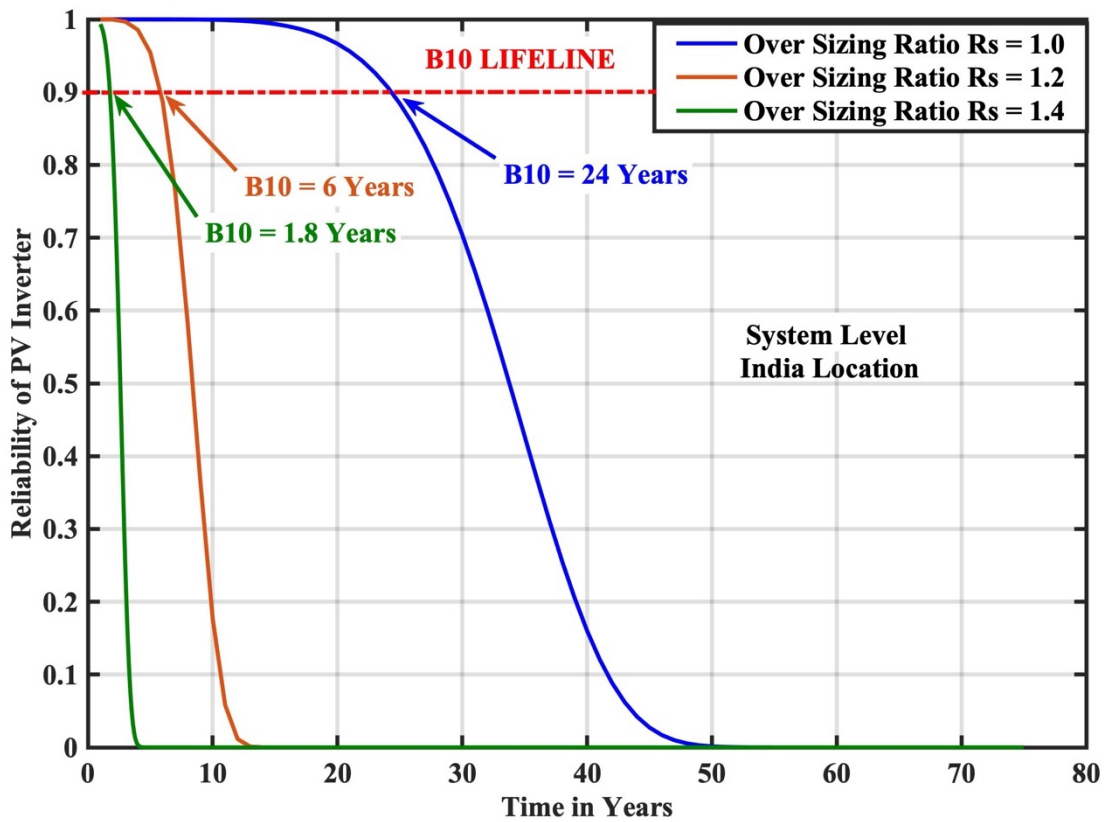


Fig. 5.21(b). Reliability (B_{10}) Evaluation of PV Inverter at India System Level

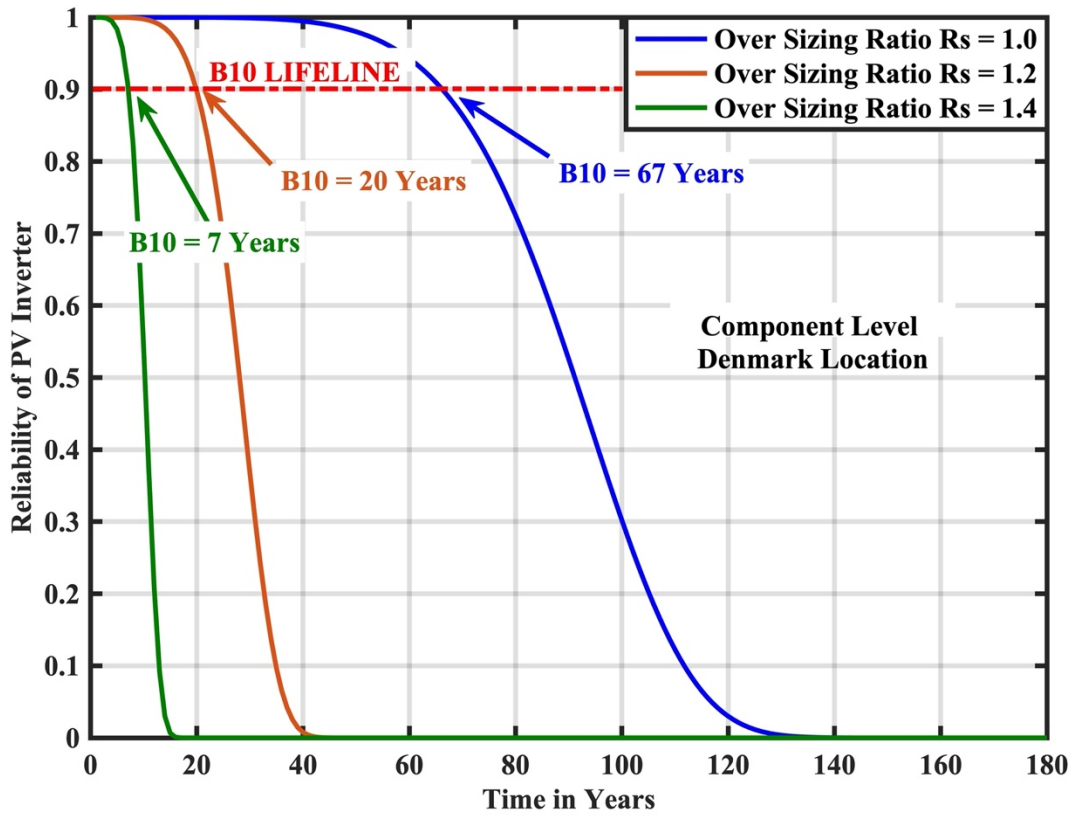


Fig. 5.22(a). Reliability (B_{10}) Evaluation of PV Inverter at Denmark Component Level

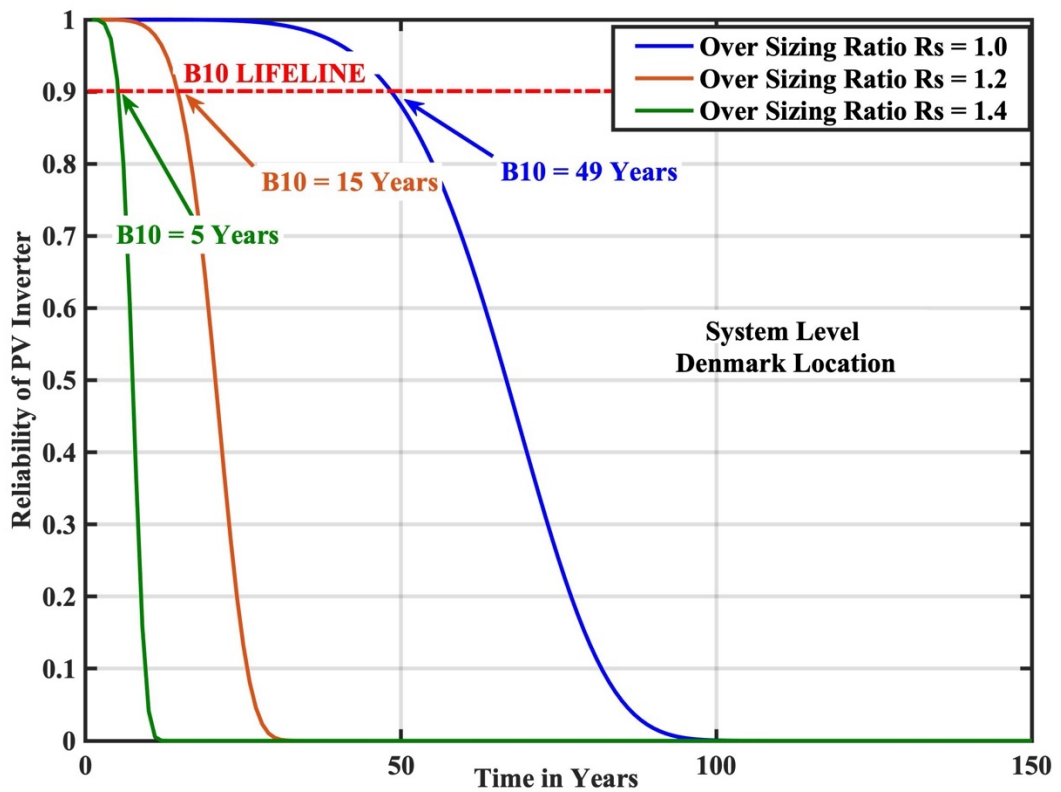


Fig. 5.22(b). Reliability (B_{10}) Evaluation of PV Inverter at Denmark System Level

From the reliability curves, it is observed that B_{10} lifetime has a significant impact when PV panel oversizing is considered. B_{10} lifetime decreases at both locations. For $R_s = 1.0$, At India component level reliability (B_{10}) is 34 years, system level reliability (B_{10}) is 24 years. Similarly, at the Denmark component level reliability (B_{10}) is 67 years, system level reliability (B_{10}) is 49 years. For $R_s = 1.2$, At India component level reliability (B_{10}) is 8 years, system level reliability (B_{10}) is 6 years. Similarly, at the Denmark component level reliability (B_{10}) is 20 years, system level reliability (B_{10}) is 15 years. For $R_s = 1.4$, At India component level reliability (B_{10}) is 2.5 years, system level reliability (B_{10}) is 1.8 years. Similarly, at the Denmark component level reliability (B_{10}) is 7 years, system level reliability (B_{10}) is 5 years

5.3.2.5. B_{10} Lifetime Comparison

PV panel oversizing on inverter reliability has a significant impact at both locations. Decrease in B_{10} lifetime is recorded at both locations, comparative analysis at the component level and system level are shown in Fig. 5.23. In India B_{10} lifetime at a component level decreased from 34 to 2.5 years, at system level decreased from 24 to 1.8 years. Similarly, in Denmark B_{10} lifetime at a component level decreased from 67 to 7 years, at system level decreased from 49 to 5 years.

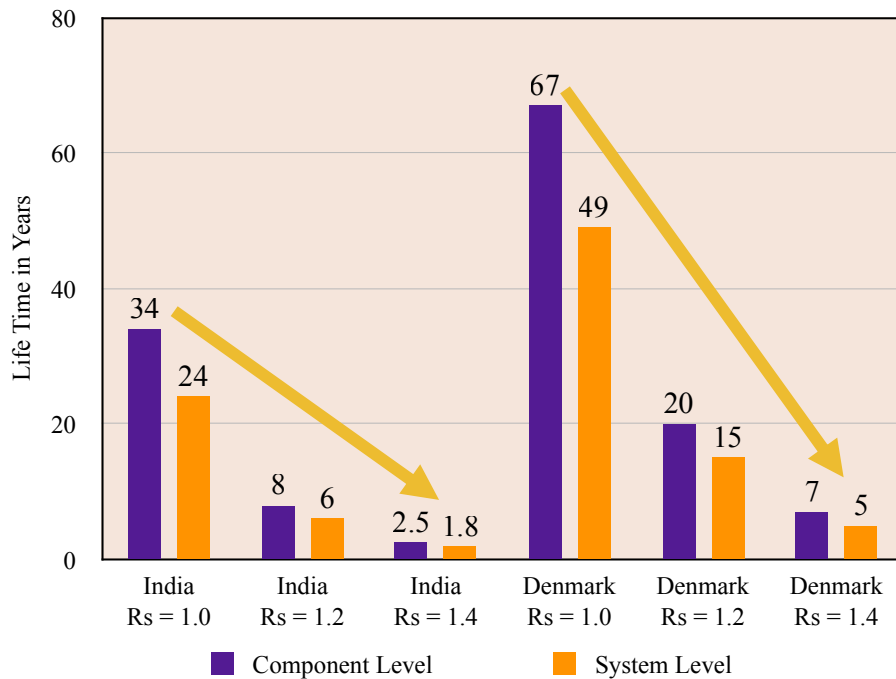


Fig. 5.23. B_{10} Lifetime Comparison

5.3.3 Impact of Bifacial PV Panel on PV Inverter Reliability:

To analyze the impact of Bifacial PV Panel on PV Inverter Reliability Bifacial PV Panel with 0%, 30%, 50% more energy yield is considered.

5.3.3.1. Junction Temperature Considering Bifacial PV Panel:

In this case, grid connected PV inverter with a Bifacial PV panel is considered. With the foster electro model of IGBT junction temperature is calculated. The junction temperature correspond to the yearly mission profile at India and Denmark locations are shown in Fig: 5.24 and Fig: 5.25 respectively.

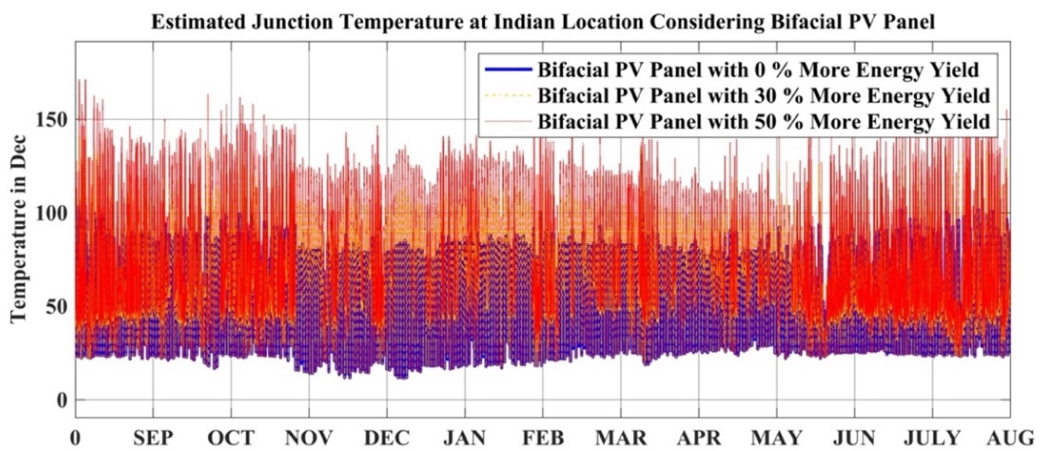


Fig. 5.24. Junction Temperature with Bifacial PV Panel at India.

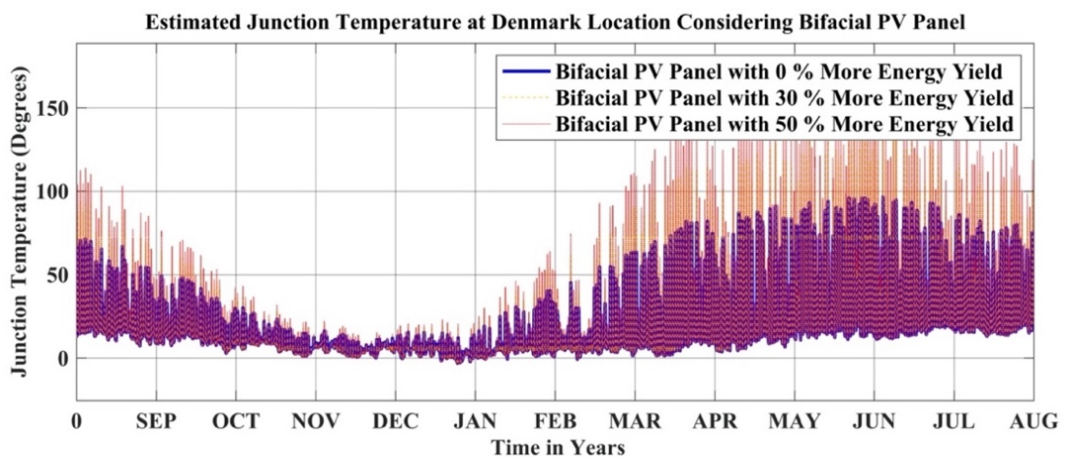


Fig. 5.25. Junction Temperature with Bifacial PV Panel at Denmark.

The junction temperature of IGBT is estimated considering a bifacial PV panel with 0 % more energy yield, 30 % more energy yield, 50 % more energy yield. In all three cases at both locations, junction temperature increases with the increase in bifacial PV panel energy yield.

The junction temperature by considering the Bifacial PV panel shows the increasing trend at both locations. The average values of calculated junction temperature at both locations are compared and presented in Fig. 5.26. In India, it is increased from 55.66 °C to 75.08 °C. Similarly, at the Denmark location, it is increased from 16.38 °C to 19.92 °C.

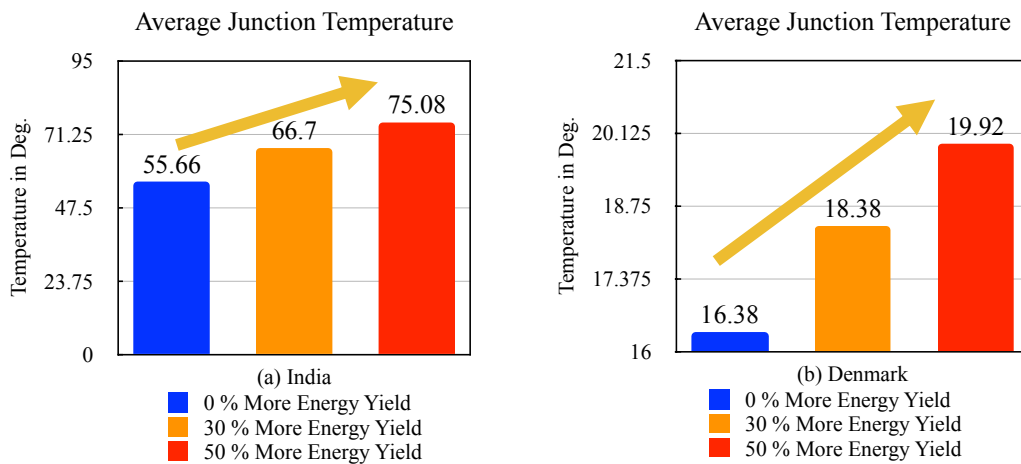


Fig. 5.26. Average Junction Temperature with Bifacial PV Panel

5.3.3.2. Rainflow Analysis:

Junction temperature variations are analyzed by rain flow counting algorithm. Number of Cycles N_i , Mean Junction Temperature T_{jm} , Cycle Amplitude ΔT_j of calculated junction temperature at India and Denmark locations are shown in Fig. 5.27.

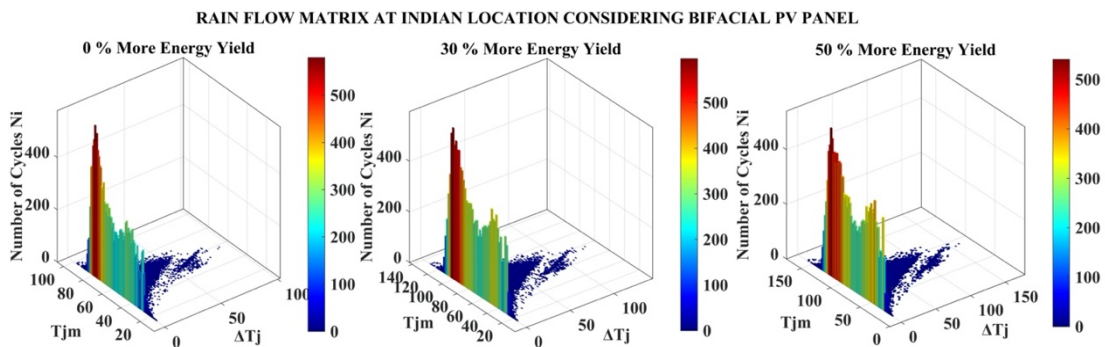


Fig: 5.27(a) Rain Flow Matrix at India Location

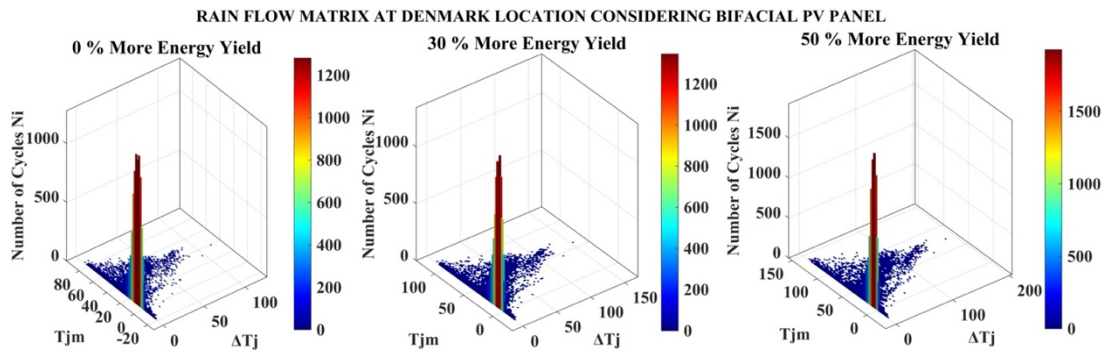


Fig. 5.27(b) Rain flow Matrix at Denmark Location.

5.3.3.3. Life Time Evaluation:

For the lifetime evaluation, static values (mean values) need to be derived from the rainflow analysis. In Table. 5.5, lifetime is evaluated for bifacial PV panel with 0 %, 30%, and 50% of energy yield.

Table. 5.5. Lifetime Evaluation for Static Parameters

Country		Mean Junction Temperature (T_{jm})	Cycle Amplitude (ΔT_j)	Life Consumption (LC)	Lifetime in Years (LF)
India	0 % of Energy Yield	59.77 °C	5.95 °C	0.02201673	45.42
	30 % of Energy Yield	72.84 °C	8.95 °C	0.1529052	6.54
	50 % of Energy Yield	82.85 °C	11.30 °C	0.47619048	2.10
Denmark	0 % of Energy Yield	19.23 °C	4.69 °C	0.01115325	89.66
	30 % of Energy Yield	21.98 °C	6.77 °C	0.05913661	16.91
	50 % of Energy Yield	24.14 °C	8.42 °C	0.15948963	6.27

At both locations with Bifacial PV panel decreased lifetime is recorded. At the India location lifetime decreased from 45.42 to 2.10 years, at Denmark location's lifetime decreased from 89.66 to 6.27 years.

5.3.3.4. Monte Carlo Simulation based Reliability (B_{10}) Evaluation:

Monte Carlo simulation is used to generate 10000 samples with five percent variation for all the parameters in Eq. 5.1. Monte Carlo Simulation lifetime distribution of PV inverter at India and Denmark locations are shown in Fig. 5.28 and Fig. 5.29 respectively

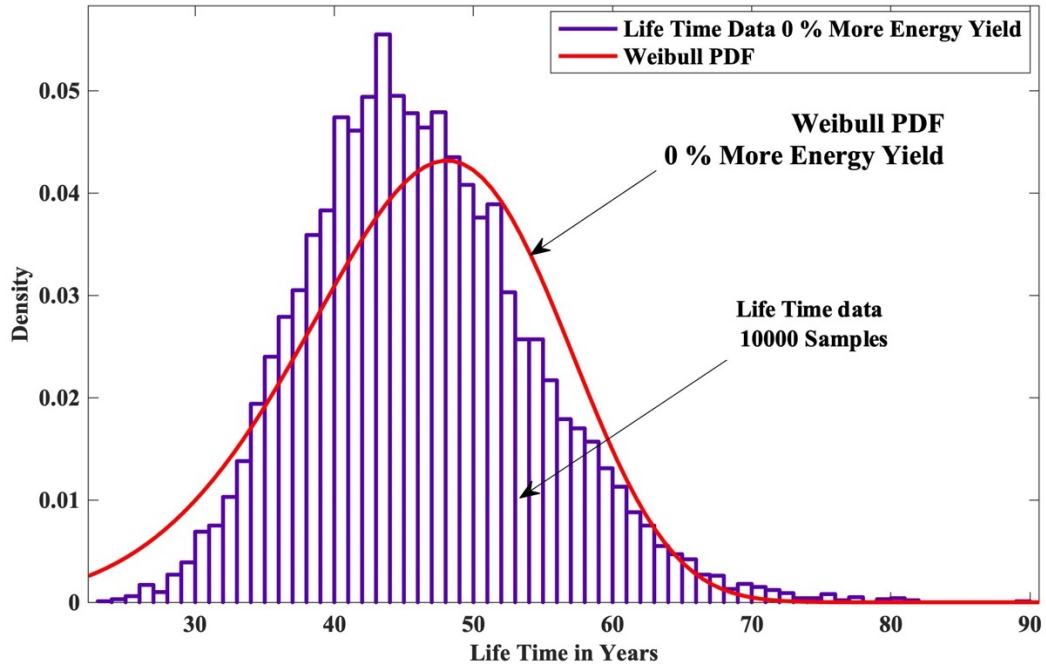


Fig. 5.28(a). Monte Carlo Simulation Lifetime distribution with 0 % More Energy Yield at India

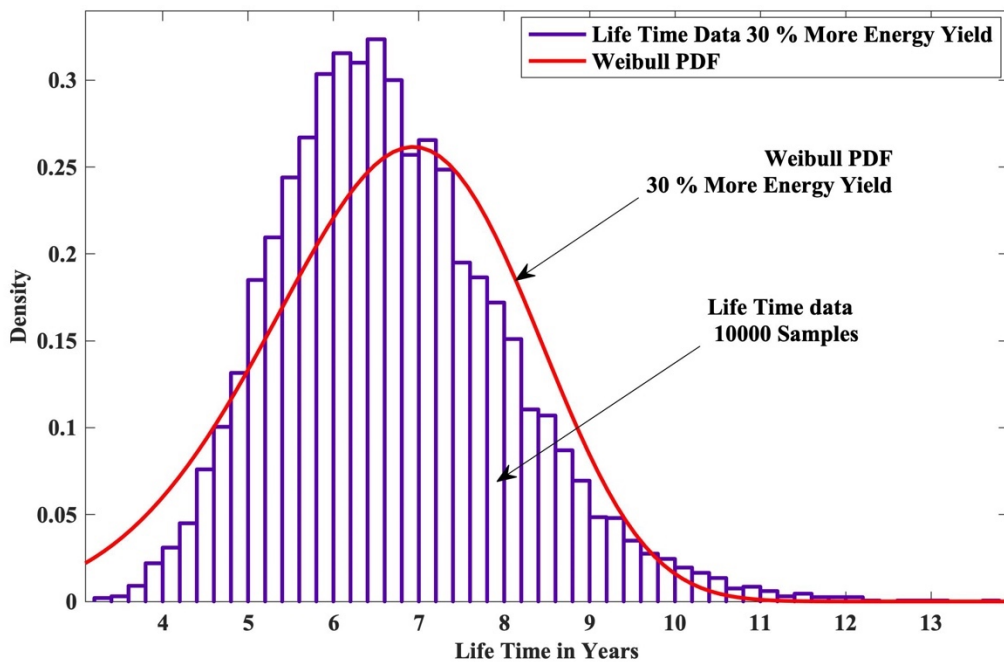


Fig. 5.28(b). Monte Carlo Simulation Lifetime distribution with 30 % More Energy Yield at India

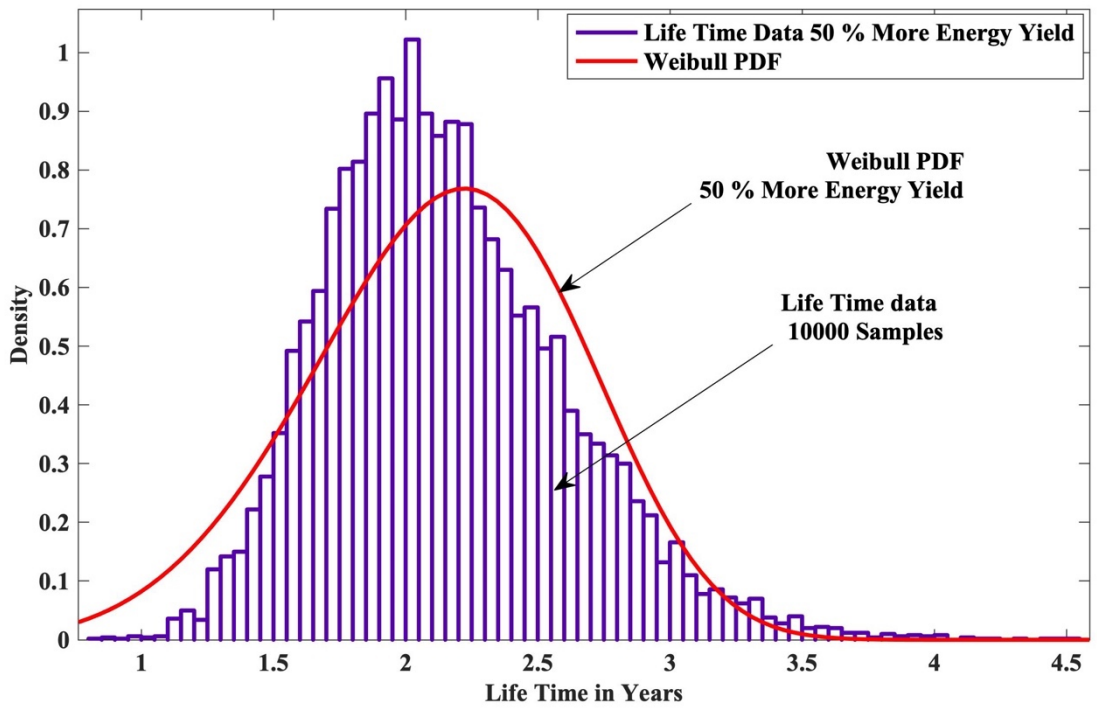


Fig. 5.28(c). Monte Carlo Simulation Lifetime distribution with 50 % More Energy Yield at India

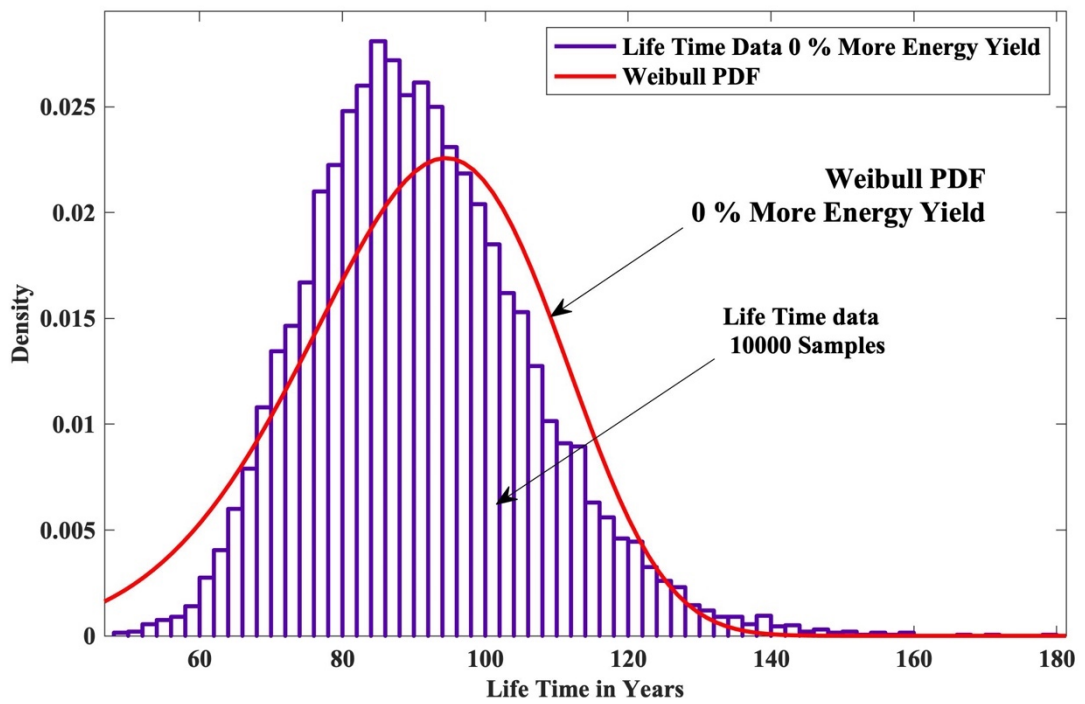


Fig. 5.29(a). Monte Carlo Simulation Lifetime distribution with 0 % More Energy Yield at Denmark

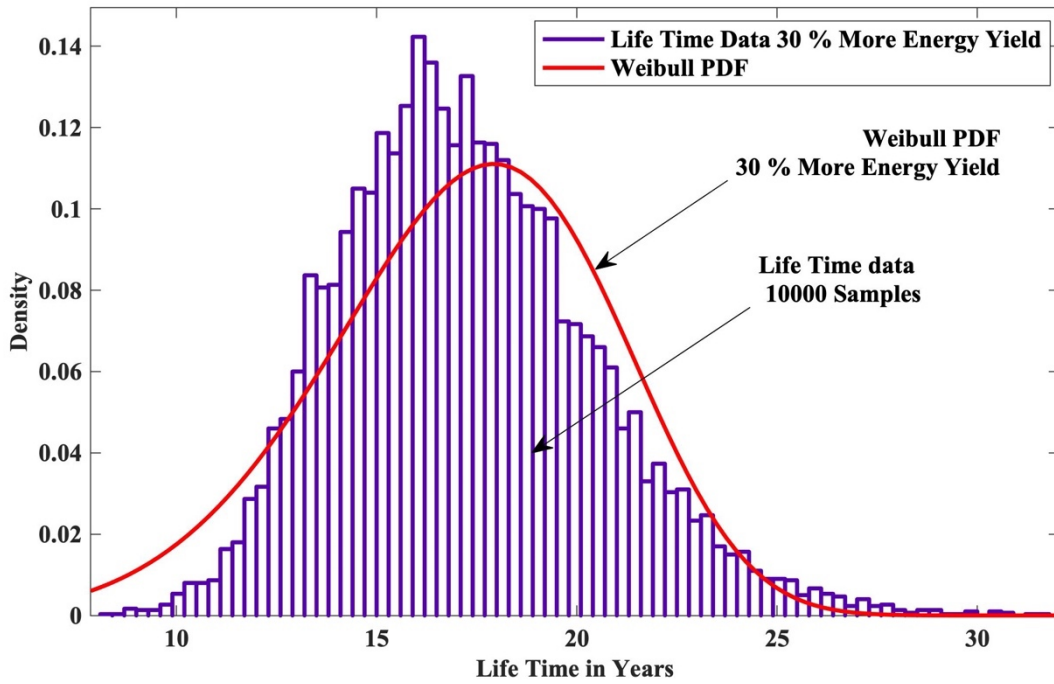


Fig. 5.29(b). Monte Carlo Simulation Lifetime distribution with 30 % More Energy Yield at Denmark

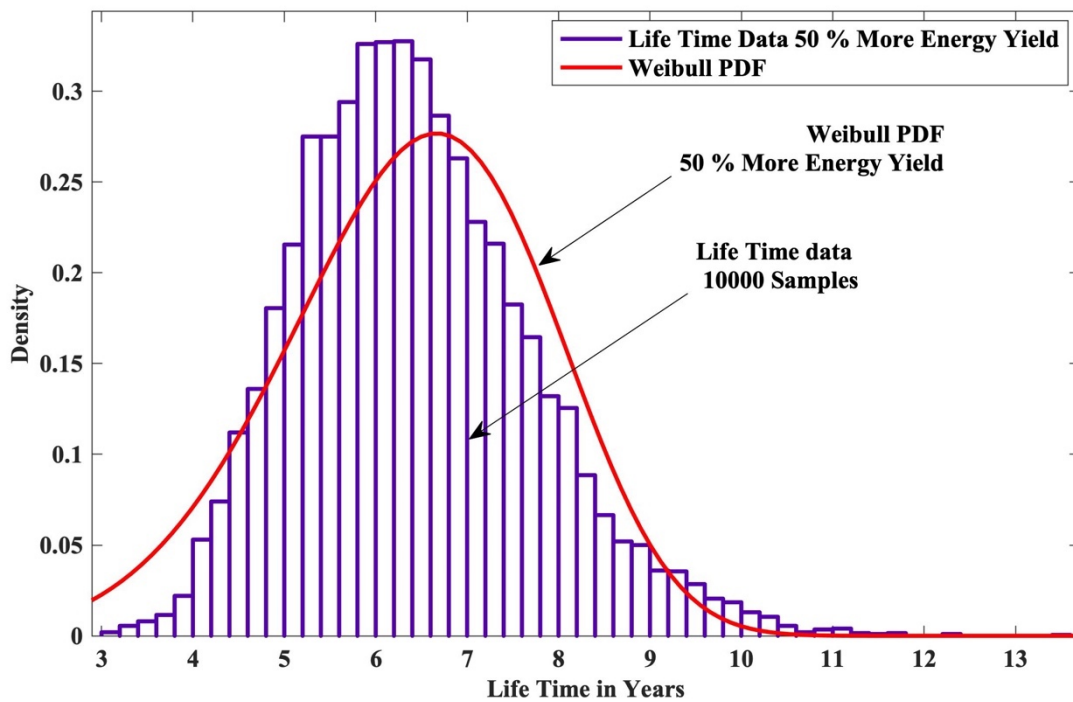


Fig. 5.29(c). Monte Carlo Simulation Lifetime distribution with 50 % More Energy Yield at Denmark

The reliability function $R(t)$ is calculated using two parameter Weibull distribution. Component level reliability is calculated using Eq. 5.4, system level

reliability is calculated using Eq. 5.5, B_{10} lifetime is calculated using Eq. 5.6. $R(t)$ at India and Denmark locations are as shown in Fig. 5.30 and Fig. 5.31 respectively.

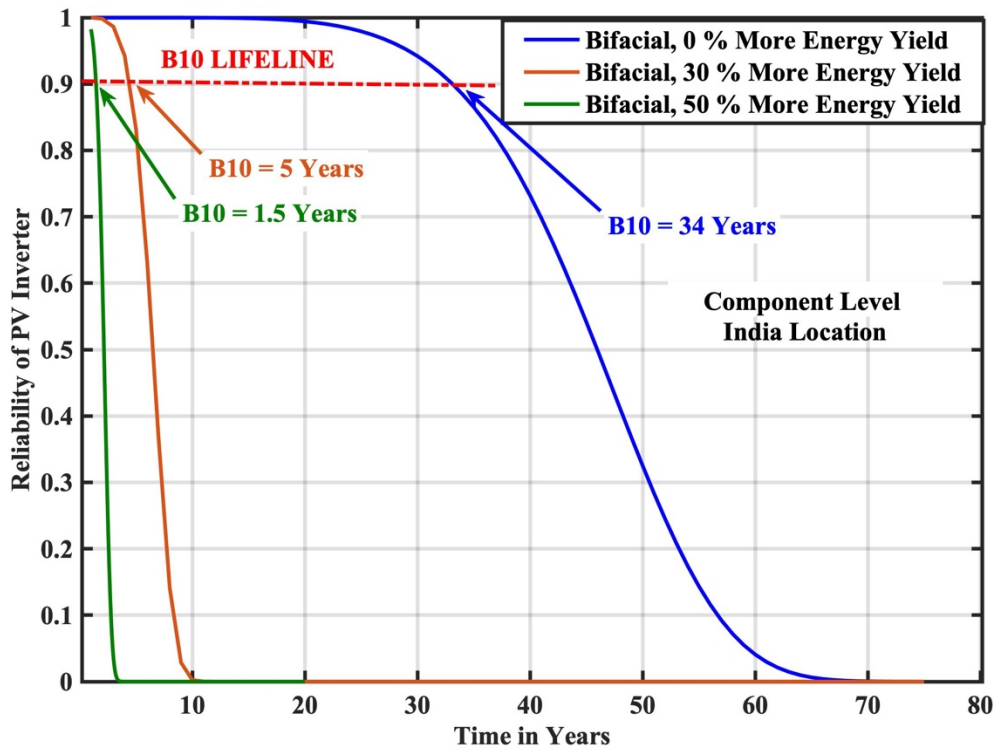


Fig. 5.30(a). Reliability function of PV inverter at India Location Component Level

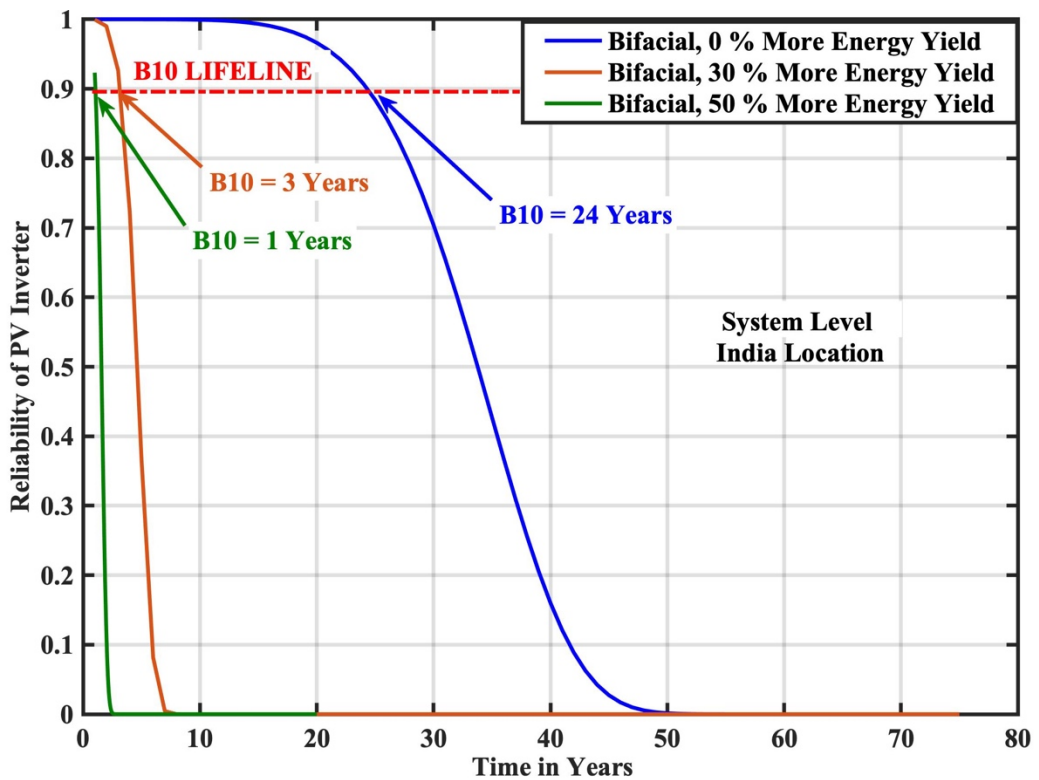


Fig. 5.30(b). Reliability function of PV inverter at India Location System Level

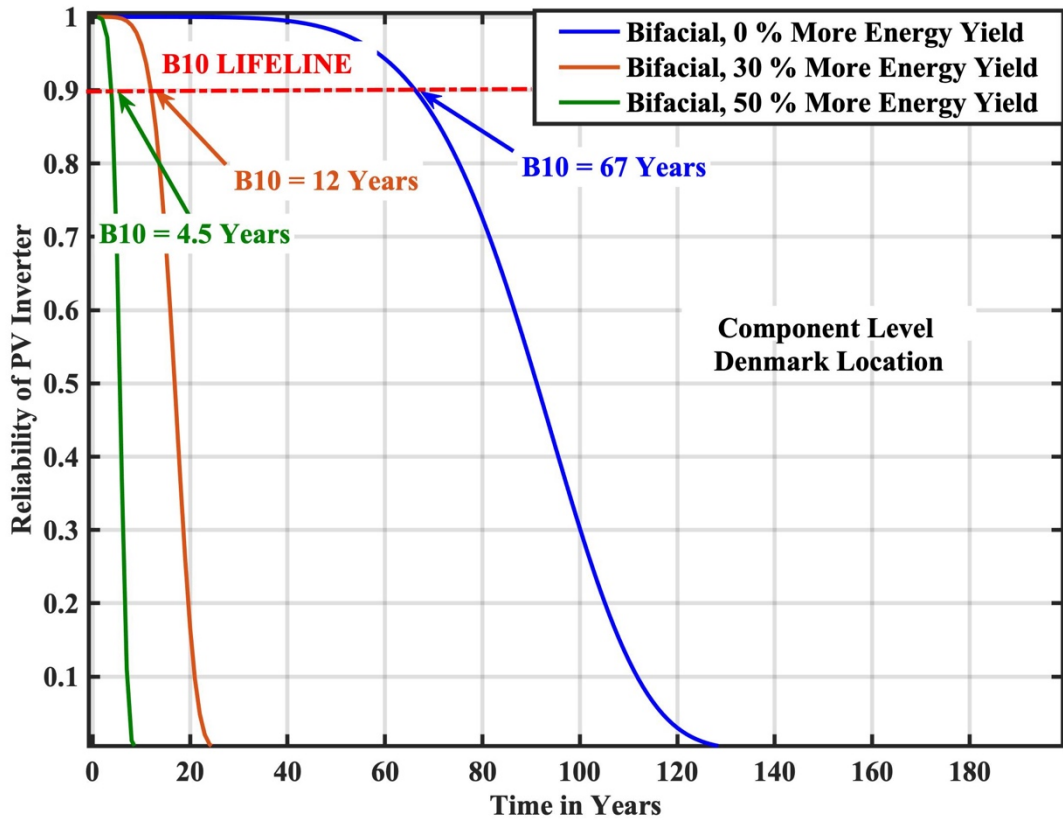


Fig. 5.31(a). Reliability function of PV inverter at Denmark Location Component Level

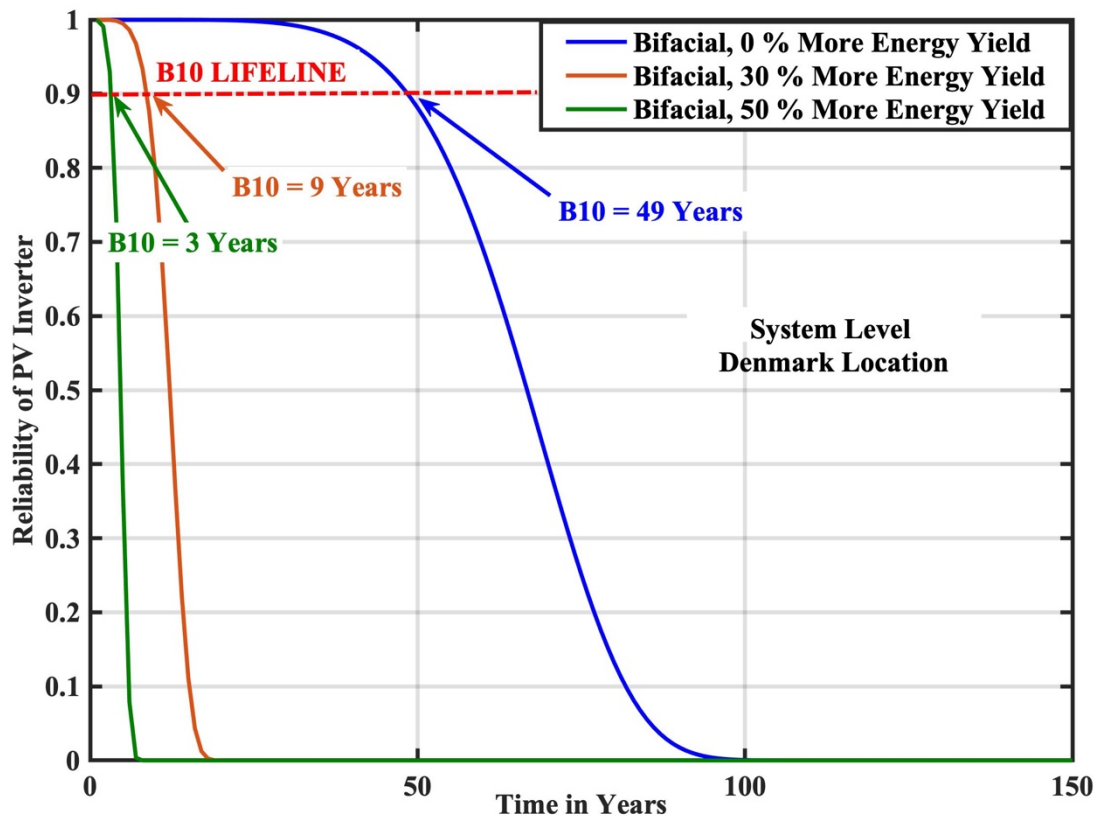


Fig. 5.31(b). Reliability function of PV inverter at Denmark Location System Level

From the reliability curves, it is observed that B_{10} lifetime has a significant impact when a Bifacial PV panel is considered. B_{10} lifetime decreases at both locations. For 0% more EY, At India component level reliability (B_{10}) is 34 years, system level reliability (B_{10}) is 24 years. Similarly, at the Denmark component level reliability (B_{10}) is 67 years, system level reliability (B_{10}) is 49 years. For 30 % more EY, At India component level reliability (B_{10}) is 5 years, system level reliability (B_{10}) is 3 years. Similarly, at the Denmark component level reliability (B_{10}) is 12 years, system level reliability (B_{10}) is 9 years. For 50 % more EY, At India component level reliability (B_{10}) is 1.5 years, system level reliability (B_{10}) is 1 year. Similarly, in Denmark component level reliability (B_{10}) is 4.5 years, system level reliability (B_{10}) is 3 years

5.3.3.5. B_{10} Lifetime Comparison

Bifacial PV panel on inverter reliability has a significant impact at both locations. Decrease in B_{10} lifetime is recorded at both locations, comparative analysis at the component level and system level are shown in Fig. 5.32. In India B_{10} lifetime at a component level decreased from 34 to 1.5 years, at the system decreased from 24 to 1 year. Similarly, in Denmark B_{10} lifetime at a component level decreased from 67 to 4.5 years, at system level decreased from 49 to 3 years.

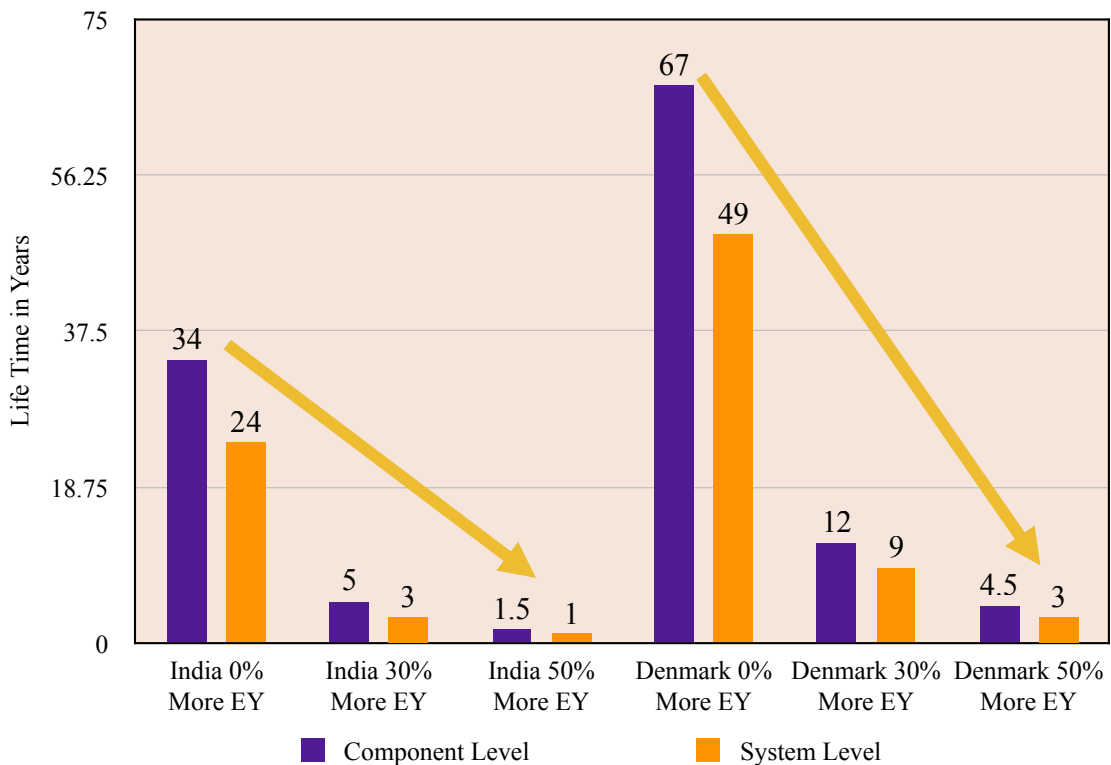


Fig. 5.32. B_{10} Lifetime Comparison

5.4 Chapter Summary

. In this chapter impact of the Installation site, PV panel degradation rate, PV panel oversizing, Bifacial PV panel are presented. Installation site has a significant impact, reliability varies from location to location based on climatic conditions. The reliability of PV inverter is reported more in cold climatic conditions. At the India component level reliability (B_{10}) is 34 years, system level reliability (B_{10}) is 24 years. Similarly at Denmark component level reliability (B_{10}) is 67 years, system level reliability (B_{10}) is 49 years.

The degradation rate exhibits an increasing trend at both locations. The degradation rate of 1.93 % per year for five years of operation is considered at the India Location and 0.15 % per year for five years of operation is considered at Denmark Location. At the India component level reliability (B_{10}) is increased from 34 years to 78 years, system level reliability (B_{10}) is increased from 24 years to 57 years. Similarly in Denmark component level reliability (B_{10}) is increased from 67 years to 71 years, system level reliability (B_{10}) is increased from 49 years to 52 years.

Oversizing of PV panel exhibits decreasing trend at both locations. To analyze the impact of PV Panel Oversizing on PV inverter panel sizing ratio $R_s = 1.0, 1.2, 1.4$ are considered. At the India component level reliability (B_{10}) is decreased from 34 years to 2.5 years, system level reliability (B_{10}) is decreased from 24 years to 1.8 years. Similarly in Denmark component level reliability (B_{10}) is decreased from 67 years to 7 years, system level reliability (B_{10}) is decreased from 49 years to 5 years.

The bifacial PV panel exhibits decreasing trend at both locations. To analyze the impact of Bifacial PV Panel on PV Inverter Reliability Bifacial PV Panel with 0%, 30%, 50% more energy yield are considered. At the India component level reliability (B_{10}) is decreased from 34 years to 1.5 years, system level reliability (B_{10}) is decreased from 24 years to 1 year. Similarly in Denmark component level reliability (B_{10}) is decreased from 67 years to 4.5 years, system level reliability (B_{10}) is decreased from 49 years to 3 years.

CHAPTER 6

RELIABILITY IMPROVEMENT SOLUTIONS

6.1 Reliability Improvement Methodology:

Conventional Si-based power electronics switches reached their theoretical limits and are not capable to address current power needs. Significant advancements are made in Si IGBTs but in the case of Si diodes, these advancements are not up to the mark, also restrict the performance of power electronic converters [97]. Hence for the Reliability Improvement of PV inverter hybrid Si/SiC switch is proposed as shown in Fig. 6.1. PV inverter consists of four 600V/30A hybrid Switch (Si-IGBT (IGW30N60H3)/SiC- diode (C3D20060D)) as shown in Fig. 6.1, its effectiveness is analyzed by comparing it with conventional Switch (Si-IGBT (IGW30N60H3)/Si-Schottky diode (IGW30N60H3)).

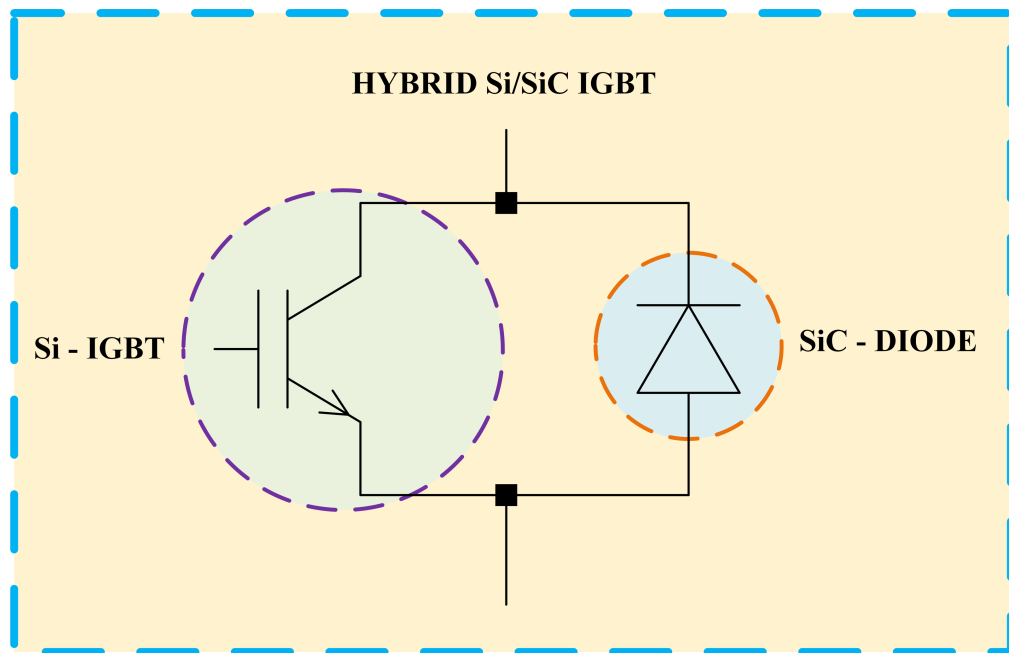


Fig. 6.1. Hybrid IGBT

6.2 Reliability Analysis of PV inverter Considering Hybrid Si/SiC Switch:

The reliability analysis of PV inverter is performed at both India and Denmark locations considering hybrid Si/SiC Switch.

6.2.1. Junction Temperature Considering Hybrid Si/SiC Switch:

The yearly mission profile is translated to Junction Temperature using foster electro thermal model. Junction Temperature with conventional Si switch and Hybrid Si/SiC switch at India and Denmark Location are shown in Fig. 6.2 and Fig. 6.3 respectively.

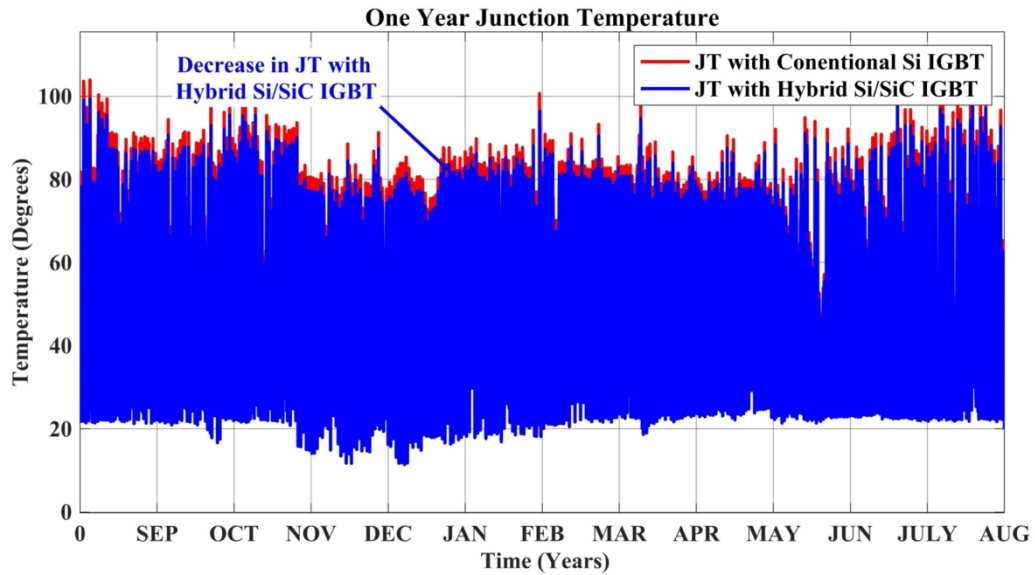


Fig. 6.2. One year estimated junction temperature at India Location

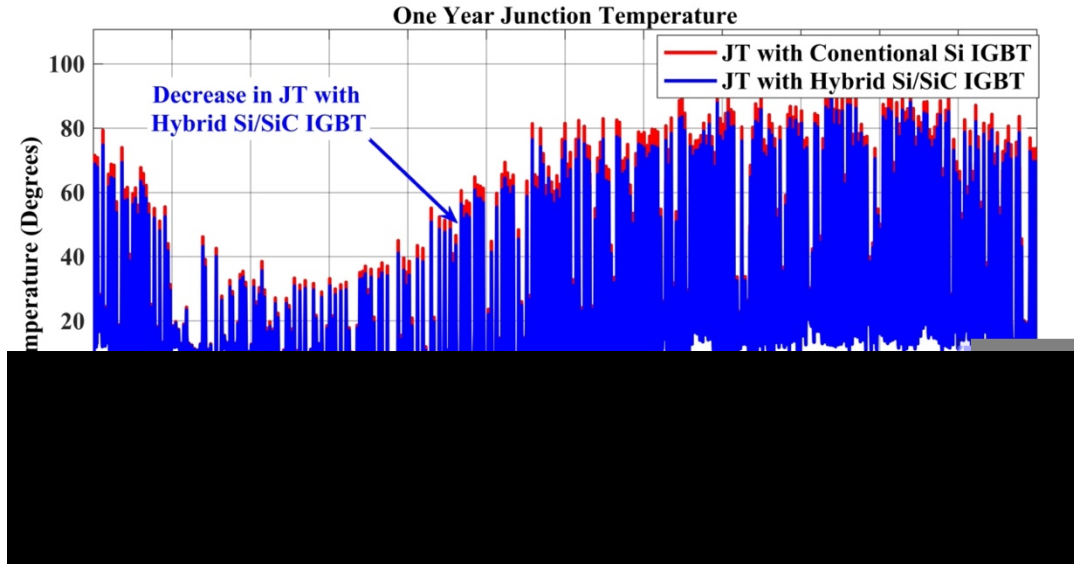


Fig. 6.3. One year estimated junction temperature at Denmark Location

The junction temperature by considering hybrid Si/SiC IGBT shows the decreasing trend at both locations. The average values of calculated junction temperature at both locations are compared and presented in Fig. 6.4. In India, it is

decreased from 55.66 °C to 53.9 °C. Similarly, at the Denmark location, it is decreased from 16.38 °C to 15.91 °C.

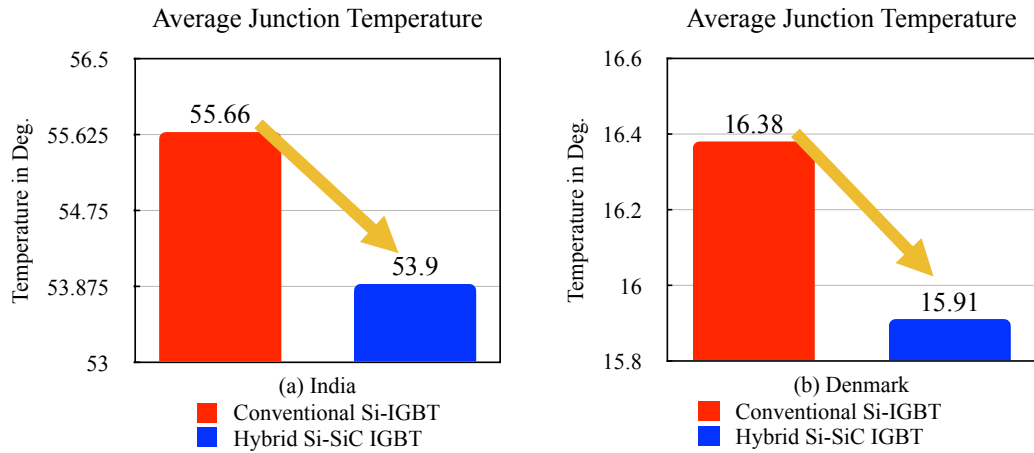
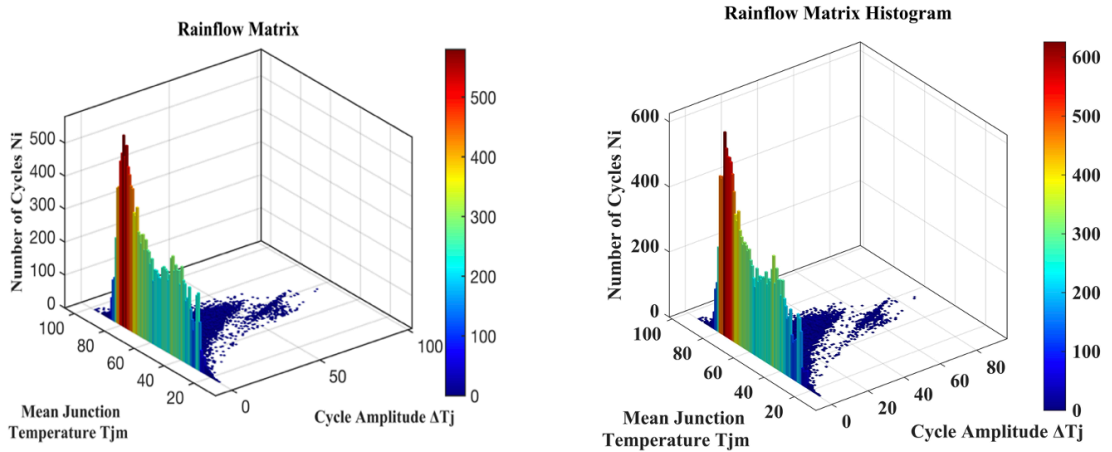


Fig. 6.4 Average Junction Temperature (a) India (b) Denmark

6.2.2 Rain Flow Analysis:

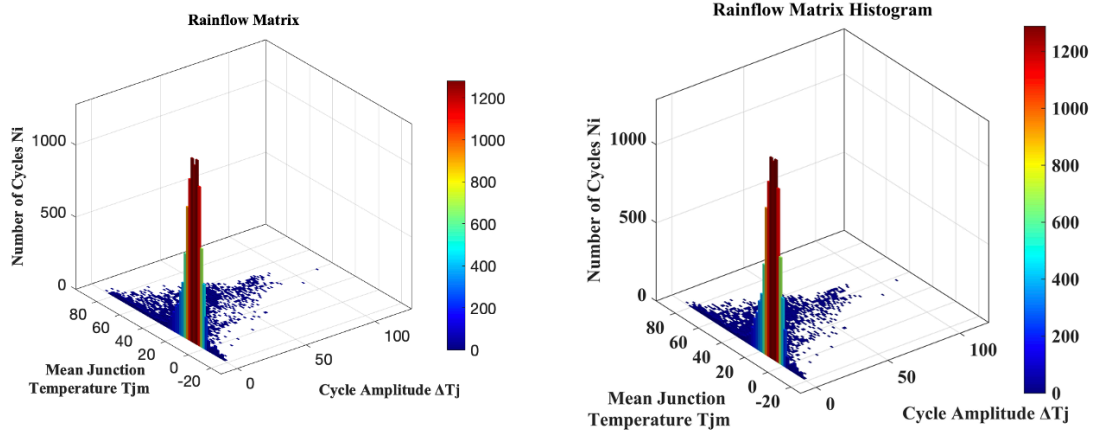
Junction temperature variations are analyzed by the rain flow counting algorithm. Number of Cycles N_i , Mean Junction Temperature T_{jm} , Cycle Amplitude ΔT_j of estimated junction temperature at India and Denmark locations are shown in Fig. 6.5.



(a) Rainflow Matrix with Si-IGBT

(b) Rainflow Matrix with Si-SiC IGBT

Fig. 6.5(a). Rain Flow Matrix at India Location



(a) Rainflow Matrix with Si-IGBT

(b) Rainflow Matrix with Si-SiC IGBT

Fig. 6.5(a). Rain flow Matrix at Denmark Location

6.2.3. Life Time Evaluation:

For the lifetime evaluation, static values (mean values) need to be derived from the rain flow analysis. The lifetime corresponds to the static values are calculated with Eq. 5.1 and are tabulated in the following Table. 6.1.

Table. 6.1. Lifetime Evaluation for Static Parameters

Country		Mean Junction Temperature (T_{jm})	Cycle Amplitude (ΔT_j)	Life Consumption (LC)	Lifetime in Years (LT)
India	Conventional Si-IGBT	59.77 °C	5.95 °C	0.02201564	45.42
	Hybrid Si-SiC IGBT	58.00 °C	5.66 °C	0.01737087	57.56
Denmark	Conventional Si-IGBT	19.23 °C	4.69 °C	0.01115268	89.66
	Hybrid Si-SiC IGBT	18.70 °C	4.36 °C	0.00809407	123.54

At both locations with a Hybrid Si/SiC switch, increased lifetime is recorded. At the India location, lifetime increased from 45.42 to 57.56 years, at Denmark location lifetime increased from 89.66 to 123.54 years. Since India's climate conditions are hot increased lifetime is observed than Denmark location while considering degradation rate.

6.2.4 Monte Carlo Simulation Based Reliability (B_{10}) evaluation:

With the Monte Carlo simulation 10000 samples are generated with five percent variation for all the parameters. Monte Carlo simulation lifetime distribution of PV inverter at India and Denmark locations are shown in Fig. 6.6 and Fig. 6.7 respectively.

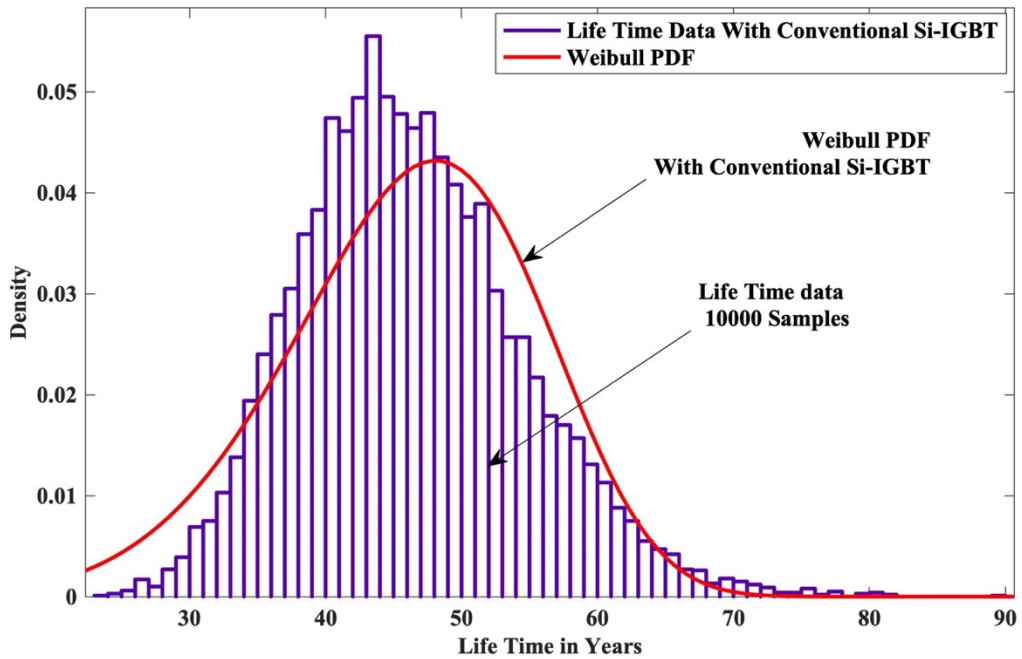


Fig. 6.6(a) Monte Carlo Simulation Lifetime Distribution of PV inverter at India Location with Conventional Si-IGBT

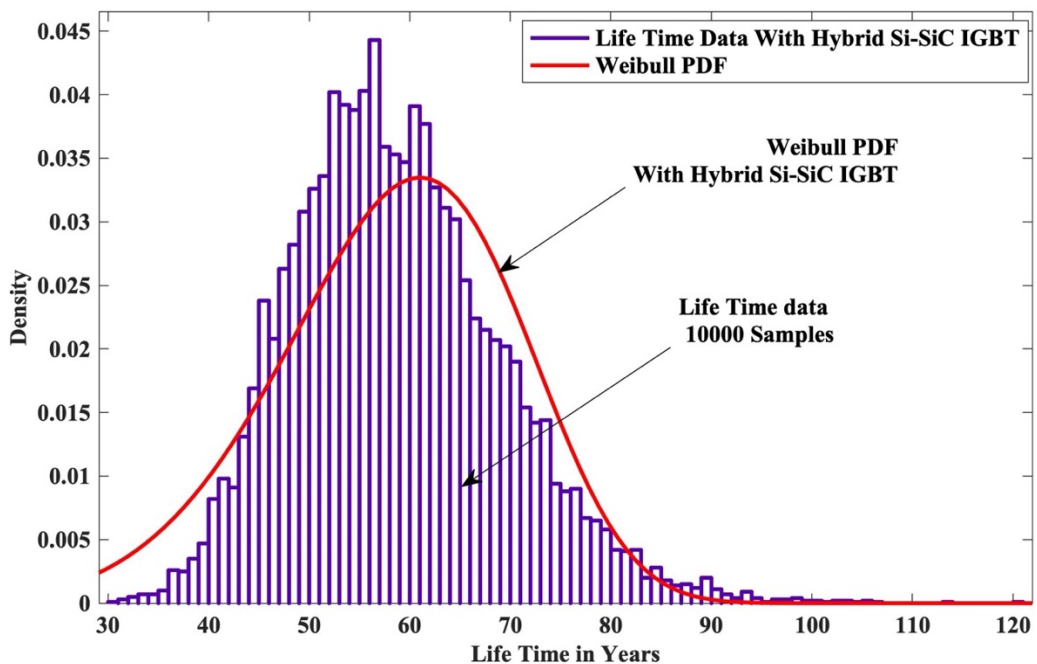


Fig. 6.6(b) Monte Carlo Simulation Lifetime Distribution of PV inverter at India Location with Hybrid Si-SiC IGBT

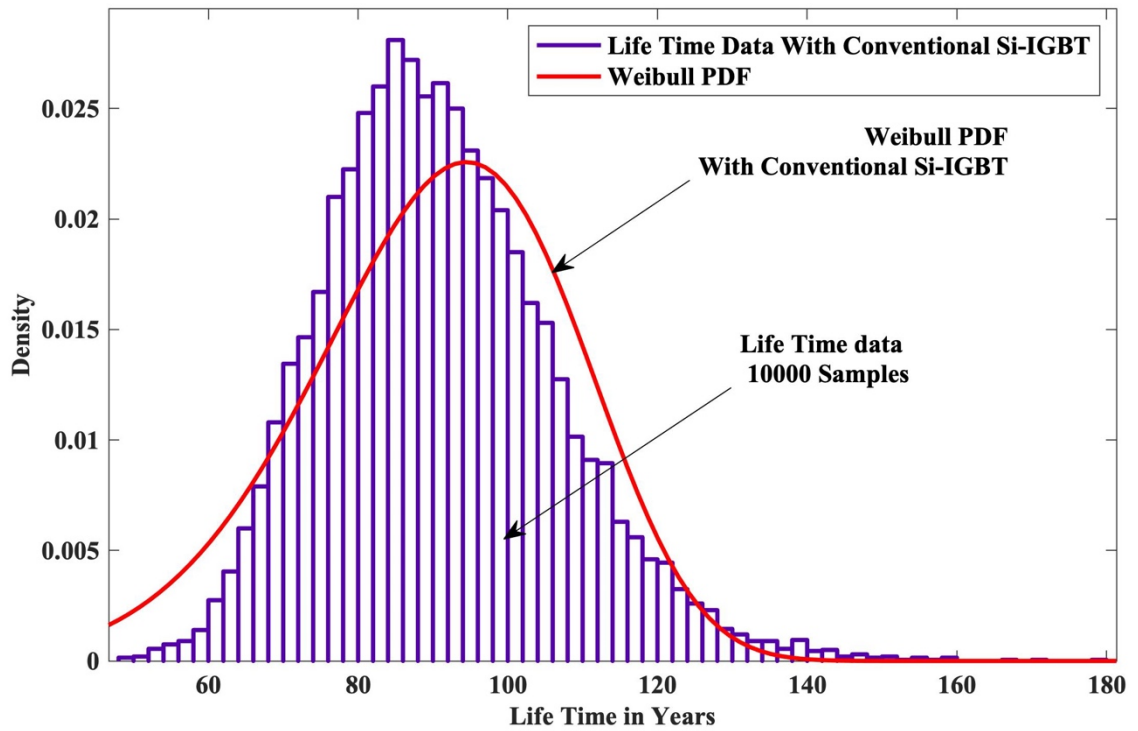


Fig. 6.7(a). Monte Carlo Simulation Lifetime Distribution of PV inverter at Denmark Location with Conventional Si-IGBT

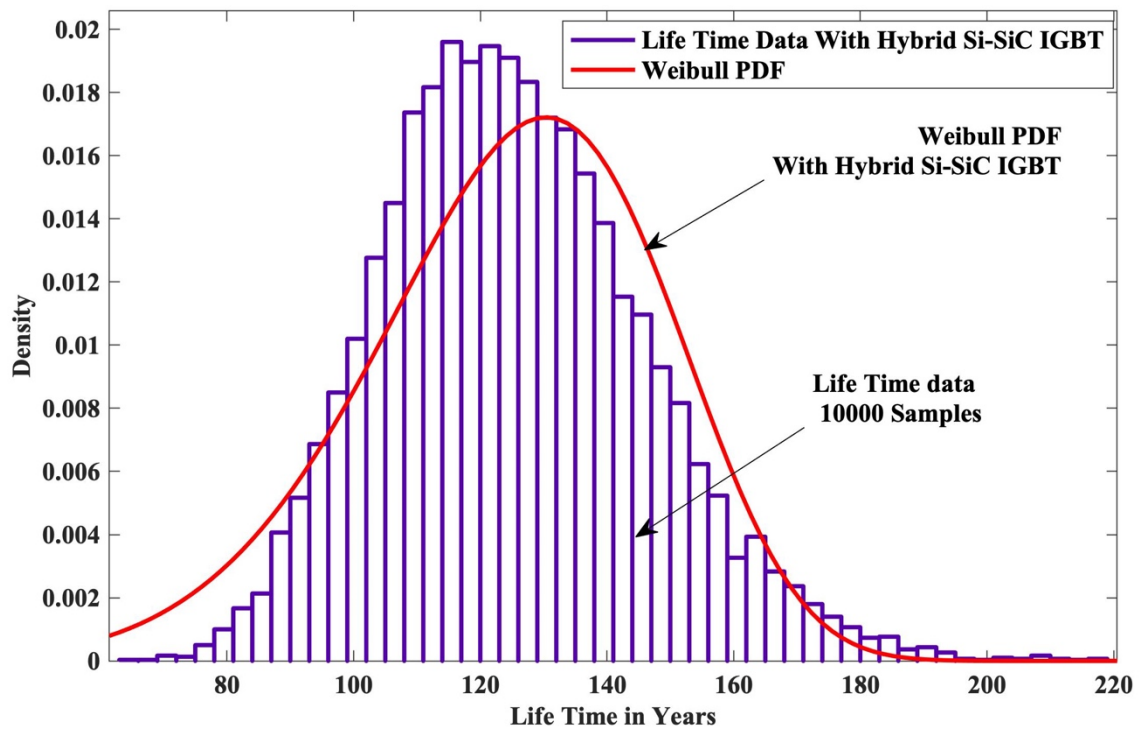


Fig. 6.7(b). Monte Carlo Simulation Lifetime Distribution of PV inverter at Denmark Location with Hybrid Si-SiC IGBT

The reliability function $R(t)$ is calculated using two parameter Weibull distribution. Component level reliability is calculated using Eq. 5.4, system level reliability is calculated using Eq. 5.5, B_{10} lifetime is calculated using Eq. 5.6. $R(t)$ at India and Denmark locations are as shown in Fig. 6.8 and Fig. 6.9 respectively.

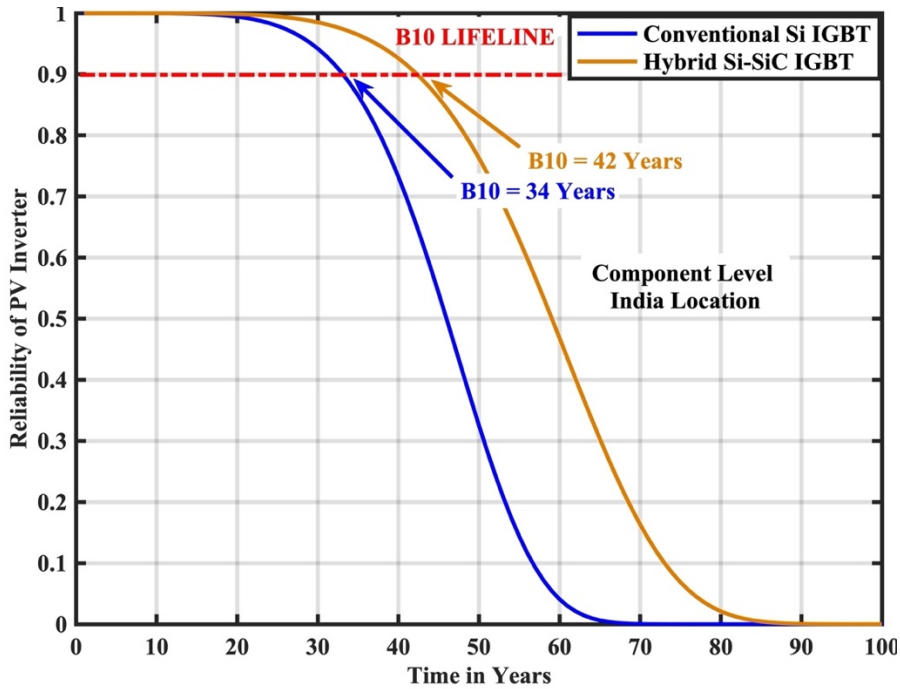


Fig. 6.8(a). Reliability function of PV inverter at India Location Component Level

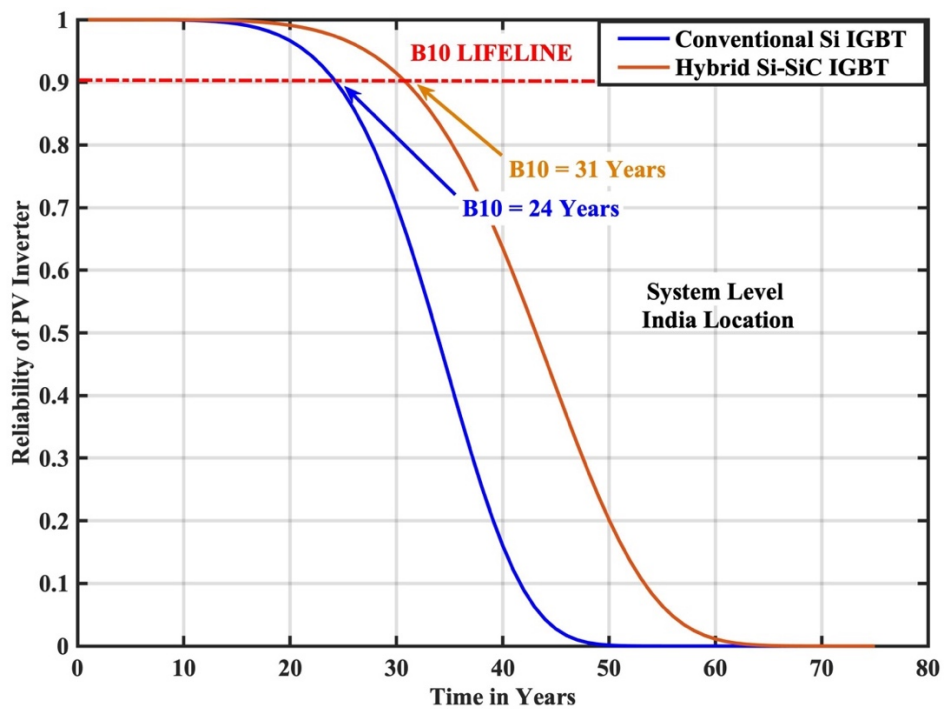


Fig. 6.8(b). Reliability function of PV inverter at India Location System Level

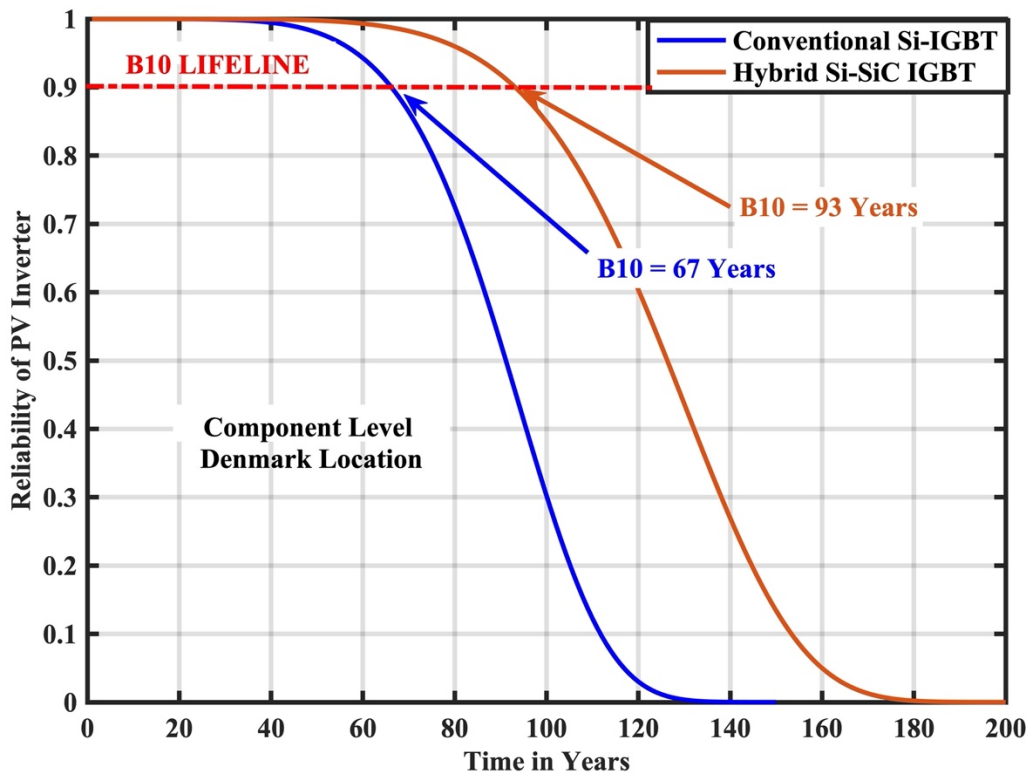


Fig. 6.9(a). Reliability function of PV inverter at Denmark Location Component Level

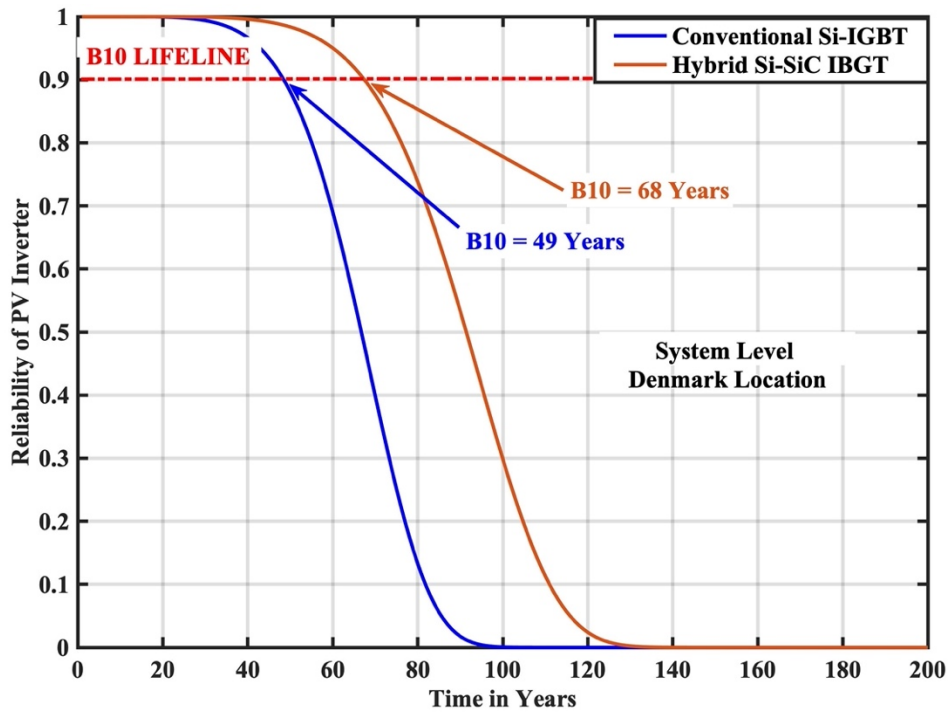


Fig. 6.9(b). Reliability function of PV inverter at Denmark Location System Level

Hybrid Si-SiC IGBT on PV inverter reliability has a significant impact at both locations. An increase in B_{10} lifetime is recorded at both locations. Reliability (B_{10})

improvement of 23.5 % at component level and 29.1 % at the system level is achieved at the India location. Similarly, reliability (B_{10}) improvement of 38.8 % at the component level and 38.7 % at the system level is achieved at Denmark location. The Junction Temperature of the proposed Hybrid Si/SiC IGBT exhibits the decreasing trend due to the lower power losses when compared with conventional Si IGBT, and hence reliability is improved.

6.2.5. B_{10} Lifetime Comparison:

Reliability analysis of PV inverter at India and Denmark locations are performed considering proposed hybrid Si/SiC power module and conventional Si power module. B_{10} lifetime is calculated in both cases and comparative analysis at the component level and system level as shown in Fig. 6.10. At both locations B_{10} lifetime of the PV inverter improved with the proposed hybrid Si/SiC power module in comparison with the conventional Si power module. Reliability improvement of 8 years at the component level and 7 years at the system level is achieved at the India location. Similarly, reliability improvement of 26 years at the component level and 19 years at the system level is achieved with the proposed Si/SiC power module.

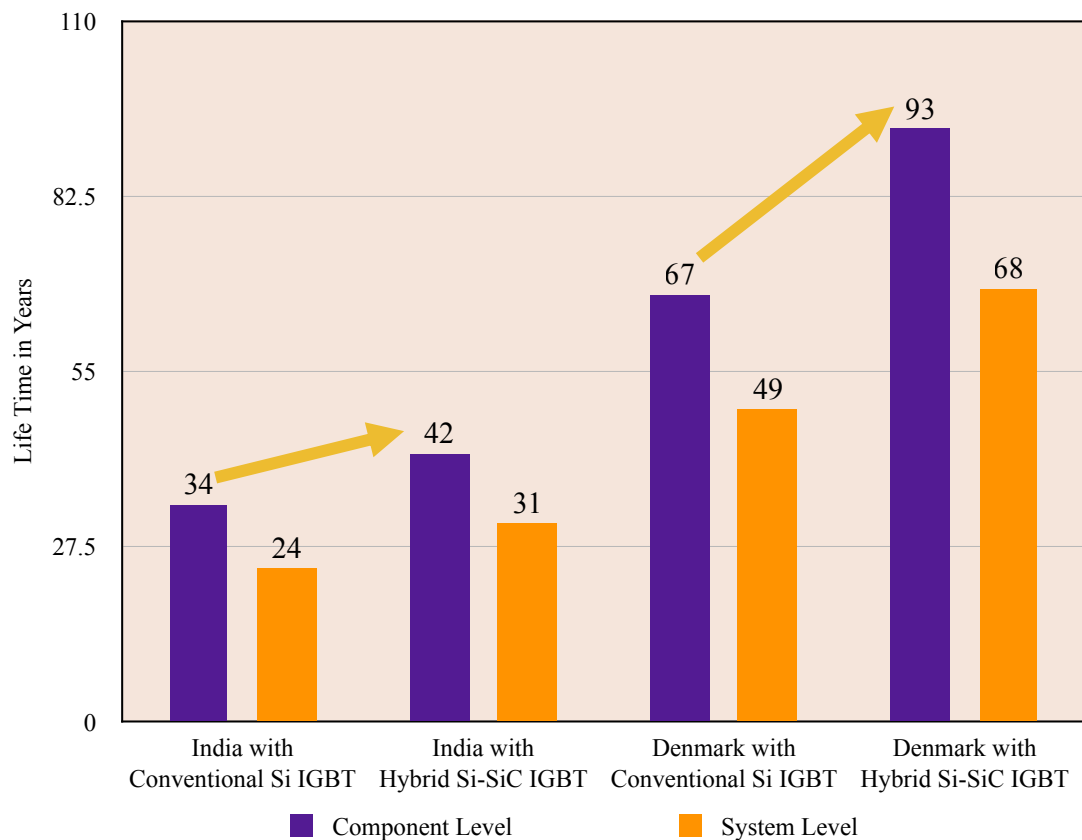


Fig. 6.10. B_{10} Lifetime Comparison

6.3 Chapter Summary:

In this chapter Hybrid Si-SiC IGBT is proposed for reliability improvement and compared with conventional Si IGBT. Reliability (B_{10}) improvement of 23.5 % at the component level and 29.1 % at the system level is achieved at the India location. Similarly, Reliability (B_{10}) improvement of 38.8 % at the component level and 38.7 % at the system level is achieved at Denmark Location.

CHAPTER 7

CONCLUSION & FUTURE SCOPE

7.1. Conclusion:

In this research work, the research focussed on reliability analysis and implementation of grid connected inverter for PV applications. Today's global PV potential growth, reliability of power electronics and its field experiences, need for PV inverter reliability analysis have been discussed and to address those, Mission profile oriented reliability analysis and improvement solutions for the PV inverter are proposed.

Mission profile impacts reliability performance of PV inverter. Hence to account for this real time mission profile data i.e., solar irradiance and ambient temperature have been logged from 01-September-2018 to 31-August-2019 at "B V Raju Institute of Technology, Narsapur, Medak, Telangana", India and Aalborg, Denmark Locations. Month-wise heat maps are presented for solar irradiance and ambient temperature at both locations to analyze the variation of mission profile. At India location, solar irradiance maximum is recorded in March, April, May, and in the remaining months, moderate values are recorded. Similarly, at Denmark location solar irradiance maximum is recorded in June, August and minimum are recorded in September, October, November, December, January, February, March. At India location, ambient temperature maximum is recorded in March, April, May, and in the remaining months, moderate values are recorded. Similarly, Denmark location ambient temperature maximum is recorded in June, August and the minimum is recorded in September, October, November, December, January, February, March.

Environmental conditions are not constant; hence mission profile always varies with respect to time, which leads to the temperature variations in the IGBT. In contrast, to assess the reliability of IGBT, the temperature at the junction layers needs to be estimated. In this work foster electro thermal model is presented and implemented on a test case of 3-kW PV inverter to estimate the yearly junction temperature at both locations. The Mean Junction Temperature ($^{\circ}\text{C}$) at the India location is 55.66°C and, at the Denmark location is 16.37°C . Junction Temperature Mean Difference ($^{\circ}\text{C}$) between both locations is 39.29°C . There is a significant amount of Mean Difference between

India and Denmark locations. This scenario leads to reliability performance deviation between India and Denmark.

As the foster electro thermal model is an indirect method for estimation junction temperature it requires validation. The validation is made by correlating the estimated junction temperature of the PV inverter with the case temperature, solar irradiance, and ambient temperature. In all the cases positive correlation is recorded. In the correlation analysis between Junction Temperature and Case Temperature, correlation coefficient $R = 0.934938$ i.e., Strong positive association. In the correlation analysis between Junction Temperature and Solar Irradiance, correlation coefficient $R = 0.978430$ i.e., Strong positive association. In the correlation analysis between Junction and Ambient Temperature, correlation coefficient $R = 0.730140$ i.e., positive association, and hence it is validated.

The variations of the estimated junction temperature follow irregular profiles to anticipate it a rain flow counting algorithm is used. From the rain flow algorithm No. of Cycles n_i , Mean Junction Temperature T_{jm} , Cycle Amplitude ΔT are calculated and lifetime is evaluated. In the obtained lifetime, all the parameters are constant i.e., all the devices should fail at the same rate but practically this is not feasible, so to overcome this the variation of 5 % is considered and 10000 samples are generated using Monte Carlo simulation. All the generated samples are fitted in Weibull distribution and reliability function at both component level and system level is obtained. From the reliability function, the B_{10} lifetime is calculated.

Several factors affect the reliability performance of the PV inverter. In this work impact of the Installation site, PV panel degradation rate, PV panel oversizing, Bifacial PV panel are presented. Installation site has a significant impact, reliability varies from location to location based on climatic conditions. The reliability of PV inverter is reported more in cold climatic conditions. At the India component level reliability (B_{10}) is 34 years, system level reliability (B_{10}) is 24 years. Similarly at Denmark component level reliability (B_{10}) is 67 years, system level reliability (B_{10}) is 49 years.

The degradation rate exhibits an increasing trend at both locations. The degradation rate of 1.93 % per year for five years of operation is considered at the India Location and 0.15 % per year for five years of operation is considered at Denmark Location. At the India component level reliability (B_{10}) is increased from 34 years to 78 years, system level reliability (B_{10}) is increased from 24 years to 57 years. Similarly

in Denmark component level reliability (B_{10}) is increased from 67 years to 71 years, system level reliability (B_{10}) is increased from 49 years to 52 years.

Oversizing of PV panel exhibits decreasing trend at both locations. To analyze the impact of PV Panel Oversizing on PV inverter panel sizing ratio $R_s = 1.0, 1.2, 1.4$ are considered. At the India component level reliability (B_{10}) is decreased from 34 years to 2.5 years, system level reliability (B_{10}) is decreased from 24 years to 1.8 years. Similarly in Denmark component level reliability (B_{10}) is decreased from 67 years to 7 years, system level reliability (B_{10}) is decreased from 49 years to 5 years.

The bifacial PV panel exhibits decreasing trend at both locations. To analyze the impact of Bifacial PV Panel on PV Inverter Reliability Bifacial PV Panel with 0%, 30%, 50% more energy yield are considered. At the India component level reliability (B_{10}) is decreased from 34 years to 1.5 years, system level reliability (B_{10}) is decreased from 24 years to 1 year. Similarly in Denmark component level reliability (B_{10}) is decreased from 67 years to 4.5 years, system level reliability (B_{10}) is decreased from 49 years to 3 years.

Furthermore, a hybrid Si/SiC switch is proposed for reliability improvement of PV inverter. The hybrid Switch consists of Si-IGBT (IGW30N60H3) and SiC- diode (C3D20060D) and its effectiveness is analyzed by comparing it with conventional Si-IGBT. Reliability (B_{10}) improvement of 23.5 % at component level and 29.1 % at the system level is achieved at the India location. Similarly, reliability (B_{10}) improvement of 38.8 % at the component level and 38.7 % at the system level is achieved at the Denmark location

7.2. Future Scope:

The following are some of the research topics that can be further investigated in the future.

7.2.1. Reliability analysis considering other stress factors:

- ⇒ Other than thermal stress, vibration, humidity, etc., impacts the reliability performance.
- ⇒ Correlation analysis needs to be developed between different stress factors.
- ⇒ Hence further investigation is required for reliability analysis.

7.2.2. Reliability analysis for different types of inverter configurations:

- ⇒ Different inverter configurations are available in today's market like NPC, FC, Cascaded H – Bridge, etc.
- ⇒ Detailed reliability analysis is required for all the configurations.

7.2.3. Reliability analysis at System Level:

- ⇒ In this work reliability is calculated for a single IGBT i.e., component level and series reliability block approach is implemented for system level reliability considering all the IGBT are the same.
- ⇒ But practically all the IGBT's exhibit the same reliable performance. Hence system level reliability if further investigated considering all IGBT's.

7.2.4. Artificial Intelligence oriented Reliability Analysis:

- ⇒ Reliability analysis of PV inverter follows several steps and takes time for the evaluation.
- ⇒ To design model-based reliability analysis Artificial Intelligence techniques are required and further investigation is needed.

REFERENCES

- [1] REN21, *Renewables 2020 Global Status Report*. 2020.
- [2] IEA, “Snapshot of Global PV Markets 2021,” 2021. [Online]. Available: <https://iea-pvps.org/snapshot-reports/snapshot-2021/>.
- [3] MNRE, “Solar Energy Overview in India,” 2020. <https://mnre.gov.in/solar/current-status/>.
- [4] Ministry of Power, “Power Growth In India,” 2021. <https://powermin.gov.in>.
- [5] F. Blaabjerg, Z. Chen, and S. B. Kjaer, “Power electronics as efficient interface in dispersed power generation systems,” *IEEE Trans. Power Electron.*, vol. 19, no. 5, pp. 1184–1194, 2004, doi: 10.1109/TPEL.2004.833453.
- [6] J. D. Van Wyk and F. C. Lee, “On a future for power electronics,” *IEEE J. Emerg. Sel. Top. Power Electron.*, vol. 1, no. 2, pp. 59–72, 2013, doi: 10.1109/JESTPE.2013.2271499.
- [7] WILLIAM E. NEWELL, “Power Electronics-merging from Limbo,” *IEEE Trans. Ind. Appl.*, vol. 10, no. 1, pp. 7–11.
- [8] W. Huai *et al.*, “Transitioning to physics-of-failure as a reliability driver in power electronics,” *IEEE J. Emerg. Sel. Top. Power Electron.*, vol. 2, no. 1, pp. 97–114, 2014, doi: 10.1109/JESTPE.2013.2290282.
- [9] L. M. Moore and H. N. Post, “Five years of operating experience at a large, utility-scale photovoltaic generating plant,” *Prog. Photovoltaics Res. Appl.*, vol. 16, no. 3, pp. 249–259, May 2008, doi: <https://doi.org/10.1002/pip.800>.
- [10] E. Koutoulakos, “Reliability of wind turbine subassemblies,” *IET Renew. Power Gener.*, vol. 3, no. 4, pp. 387-401(14), Dec. 2009, [Online]. Available: <https://digital-library.theiet.org/content/journals/10.1049/iet-rpg.2008.0060>.

- [11] Reliawind, “Project Final Report on Reliability focused research on optimizing Wind Energy systems design, operation and maintenance: Tools, proof of concepts, guidelines & methodologies for a new generation,” 2011.
- [12] IEA, “Reliability Study of Grid Connected PV Systems Field Experience and Recommended Design Practice Task 7 Report IEA-PVPS T7-08 : 2002 March 2002,” 2002.
- [13] C. Liu, F. Brem, G. Riedel, E. Eichelberger, and N. Hofmann, “The influence of thermal cycling methods on the interconnection reliability evaluation within IGBT modules,” *2012 4th Electron. Syst. Technol. Conf. ESTC 2012*, 2012, doi: 10.1109/ESTC.2012.6542180.
- [14] V. Sonti, S. Jain, and S. Bhattacharya, “Analysis of the modulation strategy for the minimization of the leakage current in the PV grid-connected cascaded multilevel inverter,” *IEEE Trans. Power Electron.*, vol. 32, no. 2, pp. 1156–1169, 2017, doi: 10.1109/TPEL.2016.2550206.
- [15] R. Kaplar *et al.*, “PV inverter performance and reliability: What is the role of the IGBT?,” in *2011 37th IEEE Photovoltaic Specialists Conference*, 2011, pp. 1842–1847.
- [16] C. Busca *et al.*, “An overview of the reliability prediction related aspects of high power IGBTs in wind power applications,” *Microelectron. Reliab.*, vol. 51, no. 9–11, pp. 1903–1907, 2011, doi: 10.1016/j.microrel.2011.06.053.
- [17] G. J. Riedel and M. Valov, “Simultaneous testing of wirebond and solder fatigue in IGBT modules,” *CIPS 2014 - 8th Int. Conf. Integr. Power Electron. Syst. Proc.*, pp. 25–27, 2014.
- [18] I. F. Kovačević, U. Drogenik, and J. W. Kolar, “New physical model for lifetime estimation of power modules,” *2010 Int. Power Electron.*

- Conf. - ECCE Asia -, IPEC 2010*, pp. 2106–2114, 2010, doi: 10.1109/IPEC.2010.5543755.
- [19] P. D. Reigosa, H. Wang, Y. Yang, and F. Blaabjerg, “Prediction of Bond Wire Fatigue of IGBTs in a PV Inverter under a Long-Term Operation,” *IEEE Trans. Power Electron.*, vol. 31, no. 10, pp. 7171–7182, 2016, doi: 10.1109/TPEL.2015.2509643.
- [20] U. M. Choi and F. Blaabjerg, “Real-time condition monitoring of IGBT modules in PV inverter systems,” *CIPS 2018 - 10th Int. Conf. Integr. Power Electron. Syst.*, pp. 412–416, 2018.
- [21] S. Yang, A. Bryant, P. Mawby, D. Xiang, L. Ran, and P. Tavner, “An industry-based survey of reliability in power electronic converters,” *IEEE Trans. Ind. Appl.*, vol. 47, no. 3, pp. 1441–1451, 2011, doi: 10.1109/TIA.2011.2124436.
- [22] K. Upadhyayula and A. Dasgupta, “Guidelines for physics-of-failure based accelerated stress testing,” *Proc. Annu. Reliab. Maintainab. Symp.*, pp. 345–357, 1998, doi: 10.1109/rams.1998.653803.
- [23] J. Reichelt, P. Gromala, and S. Rzepka, “Accelerating the temperature cycling tests of FBGA memory components with lead-free solder joints without changing the damage mechanism,” in *2009 European Microelectronics and Packaging Conference, EMPC 2009*, 2009.
- [24] K. C. Norris and A. H. Landzberg, “Reliability of Controlled Collapse Interconnections,” *IBM J. Res. Dev.*, vol. 13, no. 3, pp. 266–271, 2010, doi: 10.1147/rd.133.0266.
- [25] W. Huai *et al.*, “Transitioning to physics-of-failure as a reliability driver in power electronics,” *IEEE J. Emerg. Sel. Top. Power Electron.*, vol. 2, no. 1, pp. 97–114, 2014, doi: 10.1109/JESTPE.2013.2290282.
- [26] D. R. Tobergte and S. Curtis, “NCPV Program Review Meeting,” *J.*

- Chem. Inf. Model.*, vol. 53, no. 9, pp. 1689–1699, 2013.
- [27] K. Ma, “Reliability-Cost models for the power switching devices of wind power converters,” *Res. Top. Wind Energy*, vol. 5, pp. 123–138, 2015, doi: 10.1007/978-3-319-21248-7_9.
- [28] A. Pigazo, M. Liserre, F. Blaabjerg, and T. Kerekes, “Robustness analysis of the efficiency in PV inverters,” *IECON Proc. (Industrial Electron. Conf.)*, pp. 7015–7020, 2013, doi: 10.1109/IECON.2013.6700296.
- [29] M. Held, P. Jacob, G. Nicoletti, P. Scacco, and M. H. Poech, “Fast power cycling test for IGBT modules in traction application,” *Proc. Int. Conf. Power Electron. Drive Syst.*, vol. 1, pp. 425–430, 1997, doi: 10.1109/peds.1997.618742.
- [30] T. Solar and P. Magazine, “The » Infinity « research project is aiming to optimize,” 2015.
- [31] S. Kouro, J. I. Leon, D. Vinnikov, and L. G. Franquelo, “Grid-connected photovoltaic systems: An overview of recent research and emerging PV converter technology,” *IEEE Ind. Electron. Mag.*, vol. 9, no. 1, pp. 47–61, 2015, doi: 10.1109/MIE.2014.2376976.
- [32] S. Bennici, P. Carniti, and A. Gervasini, “Bulk and surface properties of dispersed CuO phases in relation with activity of NO_x reduction,” *Catal. Letters*, vol. 98, no. 4, pp. 187–194, 2004, doi: 10.1007/s10562-004-8679-9.
- [33] L. Zhang, K. Sun, L. Feng, H. Wu, and Y. Xing, “A family of neutral point clamped full-bridge topologies for transformerless photovoltaic grid-tied inverters,” *IEEE Trans. Power Electron.*, vol. 28, no. 2, pp. 730–739, 2013, doi: 10.1109/TPEL.2012.2205406.
- [34] A. Demirbas, “Future energy systems,” *Energy Sources, Part A Recover. Util. Environ. Eff.*, vol. 38, no. 12, pp. 1721–1729, 2016, doi: 10.1080/15567036.2014.962119.

- [35] X. Tong, M. Zhong, X. Zhang, J. Deng, and Z. Zhang, “Voltage regulation strategy of AC distribution network based on distributed PV grid-connected inverter,” *J. Eng.*, vol. 2019, no. 16, pp. 2525–2528, 2019, doi: 10.1049/joe.2018.8680.
- [36] S. Rivera, S. Kouro, B. Wu, J. I. Leon, J. Rodríguez, and L. G. Franquelo, “Cascaded H-bridge multilevel converter multistring topology for large scale photovoltaic systems,” *Proc. - ISIE 2011 2011 IEEE Int. Symp. Ind. Electron.*, pp. 1837–1844, 2011, doi: 10.1109/ISIE.2011.5984437.
- [37] C. D. Fuentes, C. A. Rojas, H. Renaudineau, S. Kouro, M. A. Perez, and T. Meynard, “Experimental Validation of a Single DC Bus Cascaded H-Bridge Multilevel Inverter for Multistring Photovoltaic Systems,” *IEEE Trans. Ind. Electron.*, vol. 64, no. 2, pp. 930–934, 2017, doi: 10.1109/TIE.2016.2619661.
- [38] Q. Huang and A. Q. Huang, “Feedforward proportional carrier-based PWM for Cascaded H-Bridge PV Inverter,” *IEEE J. Emerg. Sel. Top. Power Electron.*, vol. 6, no. 4, pp. 2192–2205, 2018, doi: 10.1109/JESTPE.2018.2817183.
- [39] T. Zhao *et al.*, “An optimized third harmonic compensation strategy for single-phase cascaded H-bridge photovoltaic inverter,” *IEEE Trans. Ind. Electron.*, vol. 65, no. 11, pp. 8635–8645, 2018, doi: 10.1109/TIE.2018.2813960.
- [40] A. Ahmed, M. Sundar Manoharan, and J. H. Park, “An Efficient Single-Sourced Asymmetrical Cascaded Multilevel Inverter with Reduced Leakage Current Suitable for Single-Stage PV Systems,” *IEEE Trans. Energy Convers.*, vol. 34, no. 1, pp. 211–220, 2019, doi: 10.1109/TEC.2018.2874076.
- [41] B. Xiao, L. Hang, J. Mei, C. Riley, L. M. Tolbert, and B. Ozpineci, “Modular Cascaded H-Bridge Multilevel PV Inverter with

- Distributed MPPT for Grid-Connected Applications,” *IEEE Trans. Ind. Appl.*, vol. 51, no. 2, pp. 1722–1731, 2015, doi: 10.1109/TIA.2014.2354396.
- [42] J. M. Lenz, H. C. Sartori, and J. R. Pinheiro, “Defining Photovoltaic Mission Profile for the Pre-Design of Static Converters,” *IEEE Lat. Am. Trans.*, vol. 16, no. 5, pp. 1402–1409, 2018, doi: 10.1109/TLA.2018.8408434.
- [43] S. Peyghami, H. Wang, P. Davari, and F. Blaabjerg, “Mission-Profile-Based System-Level Reliability Analysis in DC Microgrids,” *IEEE Trans. Ind. Appl.*, vol. 55, no. 5, pp. 5055–5067, 2019, doi: 10.1109/TIA.2019.2920470.
- [44] A. Sangwongwanich, H. Wang, and F. Blaabjerg, “Reduced-Order Thermal Modeling for Photovoltaic Inverters Considering Mission Profile Dynamics,” *IEEE Open J. Power Electron.*, vol. 1, pp. 407–419, 2020, doi: 10.1109/OJPEL.2020.3025632.
- [45] A. Sangwongwanich, Y. Yang, D. Sera, and F. Blaabjerg, “Mission Profile-Oriented Control for Reliability and Lifetime of Photovoltaic Inverters,” *IEEE Trans. Ind. Appl.*, vol. 56, no. 1, pp. 601–610, 2020, doi: 10.1109/TIA.2019.2947227.
- [46] J. He, A. Sangwongwanich, Y. Yang, and F. Iannuzzo, “Lifetime Evaluation of Power Modules for Three-Level 1500-V Photovoltaic Inverters,” in *2020 IEEE Applied Power Electronics Conference and Exposition (APEC)*, 2020, pp. 430–435, doi: 10.1109/APEC39645.2020.9124560.
- [47] T. Schütze, “Infineon AN2008-03 Thermal equivalent circuit models,” 2008.
- [48] T. K. Gachovska, B. Tian, J. L. Hudgins, W. Qiao, and J. F. Donlon, “A Real-Time Thermal Model for Monitoring of Power Semiconductor Devices,” *IEEE Trans. Ind. Appl.*, vol. 51, no. 4, pp.

- 3361–3367, 2015, doi: 10.1109/TIA.2015.2391438.
- [49] U. M. Choi, F. Blaabjerg, F. Iannuzzo, and S. Jørgensen, “Junction temperature estimation method for a 600 V, 30A IGBT module during converter operation,” *Microelectron. Reliab.*, vol. 55, no. 9–10, pp. 2022–2026, 2015, doi: 10.1016/j.microrel.2015.06.146.
- [50] Z. Wang, B. Tian, W. Qiao, and L. Qu, “Real-Time Aging Monitoring for IGBT Modules Using Case Temperature,” *IEEE Trans. Ind. Electron.*, vol. 63, no. 2, pp. 1168–1178, 2016, doi: 10.1109/TIE.2015.2497665.
- [51] U. M. Choi, S. Jorgensen, and F. Blaabjerg, “Advanced Accelerated Power Cycling Test for Reliability Investigation of Power Device Modules,” *IEEE Trans. Power Electron.*, vol. 31, no. 12, pp. 8371–8386, 2016, doi: 10.1109/TPEL.2016.2521899.
- [52] K. Górecki, P. Górecki, and J. Zarębski, “Measurements of Parameters of the Thermal Model of the IGBT Module,” *IEEE Trans. Instrum. Meas.*, vol. 68, no. 12, pp. 4864–4875, 2019, doi: 10.1109/TIM.2019.2900144.
- [53] R. B. B. Ovando, F. A. Ramírez, C. Hernandez, and M. A. Arjona, “A 2D finite element thermal model of a three-phase-inverter heat sink,” *Proc. - 2010 IEEE Electron. Robot. Automot. Mech. Conf. CERMA 2010*, pp. 696–701, 2010, doi: 10.1109/CERMA.2010.141.
- [54] M. A. Bella, C. Bailey, and H. Lu, “Electro-thermal behaviour using finite volume and Finite Element method,” *2018 19th Int. Conf. Therm. Mech. Multi-Physics Simul. Exp. Microelectron. Microsystems, EuroSimE 2018*, pp. 1–5, 2018, doi: 10.1109/EuroSimE.2018.8369916.
- [55] M. N. O. Sadiku, “A Simple Introduction to Finite Element Analysis of Electromagnetic Problems,” *IEEE Trans. Educ.*, vol. 32, no. 2, pp. 85–93, 1989, doi: 10.1109/13.28037.

- [56] Y. Xiong, S. Sun, H. Jia, P. Shea, and Z. John Shen, “New physical insights on power MOSFET switching losses,” *IEEE Trans. Power Electron.*, vol. 24, no. 2, pp. 525–531, 2009, doi: 10.1109/TPEL.2008.2006567.
- [57] M. Ciappa, W. Fichtner, T. Kojima, Y. Yamada, and Y. Nishibe, “Extraction of accurate thermal compact models for fast electro-thermal simulation of IGBT modules in hybrid electric vehicles,” *Microelectron. Reliab.*, vol. 45, no. 9–11, pp. 1694–1699, 2005, doi: 10.1016/j.microrel.2005.07.083.
- [58] T. Kojima, Y. Yamada, M. Ciappa, M. Chiavarini, and W. Fichtner, “A novel electro-thermal simulation approach of power IGBT modules for automotive traction applications,” *IEEE Int. Symp. Power Semicond. Devices ICs*, vol. 16, no. v, pp. 289–292, 2004, doi: 10.1109/wct.2004.239990.
- [59] M. Musallam and C. M. Johnson, “Real-time compact thermal models for health management of power electronics,” *IEEE Trans. Power Electron.*, vol. 25, no. 6, pp. 1416–1425, 2010, doi: 10.1109/TPEL.2010.2040634.
- [60] L. Lu, A. T. Bryant, E. Santi, P. R. Palmer, and J. L. Hudgins, “Physical modeling of fast p-i-n diodes with carrier lifetime zoning, Part II: Parameter extraction,” *IEEE Trans. Power Electron.*, vol. 23, no. 1, pp. 198–205, 2008, doi: 10.1109/TPEL.2007.911825.
- [61] M. Musallam and C. Mark Johnson, “Extraction of efficient thermal models for life limiting interfaces in power modules,” *CIPS 2008 - 5th Int. Conf. Integr. Power Electron. Syst. Proc.*, pp. 333–338, 2008.
- [62] J. T. Hsu and L. Vu-Quoc, “A rational formulation of thermal circuit models for electrothermal simulation-part I: Finite element method,” *IEEE Trans. Circuits Syst. I Fundam. Theory Appl.*, vol. 43, no. 9, pp. 721–732, 1996, doi: 10.1109/81.536742.

- [63] A. T. Bryant, P. A. Mawby, P. R. Palmer, E. Santi, and J. L. Hudgins, “Exploration of power device reliability using compact device models and fast electrothermal simulation,” *IEEE Trans. Ind. Appl.*, vol. 44, no. 3, pp. 894–903, 2008, doi: 10.1109/TIA.2008.921388.
- [64] J. Daly and D. Galipeau, “Device Models,” *Analog BiCMOS Des.*, pp. 233–243, 1999, doi: 10.1201/9781439822500.ch2.
- [65] Z. Hu, M. Du, K. Wei, and W. G. Hurley, “An Adaptive Thermal Equivalent Circuit Model for Estimating the Junction Temperature of IGBTs,” *IEEE J. Emerg. Sel. Top. Power Electron.*, vol. 7, no. 1, pp. 392–403, 2019, doi: 10.1109/JESTPE.2018.2796624.
- [66] Y. Zhang, H. Wang, Z. Wang, Y. Yang, and F. Blaabjerg, “Simplified thermal modeling for IGBT modules with periodic power loss profiles in modular multilevel converters,” *IEEE Trans. Ind. Electron.*, vol. 66, no. 3, pp. 2323–2332, 2019, doi: 10.1109/TIE.2018.2823664.
- [67] Z. Wang and W. Qiao, “A Physics-Based Improved Cauer-Type Thermal Equivalent Circuit for IGBT Modules,” *IEEE Trans. Power Electron.*, vol. 31, no. 10, pp. 6781–6786, 2016, doi: 10.1109/TPEL.2016.2539208.
- [68] M. H. M. Sathik *et al.*, “Online junction temperature estimation of IGBT modules for Space Vector Modulation based inverter system,” *2016 Int. Symp. Power Electron. Electr. Drives, Autom. Motion, SPEEDAM 2016*, pp. 156–162, 2016, doi: 10.1109/SPEEDAM.2016.7525975.
- [69] A. S. Bahman, K. Ma, and F. Blaabjerg, “A Lumped Thermal Model Including Thermal Coupling and Thermal Boundary Conditions for High-Power IGBT Modules,” *IEEE Trans. Power Electron.*, vol. 33, no. 3, pp. 2518–2530, 2018, doi: 10.1109/TPEL.2017.2694548.
- [70] A. Sangwongwanich *et al.*, “Enhancing PV inverter reliability with

- battery system control strategy,” *CPSS Trans. Power Electron. Appl.*, vol. 3, no. 2, pp. 93–101, 2018.
- [71] L. R. GopiReddy, L. M. Tolbert, B. Ozpineci, and J. O. P. Pinto, “Rainflow Algorithm-Based Lifetime Estimation of Power Semiconductors in Utility Applications,” *IEEE Trans. Ind. Appl.*, 2015, doi: 10.1109/TIA.2015.2407055.
- [72] S S Manson, *Thermal stress low-cycle fatigue*. New York, McGraw-Hill, 1966.
- [73] K. C. Norris and A. H. Landzberg, “Reliability of Controlled Collapse Interconnections,” *IBM J. Res. Dev.*, vol. 13, no. 3, pp. 266–271, 2010, doi: 10.1147/rd.133.0266.
- [74] R. Bayerer, T. Herrmann, T. Licht, J. Lutz, and M. Feller, “Model for power cycling lifetime of IGBT Modules? Various factors influencing lifetime,” in *2008 5th International Conference on Integrated Power Systems, CIPS 2008*, 2008.
- [75] S. H. Ali, M. Heydarzadeh, S. Dusmez, X. Li, A. S. Kamath, and B. Akin, “Lifetime Estimation of Discrete IGBT Devices Based on Gaussian Process,” *IEEE Trans. Ind. Appl.*, vol. 54, no. 1, pp. 395–403, 2018, doi: 10.1109/TIA.2017.2753722.
- [76] R. M. Burkart and J. W. Kolar, “Comparative Life Cycle Cost Analysis of Si and SiC PV Converter Systems Based on Advanced η - ρ - σ Multiobjective Optimization Techniques,” *IEEE Trans. Power Electron.*, vol. 32, no. 6, pp. 4344–4358, 2017, doi: 10.1109/TPEL.2016.2599818.
- [77] L. R. GopiReddy, L. M. Tolbert, B. Ozpineci, and J. O. P. Pinto, “Rainflow Algorithm-Based Lifetime Estimation of Power Semiconductors in Utility Applications,” *IEEE Trans. Ind. Appl.*, vol. 51, no. 4, pp. 3368–3375, 2015, doi: 10.1109/TIA.2015.2407055.

- [78] U. M. Choi *et al.*, “Power cycling test and failure analysis of molded Intelligent Power IGBT Module under different temperature swing durations,” *Microelectron. Reliab.*, vol. 64, pp. 403–408, 2016, doi: 10.1016/j.microrel.2016.07.020.
- [79] W. Lai, M. Chen, L. Ran, O. Alatise, S. Xu, and P. Mawby, “Low Δt_j Stress Cycle Effect in IGBT Power Module Die-Attach Lifetime Modeling,” *IEEE Trans. Power Electron.*, vol. 31, no. 9, pp. 6575–6585, 2016, doi: 10.1109/TPEL.2015.2501540.
- [80] S. H. Ali, S. Dusmez, and B. Akin, “A comprehensive study on variations of discrete IGBT characteristics due to package degradation triggered by thermal stress,” *ECCE 2016 - IEEE Energy Convers. Congr. Expo. Proc.*, pp. 1–6, 2016, doi: 10.1109/ECCE.2016.7854665.
- [81] S. Dusmez, S. H. Ali, M. Heydarzadeh, A. S. Kamath, H. Duran, and B. Akin, “Aging precursor identification and lifetime estimation for thermally aged discrete package silicon power switches,” *IEEE Trans. Ind. Appl.*, vol. 53, no. 1, pp. 251–260, 2017, doi: 10.1109/TIA.2016.2603144.
- [82] M. Novak, A. Sangwongwanich, and F. Blaabjerg, “Monte Carlo Based Reliability Estimation Methods in Power Electronics,” in *2020 IEEE 21st Workshop on Control and Modeling for Power Electronics (COMPEL)*, 2020, pp. 1–7, doi: 10.1109/COMPEL49091.2020.9265685.
- [83] N. Shahidirad, M. Niroomand, and R. Hooshmand, “Investigation of PV Power Plant Structures Based on Monte Carlo Reliability and Economic Analysis,” *IEEE J. Photovoltaics*, vol. 8, no. 3, pp. 825–833, 2018, doi: 10.1109/JPHOTOV.2018.2814922.
- [84] A. Sangwongwanich, Y. Yang, D. Sera, and F. Blaabjerg, “Lifetime Evaluation of Grid-Connected PV Inverters Considering Panel

- Degradation Rates and Installation Sites,” *IEEE Trans. Power Electron.*, vol. 33, no. 2, pp. 1125–1236, 2018, doi: 10.1109/TPEL.2017.2678169.
- [85] V. K. Rajiv Dubey, Shashwata Chattopadhyay and A. K. and O. S. S. S. Jim Joseph John, B. M. Arora, Anil Kottantharayil, K. L. Narasimhan, Chetan S. Solanki, Vaman Kuber and Juzer Vasi, “All-India India Survey of Photovoltaic Module Degradation : 2013,” *Rep. Natl. Cent. Photovolt. Res. Educ. IIT Bombay Sol. Energy Cent. (Gurgaon)*; , no. June, p. 273, 2013.
- [86] S. Bouguerra, S. Member, M. R. Yaiche, O. Gassab, and S. Member, “The Impact of PV Panel Positioning and Degradation on the PV Inverter Lifetime and Reliability,” vol. 6777, no. c, pp. 1–14, 2020, doi: 10.1109/JESTPE.2020.3006267.
- [87] A. Sangwongwanich, Y. Yang, D. Sera, and F. Blaabjerg, “Impacts of PV array sizing on PV inverter lifetime and reliability,” *2017 IEEE Energy Convers. Congr. Expo. ECCE 2017*, vol. 2017-Janua, pp. 3830–3837, 2017, doi: 10.1109/ECCE.2017.8096675.
- [88] W. Mackenzie, “Global bifacial module market report 2019,” *Wood Mackenzie*, Sep. 2019.
- [89] X. Sun, M. R. Khan, A. Hanna, M. M. Hussain, and M. A. Alam, “The Potential of Bifacial Photovoltaics: A Global Perspective,” in *2017 IEEE 44th Photovoltaic Specialist Conference (PVSC)*, 2017, pp. 1055–1057, doi: 10.1109/PVSC.2017.8366353.
- [90] T. S. Liang, M. Pravettoni, J. P. Singh, and Y. S. Khoo, “A Metrological Study of Accurate Indoor Characterisation of Commercial Bifacial Photovoltaic Module with Single Light Source,” *IEEE J. Photovoltaics*, vol. 10, no. 5, pp. 1448–1454, 2020, doi: 10.1109/JPHOTOV.2020.3004932.
- [91] S. A. Pelaez, C. Deline, S. M. Macalpine, B. Marion, J. S. Stein, and

- R. K. Kostuk, “Comparison of Bifacial Solar Irradiance Model Predictions with Field Validation,” *IEEE J. Photovoltaics*, vol. 9, no. 1, pp. 82–88, 2019, doi: 10.1109/JPHOTOV.2018.2877000.
- [92] Z. Zengwei, Z. Zhen, J. Yongfeng, L. Haolin, and Z. Shengcheng, “Performance analysis on bifacial pv panels with inclined and horizontal east-west sun trackers,” *IEEE J. Photovoltaics*, vol. 9, no. 3, pp. 636–642, 2019, doi: 10.1109/JPHOTOV.2019.2899472.
- [93] A. A. Widayat, S. Ma’arif, K. D. Syahindra, A. F. Fauzi, and E. A. Setiawan, “Comparison and Optimization of Floating Bifacial and Monofacial Solar PV System in a Tropical Region,” in *2020 9th International Conference on Power Science and Engineering (ICPSE)*, 2020, pp. 66–70, doi: 10.1109/ICPSE51196.2020.9354374.
- [94] O. Ayadi, M. Jamra, A. Jaber, L. Ahmad, and M. Alnaqep, “An Experimental Comparison of Bifacial and Monofacial PV Modules,” in *2021 12th International Renewable Engineering Conference (IREC)*, 2021, pp. 1–8, doi: 10.1109/IREC51415.2021.9427864.
- [95] M. H. Riaz, H. Imran, R. Younas, M. A. Alam, and N. Z. Butt, “Module Technology for Agrivoltaics: Vertical Bifacial Versus Tilted Monofacial Farms,” *IEEE J. Photovoltaics*, vol. 11, no. 2, pp. 469–477, 2021, doi: 10.1109/JPHOTOV.2020.3048225.
- [96] M. Rouholamini, L. Chen, and C. Wang, “Modeling, Configuration, and Grid Integration Analysis of Bifacial PV Arrays,” *IEEE Trans. Sustain. Energy*, vol. 12, no. 2, pp. 1242–1255, 2021, doi: 10.1109/TSTE.2020.3040427.
- [97] L. Amber and K. Haddad, “Hybrid Si IGBT-SiC Schottky diode modules for medium to high power applications,” *Conf. Proc. - IEEE Appl. Power Electron. Conf. Expo. - APEC*, pp. 3027–3032, 2017, doi: 10.1109/APEC.2017.7931127.

- [98] Z. Feng, X. Zhang, J. Wang, and S. Yu, "A high-efficiency three-level ANPC inverter based on hybrid SiC and Si devices," *Energies*, vol. 13, no. 5, 2020, doi: 10.3390/en13051159.
- [99] D. Zhang, J. He, and D. Pan, "A Megawatt-Scale Medium-Voltage High-Efficiency High Power Density ' SiC + Si ' Hybrid Three-Level Propulsion Systems," vol. 55, no. 6, pp. 5971–5980, 2019.
- [100] Z. Peng *et al.*, "Adaptive Gate Delay-Time Control of Si/SiC Hybrid Switch for Efficiency Improvement in Inverters," *IEEE Trans. Power Electron.*, vol. 36, no. 3, pp. 3437–3449, 2021, doi: 10.1109/TPEL.2020.3015803.
- [101] P. Ning, L. Li, X. Wen, and H. Cao, "A hybrid Si IGBT and SiC MOSFET module development," *CES Trans. Electr. Mach. Syst.*, vol. 1, no. 4, pp. 360–366, 2020, doi: 10.23919/tems.2017.8241357.
- [102] T. Mishima, "A Time-Sharing Current-Fed ZCS High-Frequency Inverter-Based Resonant DC-DC Converter with Si-IGBT/SiC-SBD Hybrid Module for Inductive Power Transfer Applications," *IEEE J. Emerg. Sel. Top. Power Electron.*, vol. 8, no. 1, pp. 506–516, 2020, doi: 10.1109/JESTPE.2019.2927723.
- [103] D. Han, J. Noppakunkajorn, and B. Sarlioglu, "Comprehensive efficiency, weight, and volume comparison of SiC- and Si-based bidirectional dc-dc converters for hybrid electric vehicles," *IEEE Trans. Veh. Technol.*, vol. 63, no. 7, pp. 3001–3010, 2014, doi: 10.1109/TVT.2014.2323193.
- [104] K. Saito, T. Miyoshi, D. Kawase, S. Hayakawa, T. Masuda, and Y. Sasajima, "Simplified Model Analysis of Self-Excited Oscillation and Its Suppression in a High-Voltage Common Package for Si-IGBT and SiC-MOS," *IEEE Trans. Electron Devices*, vol. 65, no. 3, pp. 1063–1071, 2018, doi: 10.1109/TED.2018.2796314.
- [105] Z. Li *et al.*, "Active Gate Delay Time Control of Si/SiC Hybrid

- Switch for Junction Temperature Balance over a Wide Power Range,” *IEEE Trans. Power Electron.*, vol. 35, no. 5, pp. 5354–5365, 2020, doi: 10.1109/TPEL.2019.2942044.
- [106] Q. X. Guan *et al.*, “An Extremely High Efficient Three-Level Active Neutral-Point-Clamped Converter Comprising SiC and Si Hybrid Power Stages,” *IEEE Trans. Power Electron.*, vol. 33, no. 10, pp. 8341–8352, 2018, doi: 10.1109/TPEL.2017.2784821.
- [107] D. Li *et al.*, “Characterization of a 3.3-kV Si-SiC Hybrid Power Module in Half-Bridge Topology for Traction Inverter Application,” *IEEE Trans. Power Electron.*, vol. 35, no. 12, pp. 13429–13440, 2020, doi: 10.1109/TPEL.2020.2995698.
- [108] Z. Feng, X. Zhang, S. Yu, and J. Zhuang, “Comparative Study of 2Si&C4Si Hybrid Configuration Schemes in ANPC Inverter,” *IEEE Access*, vol. 8, pp. 33934–33943, 2020, doi: 10.1109/ACCESS.2020.2974554.
- [109] J. Wang, Z. Li, X. Jiang, C. Zeng, and Z. J. Shen, “Gate Control Optimization of Si/SiC Hybrid Switch for Junction Temperature Balance and Power Loss Reduction,” *IEEE Trans. Power Electron.*, vol. 34, no. 2, pp. 1744–1754, 2019, doi: 10.1109/TPEL.2018.2829624.
- [110] Z. Li, J. Wang, Z. He, J. Yu, Y. Dai, and Z. John Shen, “Performance Comparison of Two Hybrid Si/SiC Device Concepts,” *IEEE J. Emerg. Sel. Top. Power Electron.*, vol. 8, no. 1, pp. 42–53, 2020, doi: 10.1109/JESTPE.2019.2947252.
- [111] Z. Li, J. Wang, B. Ji, and Z. J. Shen, “Power loss model and device sizing optimization of Si/SiC hybrid switches,” *IEEE Trans. Power Electron.*, vol. 35, no. 8, pp. 8512–8523, 2020, doi: 10.1109/TPEL.2019.2954288.
- [112] P. Ning, T. Yuan, Y. Kang, C. Han, and L. Li, “Review of Si IGBT

- and SiC MOSFET based on hybrid switch,” *Chinese J. Electr. Eng.*, vol. 5, no. 3, pp. 20–29, 2019, doi: 10.23919/cjee.2019.000017.
- [113] X. Song, L. Zhang, and A. Q. Huang, “Three-Terminal Si/SiC Hybrid Switch,” *IEEE Trans. Power Electron.*, vol. 35, no. 9, pp. 8867–8871, 2020, doi: 10.1109/TPEL.2020.2969895.
- [114] J. Noppakunkajorn, D. Han, and B. Sarlioglu, “Analysis of High-Speed PCB with SiC Devices by Investigating Turn-Off Overvoltage and Interconnection Inductance Influence,” *IEEE Trans. Transp. Electrification*, vol. 1, no. 2, pp. 118–125, 2015, doi: 10.1109/TTE.2015.2426503.
- [115] Global Modelling and Assimilation Office, “MERRA-2 Re-Analysis,” *Web site*, 2018. .
- [116] Infineon Technologies, “IGW30N60H3 IGBT module Data sheet,” 2014.
- [117] J. Schönberger, “Modeling a Photovoltaic String using PLECS,” *PLECS Appl. Ex.*, pp. 4–6, 2013, [Online]. Available: https://www.plexim.com/sites/default/files/plecs_pvstring.pdf.
- [118] S. Kumar and I. Chong, “Correlation Analysis to Identify the Effective Data in Machine Learning: Prediction of Depressive Disorder and Emotion States,” 2018, doi: 10.3390/ijerph15122907.
- [119] Y. Yang, A. Sangwongwanich, and F. Blaabjerg, “Design for Reliability of Power Electronics for,” *CPSS Trans. Power Electron. Appl.*, vol. 1, no. 1, 2016.
- [120] H. S. H. Chung, H. Wang, F. Blaabjerg, and M. Pecht, *Reliability of power electronic converter systems*. 2016.

APPENDICES

A.1. Derivation for B_x Lifetime Equation:

Reliability function for 2-parameter Weibull distribution is

$$\Rightarrow R(t) = e^{-\left(\frac{t}{\alpha}\right)^\gamma}$$

Apply log on both sides for the above equation

$$\Rightarrow \ln[R(t)] = \ln\left[e^{-\left(\frac{t}{\alpha}\right)^\gamma}\right]$$

$$\Rightarrow \ln[R(t)] = -\left(\frac{t}{\alpha}\right)^\gamma$$

$$\Rightarrow t = \left(-\ln[R(t)] \times \alpha^\gamma\right)^{\frac{1}{\gamma}}$$

$$\Rightarrow t = \left(\ln\left[\frac{1}{R(t)}\right] \times \alpha^\gamma\right)^{\frac{1}{\gamma}}$$

Now replace 't' and 'R(t)' by B_x and $\left[\frac{100}{100-x}\right]$ respectively for simplification no the equation becomes

$$\Rightarrow B_x = \left[\ln\left(\frac{100}{100-x}\right) \times (\alpha)^\gamma\right]^{\frac{1}{\gamma}} \quad \text{a.1}$$

The above shown is B_x equation

were

x is percentage of population

α is Scale Parameter

γ is Shape Parameter.

A.2. Thermal Parameters of Si-IGBT (IGW30N60H3)

Parameter	1	2	3	4
R _{th}	0.052 K/W	0.193 K/W	0.257 K/W	0.295 K/W
C	0.001 J/K	0.002 J/K	0.023 J/K	0.216 J/K

A.3. Thermal Parameters of SiC-Diode (C3D20060D)

Parameter	1	2	3	4
R _{th}	0.0631 K/W	0.3651 K/W	0.1093 K/W	0.107 K/W
C	0.00165 J/K	0.00749 J/K	0.03105 J/K	0.1424 J/K

A.4. Cost Comparison of Switches

Cost Comparison	
Type of Switch	Cost in Rs.
Conventional IGBT	237.02
Hybrid Si/SiC IGBT	1095.28

A.5. Algorithm steps for Monte Carlo simulation and obtaining Weibull distribution

Step: 1 Select sample size of the population.

Step: 2 Select the probability distribution type for the sample.

Step: 3 Using the probability distribution generate samples with uncertainties.

Step: 4 Calculate lifetime at each sample

Step: 5 Fit all the calculated lifetimes in the Weibull distribution

Step: 6 Calculate the B₁₀ lifetime using Eq. a.1.

A.6. Probability Density Function

The Normal distribution PDF is given as

$$f(t) = \frac{1}{\sigma\sqrt{2\pi}} e^{-\frac{1}{2}\left(\frac{t-\mu}{\sigma}\right)^2} \quad \text{a.2}$$

where

$f(t)$ is Probability Density Function

σ is Standard Deviation

μ is Mean

The two parameter Weibull distribution PDF is given as

$$f(t) = \frac{\gamma}{\alpha} \left(\frac{t}{\alpha}\right)^{\gamma-1} e^{-\left(\frac{t}{\alpha}\right)^\gamma} \quad \text{a.3}$$

where

$f(t)$ is Probability Density Function

α is Scale Parameter

γ is Shape Parameter

LIST OF PUBLICATIONS

The following publications are the contributions related to this work. It includes peer reviewed journals, conference presentations and book chapter contributions (Published/Under Review).

1. Kshatri, S.S., Dhillon, J., Mishra, S. “Impact of solar irradiance and ambient temperature on PV inverter reliability considering geographical locations”. **International Journal of Heat and Technology**, Vol. 39, No. 1, pp. 292-298, 2021. <https://doi.org/10.18280/ijht.390132>. (SCOPUS, ESCI) – **Published**.
2. S. S. Kshatri, J. Dhillon, and S. Mishra, “Reliability Evaluation of Grid Connected PV Inverter Considering Panel Degradation Rate And Oversizing”. **Journal of Critical Review**, vol. 7, no. 19, pp. 1710–1714, 2020. (SCOPUS) – **Published**
3. S. S. Kshatri and J. Dhillon, “Reliability Assessment Methodologies For Grid Connected PV Inverter,” **Think India Journal**, no. 17, pp. 908–917, 2019. (UGC Approved) - Published
4. Kshatri S.S., Dhillon J., Mishra S. “Mission Profile Oriented Reliability Evaluation of Grid-Connected PV Inverter Considering Panel Degradation and Uncertainties at Indian Location” **Renewable Energy and Future Power Systems. Energy Systems in Electrical Engineering. Springer, Singapore**, Chapter 3, 2021. (Book Chapter) – **Published**.
5. “Impact of Geographical Locations on the PV Inverter Lifetime Considering Mission Profile and Uncertainties”, Presented at **ICICS 2020**, Lovely Professional University, Punjab. (Conference) – **Presented**.
6. “Mission Profile Oriented Estimation and Validation of Junction Temperature of IGBT Using ETM for Grid Connected PV Inverter Applications” Presented at **ICSTEESD-20**, G H Rasoni College of Engineering, Maharashtra. (Conference) – **Presented**.
7. “High Resolution MP Based Electro Thermal Modelling of PV Inverter for Junction Temperature Estimation” Submitted to **International Journal of Ambient Energy**, Taylor and Francis. (SCOPUS, ESCI) – **Under Review**
8. “Impact of Bifacial PV panel on Inverter Reliability Considering Geographical Locations”, Submitted to **International Journal of Ambient Energy**, Taylor and Francis, (SCOPUS, ESCI) – **Under Review**.

9. “Reliability Improvement of a Grid Connected PV Inverter Considering Hybrid Si/SiC Power Module”, Submitted to **Arabian Journal of Science and Engineering Research, (SCOPUS, SCI) – Under Review**
10. “Reliability Evaluation of PV Inverter Considering Bifacial and Monofacial Panel”, Submitted to **IEEE Access, (SCOPUS, SCI) – Under Review**
11. “Impact of Geographical Locations on the PV Inverter Lifetime Considering Mission Profile and Uncertainties”, Submitted to Taylor and Fransis Book Chapter, Intelligent Circuits and Systems. **(Book Chapter) – Published.**
12. “Mission Profile Oriented Estimation and Validation of Junction Temperature of IGBT Using ETM for Grid Connected PV Inverter Applications” Submitted to Springer Book Chapter, Smart Technologies for Energy, Environment and Sustainable Development. **(Book Chapter) – Accepted.**
13. “Impact of panel degradation rate and oversizing on PV inverter reliability”, Presented at **RDCAPE 2021**, Amity University, UP. **(Conference) – Presented.**

LIST OF PATENTS

The following patent is the contributions related to this work, Filed on 09/09/2021,
Published on 22/10/2021.

1. Hybrid Photovoltaic (PV) Inverter, App.No. 202111041030, **PUBLISHED**.